GENES CONTROLLING CONJUGATION AND MITOTIC CELL DIVISION IN YEAST SACCHAROMYCES CEREVISIAE

by

JINMI KIM

B.S. Microbiology, Seoul National University
(1981)

SUBMITTED TO THE DEPARTMENT OF BIOLOGY
IN PARTIAL FULFILLMENT OF THE REQUIREMENTS
FOR THE DEGREE OF DOCTOR OF PHILOSOPHY

at the

MASSACHUSETTS INSTITUTE OF TECHNOLOGY

May 1988

c Jinmi Kim 1988. All rights reserved

The author hereby grants to MIT permission to reproduce and to distribute copies of this thesis document in whole or in part.

Signature of Author _____
Department of Biology
May 9, 1988

Certified by_____
Gerald R. Fink
Thesis Supervisor

Accepted by_____
Robert T. Sauer
Chairman, Departmental Committee
on Graduate Studies

MASSACHUSETTS INSTITUTE OF TECHNOLOGY
MAY 13 1988
LIBRARIES ARCHIVES

GENES CONTROLLING CONJUGATION AND MITOTIC CELL DIVISION IN YEAST SACCHAROMYCES CEREVISIAE

by

JINMI KIM

Submitted to the Department of Biology
in May 1988 in partial fulfillment of the requirements
for the Degree of Doctor of Philosophy

Abstract

New mutations were isolated that affect nuclear fusion during conjugation in the yeast Saccharomyces cerevisiae. These mutations, called kem (Kar⁻ enhancing mutation), enhance the nuclear fusion defect of the kar1-1 mutation. In crosses of kar1-1 strains, 10 - 15% of zygotes undergo nuclear fusion forming stable diploids whereas 85 - 90% of zygotes fail to have nuclei fused. The nuclear fusion defect of kar1-1 leads to formation of a heterocaryon which buds off a cytoductant with a parental haploid nucleus and a mixed cytoplasm. Newly isolated kem mutations block the residual nuclear fusion of kar1-1 crosses. This block in nuclear fusion has been confirmed by the genetic assay measuring cytoductant formation and the cytological observation of nuclear DNA in zygotes stained with DAPI. Nuclear fusion is normal in crosses of kem x KAR. Eight independent kem mutations were isolated. These eight mutations define at least three genes KEM1, KEM2, and KEM3. The KEM1 and KEM3 genes are located on the left arm of chromosome VII; CenV met13 (16 cM) kem3 (18 cM) lys5 (13 cM) kem1.

I have characterized mutations in KEM1 in a Kar⁺ background. Several phenotypes of the kem1 mutants suggest that kem1 mutations affect the microtubule or spindle pole body function. The kem1-1 and kem1-5 mutations cause a bilateral nuclear fusion defect. In crosses where both parents are kem1, about 30% of the zygotes fail to fuse nuclei with the result that cytoductants are produced at high frequency. The growth of kem1 mutants was examined at various concentrations of the anti-microtubule drug, benomyl. As compared with KEM1, the kem1 mutants are hypersensitive to benomyl. kem1/kem1 diploids lose chromosomes with a frequency of 10 - 20 fold higher than Kem⁺ diploids. These results are consistent with the idea that KEM1 has a role in microtubule function.

The KEM1 gene was disrupted by replacing the internal fragment of the KEM1 gene with a fragment carrying the URA3 gene. The null allele kem1::URA3 is viable but causes a slow-growth phenotype and an altered cell morphology during the mitotic cell cycle. Microscopic examination of cell culture has shown that about 80% of kem1::URA3 cells have an elongated rod-shape and twice the size of a wild type cell. In these cells spindle pole body duplication/separation is defective as visualized by indirect immunofluorescence microscopy using anti-tubulin antibodies. A high proportion of large budded cells in kem1::URA3

culture contained a single spindle pole body region without progression to the stage where the intranuclear spindles being developed. Approximately 10% of cells contained two nuclei.

kem1 strains lose viability upon nitrogen starvation and kem1/kem1 diploids have a defect in sporulation. The initial response of kem1 strains to nitrogen starvation is similar to that of a wild type strain: 90 - 95% of cells arrest as unbudded cells. However, upon further starvation, the kem1 strains lose viability: after 4 days only 5% of kem1 cells were viable. These observations support the notion that mutations in KEM1 cause a defect in the proper response to nutritional changes. I infer that the KEM1 gene is involved in a regulatory mechanism controlling the spindle pole body or microtubules in response to the nutritional state of the cell.

Transposon insertions were performed in the cloned KEM1 gene using mini-Tn10-LUK element (carrying the E. coli β-galactosidase structural gene and the yeast URA3 gene). A collection of random Tn10-LUK insertions defined an approximately 3.5 kb region required for the KEM1 function. From this collection functional KEM1::lacz protein fusions were identified. Indirect immunofluorescence using anti-β-galactosidase antibodies localized KEM1::lacz fusion proteins to the periphery of the nucleus.

Thesis supervisor: Gerald R. Fink

Professor of Genetics

ACKNOWLEDGEMENTS

I would like to give my deep gratitute to all those who have helped me through the years of my graduate life. I, first, thank my advisor, Gerry Fink, for teaching me to do good science and to love genetics, for his stimulating advice and encouragement which helped me to find the direction and the main points in my studies, and for his understanding, unwavering patience, and caring support.

I also thank many professors in the Department of Biology including my thesis committee for their instruction and helpful discussion. I specially thank Prof. Frank Solomon for his helpful support and suggestions of my graduate work.

I thank Andy Hoyt and Chris Kaiser for the strains, plasmids, and technical help.

I am grateful fo the members of the Fink' laboratory for cheerful communications of science and other matters as well; Cora Styles, Mark Rose, Fred Winston, David Garfinkel, Jef Boeke, John Teem, Isabel Chiu, Josh Trueheart and Vivian Berlin. They helped me with experimental techniques, excellent ideas, critical suggestions, and for the most, a sense of humor.

I am grateful to all my good friends who have supported me, shared good and bad times in Cambridge, patiently listened to my complaints,...

My special thanks to my parents for their love, unlimited support, and showing me to live with a sincere heart.

TABLE OF CONTENTS

ABSTRACT 2

ACKNOWLEDGEMENTS 4

TABLE OF CONTENTS 5

LIST OF FIGURES 8

LIST OF TABLES 10

CHAPTER 1: Introduction 11

I. Conjugation pathway in Saccharomyces cerevisiae 12

II. Spindle pole body 22

III. Microtubues in yeast Saccharomyces cerevisiae 24

IV. Signal transduction 26

CHAPTER 2: Isolation and characterization of kem mutations which enhance the nuclear fusion defect of kar1-1. 31

Introduction 32

Materials and methods 33

Results 40

Isolation of kem mutants. 40

kem enhances the nuclear fusion defect of kar1-1. 45

Dominance-recessiveness and complementation test. 55

Mapping of KEM1 and KEM3. 58

Discussion 62

CHAPTER 3: kem1 mutations cause a defect in microtubule and spindle pole body function and in the cellular response to nutritional conditions. 66

Introduction 67

Materials and Methods 69

Results 77

kem1 has a bilateral nuclear fusion defect. 77

kem1 mutants are hypersensitive to the antimicrotubule drug benomyl. 82

kem1 causes a defect in mitotic chromosome transmission. 82

Cloning of KEM1. 88

Disruption of KEM1 affects the mitotic cell division. 93

kem1 null mutation affects the spindle pole body. duplication. 96

kem1/kem1 diploids fail to sporulate. 103

kem1 mutants lose viability upon nutritional starvation. 107

kem interaction with the RAS/adenylate cyclase pathway. 114

kem1 mutants are sensitive to EGTA. 118

Discussion 118

CHAPTER 4: Transposon insertions in KEM1 and localization of KEM1::lacz fusion proteins. 125

Introduction 126

Materials and Methods 127

Results 132

Transposon insertions in KEM1 using mini-Tn10-LUK. 132

Insertion mutations define a 3.5 kb region required for KEM1 function. 133

KEM1::lacz protein fusion. 136

Localization of KEM1::lacz protein fusions. 142

Discussion 145

APPENDIX I: Cloning and disruption of KEM3. 148

LITERATURE CITED 156

LIST OF FIGURES

Figure 1-1.	Schematic diagram of yeast conjugation cycle.	13
Figure 2-1.	Schematic diagram describing two schemes for isolating kem mutants.	41
Figure 2-2.	Diploid formation in crosses of kar1-1 and kem1 mutants as measured by a plate mating assay.	46
Figure 2-3.	Diagram describing quantitative mass mating assay for measuring the frequency of cytoductant and diploid formation.	49
Figure 2-4.	Genetic method for constructing diploids homozygous for the mating type locus.	56
Figure 2-5.	Map location of KEM genes.	60
Figure 3-1.	Nuclear fusion defect in kem1 x kem1 crosses as revealed by DAPI-staining and anti-tubulin immunofluorescence.	78
Figure 3-2.	Benomyl-hypersensitivity of kem1 strains.	84
Figure 3-3.	Diagram describing an assay for chromosome loss.	86
Figure 3-4.	DNA inserts of the plasmid vectors used in this study	91
Figure 3-5.	2:2 segregation of the slow-growth phenotype in the tetrads from +/kem1::URA3 diploids.	94
Figure 3-6.	Southern blot analysis of total yeast DNA from strain a parent (JK200), a Ura^+ transformant, and four spores from a resulting tetrad.	97
Figure 3-7.	Morphology of mitotically growing kem1::URA3 cells	99

compared with KEM1 cells.

Figure 3-8. (a) Nuclear and microtubular staining of large-budded cells of KEM1 strain. 101

(b) Defects in nuclear division and spindle pole body separation of kem1::URA3 cells as revealed by nuclear and microtubular staining. 104

Figure 3-9. Sporulation defect in kem1/kem1 dipoids as revealed by cell morphology and DAPI-staining. 108

Figure 3-10. Sensitivity of the kem1 mutants to the nutritional starvation. 110

Figure 3-11. Viability of kem1 mutants after nitrogen starvation. 112

Figure 3-12. Budding pattern of kem1 bcy1 double mutants. 116

Figure 3-13. Sensitivity of kem mutants to EGTA. 119

Figure 4-1. Restriction map of the plasmid vector used for transposon insertion analysis as well as the structure of mini-Tn10-LUK element. 134

Figure 4-2. Western blot analysis of KEM1::lacz fusion proteins. 140

Figure 4-3. Intracellular localization of KEM1::lacz fusion proteins revealed by indirect immunofluorescence. 143

Figure 5-1. Restriction map of the plasmid inserts containing KEM3 and kem3 disruption. 149

Figure 5-2. 2:2 segregation of lethality in tetrads from +/kem3::HIS3. 152

LIST OF TABLES

Table 2-1. Yeast strains used in this study. 34

Table 2-2. The ratio of cytoductants to diploids produced in crosses of kem and kar1-1 mutants as measured by quantitative mass matings. 51

Table 2-3. Efficiency of nuclear fusion in crosses of kem and kar1-1 mutants as measured by DAPI-staining of zygotes. 53

Table 2-4. Efficiency of diploid formation in crosses of kem and kar1-1 mutants measured by micromanipulation of zygotes. 54

Table 2-5. Mapping data. 59

Table 3-1. Yeast strains used in this study. 70

Table 3-2. Failure of nuclear fusion in crosses of kem1 mutants as measured by examining DAPI-stained nuclear DNA. 81

Table 3-3. Ratio of cytoductant to diploid in crosses of kem1-5 mutants as measured by quantitative mass mating. 83

Table 3-4. Frequency of chromosome loss and mitotic recombination in kem1/kem1 diploids. 89

Table 3-5. Nuclear division and spindle pole body separation in large budded cells of KEM1 and kem1::URA3 strains. 106

Table 4-1. Complementing acitivity of transposon insertion plasmids. 137

Chapter 1. Introduction

During conjugation in the yeast Saccharomyces cerevisiae, nuclear fusion occurs immediately after cell fusion. An early step in nuclear fusion is the movement of the two parental nuclei toward one another to permit precise positioning of the nuclei, so that subsequent fusion can take place. The mechanism by which each of these processes (nuclear migration, membrane fusion, and spindle pole body fusion) takes place is of great interest.

The primary aim of this thesis is the isolation and genetic analysis of genes involved in nuclear fusion in order to provide a clearer picture of the nuclear fusion pathway. I have isolated mutations that affect nuclear fusion during conjugation in yeast. One of these appears to be involved in signal transduction as well as microtubule or spindle pole body function. This leads me to speculate that this gene could encode a protein that relays information to the spindle pole body or microtubules concerning the nutritional state of the cell. Such a protein would tell the spindle pole body whether to carry out events required for mitosis or conjugation.

This introduction reviews what is known about the function of the spindle pole body and microtubules in both the mitotic and the conjugation pathways. I will first review the sequence of events that occur during the yeast conjugation cycle (cell biological studies and genetic analysis). Then, I will discuss the involvement of microtubules and spindle pole bodies. Finally, I will review what is known about

signal transduction in yeast, particularly with a view towards its implication in conjugation.

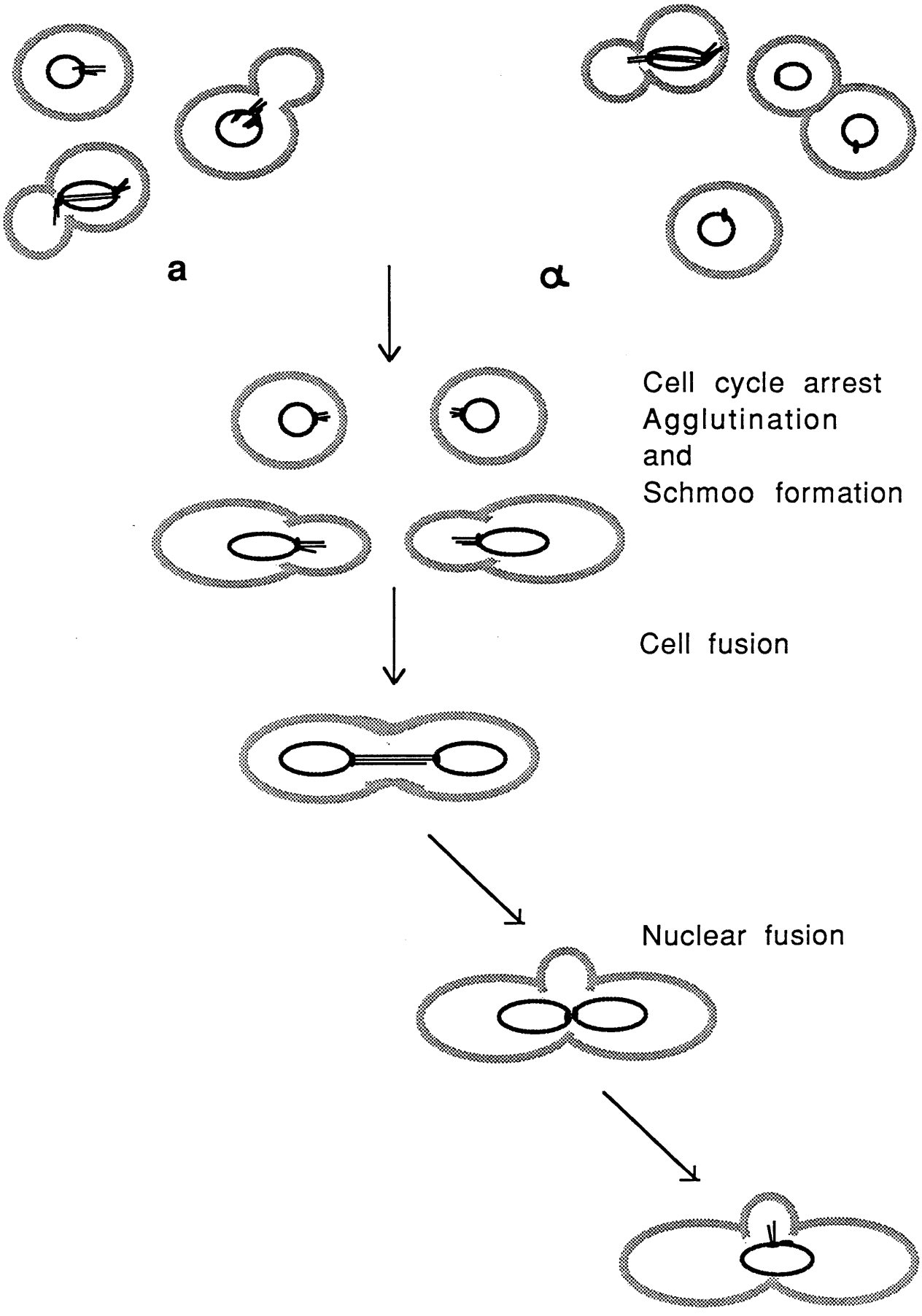
I. Conjugation pathway in Saccharomyces cerevisiae

Haploid cells make a developmental decision each cell cycle. In the presence of nutrients they divide mitotically by budding. In the presence of cells of opposite mating type, cells leave the mitotic cell division cycle and conjugate, fusing with cells of opposite mating type to form a diploid zygote. Each of the haploid cells secretes a pheromone that inhibits growth of cells of opposite mating type and induces the conjugation pathway. The mating type in Saccharomyces cerevisiae is determined by alleles of the mating-type locus MATa and MATα (Herskowitz and Oshima, 1981, Nasmyth, 1982).

Direct observations of a mixture of MATa and MATα cells in the light microscope provided an early description of the sequential steps during conjugation (Levi, 1956, Hartwell, 1973). As diagramed in Figure 1-1, cells arrest at the G1 phase of the cell cycle and undergo morphological changes forming an elongated cell called a "shmoo". The cells agglutinate and then each pair of cells fuses at the cytoplasmic level producing a transient heterokaryon. Nuclear fusion occurs immediately to form a stable diploid. The cytological studies of mating cells by electron microscopy (Byers and Goetsch, 1974, 1975) and the genetic analysis of mutants defective in mating (Mackay and Manney, 1974a, 1974b, Manney and Woods, 1976, Trueheart et al., 1987, Conde and

Figure 1-1. Schematic diagram of yeast conjugation cycle

Mating factors produced by haploid cells of each mating type induce the initial steps of conjugation; G1 arrest, agglutination, and shmoo formation. When cells of opposite mating type pair, the cell walls separating two cells are degraded and cell fusion occurs with cytoplasmic mixing. Two parental nuclei are brought together and nuclear fusion occurs starting at the spindle pole body. When a diploid nucleus is formed, the zygote initiate the mitotic cell cycle, budding off a diploid cell.


a
α
Cell cycle arrest
Agglutination
and
Schmoo formation
Cell fusion
Nuclear fusion

Fink, 1976, Polaina and Conde, 1982, Dutcher and Hartwell, 1983) have provided a clearer view of each discrete step in the pathway.

Initial steps for conjugation

Conjugation is initiated by constitutively secreted mating factors. Cells of each mating type produce a diffusible oligopeptide pheromone α-factor or a-factor that stimulates cells of the opposite mating type (Levi, 1956, Duntze et al., 1970, 1973, Betz et al., 1977, Wilkinson and Pringle, 1974). A strong indication that these mating factors are functionally involved in the conjugation processes comes from the findings that many nonmating mutants (ste) fail to produce or respond to their particular mating factors (Mackay and Manney, 1974a, 1974b) and that all mutants isolated as resistant to α-factor are mating defective (Manney and Woods, 1976). The mating defect of one of these mutants, ste13, was restored by adding α-factor to mating mixtures (Chan et al., 1983). Mating type **a** cells, upon treatment with α-factor, undergo morphological changes closely resembling those seen in mating mixtures (Hartwell, 1973, Bücking-Throm et al., 1973). The mating factor response is mediated by mating-type specific receptors encoded by the STE2 gene (α-factor receptor) and the STE3 gene (a-factor receptor) which were originally identified by the ste mutations (Burkholder and Hartwell, 1985, Nakayama et al., 1985, Hagen et al., 1986).

The synchronization of cell cycles is the critical step in conjugation and is mediated by the mating factors. When asynchronous cultures of a and α haploid cells are mixed or when asynchronous a cells are treated with α-factor, cells of both mating types are inhibited at a

specific point in the early G1 phase of the cell cycle leading to the accumulation of unbudded mononucleate cells (Hartwell, 1973, Bücking-Throm et al., 1973). Kinetic analysis of the morphology of mating cells has suggested that **a** and α haploid cells are in the unbudded stage of the cell cycle at the time of fusion (Hartwell, 1973). The cell-cycle block is prior to initiation of DNA synthesis, bud emergence, and duplication of a spindle pole body (Byers and Goetsch, 1974, 1975). However, the synthesis of RNA, protein, and polysaccharide is relatively unaffected (Thorner, 1981, Bücking-Throm and Duntze, 1970, Sumurada and Cooper, 1978, Schekman and Brawley, 1979).

Sexual agglutination is another characteristic of yeast mating cells. When a and α haploid cells are mixed, cells adhere to opposite mating types forming large aggregates (Shimoda et al., 1978, Betz et al., 1978). The agglutination presumably facilitates mating by providing cells with the opportunity to contact with cells of opposite mating type as well as the physiological conditions favorable for mating (Kawanabe et al, 1979). Several groups have reported that the sexual agglutinability is expressed constitutively in haploid yeast cells (constitutive agglutination) and enhanced during mating or by treating cells with mating factors (inducible agglutination) (Shimoda et al., 1978, Fehrenbacher et al., 1978, Terrance and Lipke, 1981, Thorner, 1981). The level of constitutive agglutination activity, however, appears to vary among yeast strains; in some strains the constitutive agglutination is weak (Betz et al., 1978), but in others it is strong (Terrance and Lipke, 1981). Because the data varied depending on the yeast strains or the agglutination assays being used, the level of

constitutive agglutination activity is still not clear. The mechanism by which cells agglutinate is suggested to be through a complementary binding of agglutination factors located on the cell surface (Burke et al., 1980, Terrance end Lipke, 1981)). Several groups have tried to isolate the agglutination factors from Saccharomyces cerevisiae cells by treating haploid cells with snail juice glusulase (Shimoda and Yanagishima, 1975), by autoclaving haploid cells (Hagiya et al., 1977), or by breaking cells (Terrance et al., 1987). The mating type-specific glycoproteins released by these treatments were shown to be adsorbed specifically to cells of opposite mating type and to inhibit the agglutinability of these cells.

There are also significant changes occurring in the cell surface and in the cell wall organization during conjugation. The yeast cell wall is composed primarily of glucans, manno-proteins, and chitins (Ballou, 1981). Mating type **a** cells treated with α-factor contain more glucan and less mannan than untreated control cells and the mannan of treated cells contain shorter side chains and unsubstituted backbone mannose units (Lipke et al., 1976). The synthesis of chitin is induced by α-factor and chitins are accumulated in the area of α-factor stimulated growth (Schekman and Brawley, 1979). Thin-section electron microscopy of treated cells reveals that the outer layer of the cell wall becomes diffuse and thinner at the region of α-factor induced cell enlargement (Lipke et al., 1976). These changes in cell wall are accompanied by an alteration in the expression of surface antigens (Lipke and Ballou, 1980).

Trueheart et al. (1987) have identified two genes, FUS1 and FUS2, which are required for cell fusion during yeast mating. The FUS1 gene encodes a glycoprotein whose production is induced by α-factor. Immunofluorescence microscopy of α-factor induced **a** cells carrying a fus1::lacz fusion has shown that the fusion protein was localized at the cell surface, concentrated at the tip of the elongated cell (shmoo) (Trueheart et al., 1987). These results suggest that the glycoprotein encoded by FUS1 is localized to the cell surface in response to α-factor and participates in mating processes.

Growth without division produces cells with a localized elongation called a "shmoo" (Thorner, 1981). The nucleus in this cell tends to be located at the neck of the shmoo structure. Studies thin sections in the electron microscope and indirect immunofluorecence with anti-tubulin antibody in the light microscope have revealed the spindle pole body and microtubule structure in α-factor induced shmoo cells. The spindle pole body, a densely stained structure embedded in nuclear envelope, is arrested as the single unduplicated spindle pole body and found adjacent to the shmoo neck. The extramicrotubules radiate from a point on this spindle pole body toward the shmoo tip (Byers and Goetsch, 1975, Rose and Fink, 1987).

Cell fusion

After the initial conjugation steps (G1 arrest, cell surface changes, agglutination, etc.), **a** and α haploid cells become appropriately prepared for cell fusion. The agglutinated cells are sensitive to sonication and disperse easily. The two-cell structure in

the early stage of cell fusion (called a "prezygote") is resistant to sonication (Hartwell, 1973). Fusion requires the removal of the cell wall separating the two cells with the subsequent fusion of the two plasma membranes. Shimoda and Yanagishima (1972) have suggested that the early breakdown of the cell wall is due to autolytic activity. The electron micrographic studies of mating pairs have indicated that the layers of intervening cell wall at the site of the cell-cell contact become progressively thinner, allowing the fusions of the two menbranes (Osumi et al., 1974). In support of this description is the finding that fus mutants defective in cell fusion form a prezygote structure in which there is no membrane fusion and remnants of undegraded cell wall remain between the paired cells (Trueheart et al., 1987). Electron microscopic observations of prezygotes that have undergone partial perforation in the region of the fused walls has revealed that cytoplasmic microtubules arising from the cytoplamic side of a spindle pole body penetrate through the perforation and entering the cytoplasm of the opposing cell (Byers and Goetsch, 1975).

Nuclear fusion

Cytoplasmic fusion of two haploid cells of opposite mating type results in formation of a transient heterokaryon. Nuclear fusion, a union of two parental nuclei, occurs immediately. Current knowledge on the nuclear fusion process has come mainly from the cytological observations of serial thin sections in the electron microscope and the identification and analysis of mutations defective in nuclear fusion. Serial thin sections examined by electron microscopy suggest that the

two nuclei are brought together by the extranuclear microtubules which interconnect the outer surface of the spindle pole body (Byers and Goetsch, 1974, 1975). The first site of contact between the two nuclei appears to be at the position of the spindle pole bodies. Subsequently the two precisely aligned spindle pole bodies fuse and, in an as yet undefined way, the contiguous nuclear envelopes follow.

A mutational analysis of the sequence of events leading to nuclear fusion has uncovered several genes required for the process. These include KAR1, KAR2, KAR3 (Conde and Fink, 1976, Fink and Conde, 1976, Polaina and Conde, 1982), TUB2 (Thomas, 1984, Huffaker et al., 1988), CDC4, CDC37 (Dutcher and Hartwell, 1982, 1983), and BIK1 (Berlin, personal communication). Conde and Fink isolated a set of kar mutants, using a scheme which relies on the phenotypes expected from the failure of nuclear fusion (Conde and Fink, 1976, Fink and Conde, 1976, Polaina and Conde, 1982C). The KAR1 gene, one of three KAR genes identified through this scheme, is likely to code for a component of the spindle pole body (Rose and Fink, 1987). Mutations in the β-tubulin gene also cause a defect in nuclear fusion (Thomas, 1984, Huffaker et al., 1988). Among the cell cycle mutations tested, cdc4 and cdc37 are shown to have a nuclear fusion defect (Dutcher and Hartwell, 1982, 1983). CDC37 is necessary for the duplication of spindle pole body and CDC4 is necessary for the separation of the duplicated spindle pole bodies (Byers, 1981b). Nuclear fusion defects are of two types; unilateral or bilateral. In the unilateral pattern, only one parent of the cross need be mutant for nuclear fusion to fail. The kar1-1, kar2, and kar3 mutations are

unilateral. In the bilateral pattern, both parents must be mutant for nuclear fusion to fail. The tub2 and bik1 mutations are bilateral.

A failure of nuclear fusion leads to the formation of a distinctive class of progeny called cytoductants. A cytoductant is a haploid exoconjugant containing the nuclear genotype of one parent and the cytoplasmic components of both parents (Fink and Conde, 1976, Dutcher, 1982, Dutcher and Hartwell, 1983). Cytoductant progeny have also been identified in a wild type crosses at a low frequency (Wright and Lederberg, 1957) indicatative of the spontaneous failure of nuclear fusion. Cytoductants are a good assay for a defect in nuclear fusion because their presence indicates a mating occurred (cell fusion) without diploid formation (Dutcher, 1982, Dutcher and Hartwell, 1983). Studies of genes affecting nuclear fusion in this thesis also involves this assay.

Nuclear fusion, like cell fusion, requires potentiation by the mating factors (Rose et al, 1986, Curran and Carter, 1986). Little is understood about the effects of mating factors in the nuclear envelope or the spindle pole body during conjugation, although cell cycle arrest by mating factors is shown to be at the point prior to the duplication of the spindle pole body. This thesis addresses questions concerning the mechanism by which the spindle pole body and microtubules change during conjugation.

II. Spindle pole body

The spindle pole body of the yeast Saccharomyces cerevisiae is a dense discoidal structure embedded in the nuclear envelope thought to be a microtubule organizing center (Pickett-Heaps, 1969). The analogous structure in the animal cell is the centrosome where the pair of centrioles and the pericentriolar material reside (Pickett-Heaps, 1971). The spindle pole body is associated with at least one end of every microtubule throughout the life cycle serving as the focus for microtubule organization (Robinow and Mark, 1966). Byers group (1978) has isolated spindle pole bodies from yeast lysates and shown that the spindle pole bodies devoid of native microtubules have the ability to initiate the polymerization of chick neurotubulin.

During the mitotic cell division cycle, the single spindle pole body duplicates resulting in two structures in a side-by-side configuration with a bridge between them. The two duplicated spindle pole bodies move apart until they are at oppositing positions on the nuclear envelope. Each spindle pole body is transmitted to the daughter cells as the cell divides. During the conjugation cycle, the spindle pole body in each parent nucleus arrests at a stage prior to duplication. The nuclear fusion process appears to initiate at the site of contact between the spindle pole bodies of each nucleus.

Various approaches have been undertaken to define the structural components and the in vivo function of the spindle pole body. The KAR1 gene, originally defined by the kar1-1 mutation, is associated with the spindle pole body function (Rose and Fink, 1987). Cells with

temperature-sensitive kar1 mutations, or in which the KAR1 gene product is overproduced, show a cell division cycle (cdc) phenotype, arresting as large budded cells. When examined by electron microscopy and light microscopy they have defects in duplication of the spindle pole body and abnormally long extranuclear microtubules. Recent indirect immunofluorescent study with kar1::lacz protein fusions suggest that the KAR1 gene product is likely to be a component of the spindle pole body (Rose, personal commmunication).

The SPA1 gene was isolated by immunoscreening a yeast genomic DNA expression library with human serum that reacts with mammalian spindle pole (Snyder and Davis, 1986). Evidences suggest that the SPA1 gene product may be a component of the spindle pole body. A 59 kd protein encoded by the SPA1 gene copurifies with a yeast nuclear fraction. In esp1 mutant cells that overproduce spindle pole bodies (Baum et al., 1986a), the SPA1 proteins is enriched. The spa1 null allele has several interesting phenotypes expected for a defect in the spindle pole body function: a high frequency of chromosome loss, abnormal numbers of nuclei per cell in mitotically growing cells, a nuclear fusion defect during mating, and temperature sensitivity at 38^{o}C with a slow growth at 30^{o}C (Snyder and Davis, 1986).

Cells containing the mutation cdc31-1 arrest as large budded cells with a single nucleus at the non-permissive temperature. cdc31-1 cells arrested at the non-permissive temperature have a spindle pole body which is doubled in size, but this enlarged spindle pole body fails to duplicate (Byers, 1981b). The amino acid sequence of the CDC31 gene shows a great similarity to those of known Ca^{++}-binding protein family,

suggesting that the CDC31 gene has a specific role in spindle pole body duplication perhaps responding to Ca^{++} at a specific stage of the cell cycle (Baum et al., 1986b).

III. Microtubules in the yeast Saccharomyces cerevisiae

In the yeast cells, microtubules closely similar to those of higher eucaryotes are found. Microtubules are tubular fibrous elements composed of globular protein subunits, tubulins, stacked in a regular helical array. The tubulins exist as a 110 kd heterodimer of α- and β-tubulin and probably serve as the funtional unit in microtubule assembly (Bryan and Wilson, 1971, Raff, 1984). The spatial and extremly dynamic organization of microtubules is well correlated with the functions of microtubules; that is, governing cell motility, structure, and morphology. Yeast microtubules function in a small number of defined cellular processes including chromosome separation during mitosis and meiosis, nuclear movement and division during mitosis, and nuclear fusion during conjugation (Thomas et al., 1985, Huffaker et al, 1987, 1988, Schatz, 1987, Delgado and Conde, 1984). The arrangement of microtubules in the yeast cell has been described by both electron microscopy (Byers, 1981, Byers and Goetsch, 1974, 1975, Robinow and Mark, 1966, Peterson and Ris, 1976) and indirect immunofluorescence using anti-tubulin antibodies (Adams and Pringle, 1984, Kilmartin and Adams, 1984).

Yeast microtubules radiate from the spindle pole body; the intranuclear spindles from the nuclear face and the cytoplasmic

microtubules from the cytoplasmic side. In the early stage of the mitotic cell cycle, unbudded or small-budded cells do not have a complete intranuclear spindle. As the cell cycle proceeds, the spindle pole body duplicates and separates. At the point where there are two spindle pole bodies opposed to each other on the nuclear membrane, a complete intranuclear spindle is found and microtubules span the nucleus from one spindle pole body to another. The intranuclear spindles become longer as the nucleus elongates and divide in large-budded cells. Finally, they break when cytokinesis and cell division occur.

The cytoplasmic microtubules arising from the cytoplasmic face of the spindle pole body are less easily observed. During cell division they frequently orient toward the bud. It has been suggested that they are involved in the delivery of secretory vesicles to the bud (Huffaker et al., 1987). Cytoplasmic microtubules appear to play an important role in nuclear movement, positioning, and fusion during conjugation (Huffaker et al., 1988). The extranuclear microtubules connect two nuclei in the zygote and appear to shorten as the two nuclei move toward one another (Byers and Goetsch, 1974, 1975). The obvious implication is that the microtubules provide the motive force for nuclear movement.

The functions attributed to microtubules by these cytological observations are supported by studies of tubulin genes using classical and molecular genetic techniques. The haploid yeast genome possesses a single essential β-tubulin gene, TUB2 (Neff et al., 1983), and two α-tubulin genes, TUB1 and TUB3 (Schatz et al., 1986a). Cold-sensitive mutations in the TUB2 gene, isolated either by selecting cells resistant to antimicrotubule drug benomyl (Thomas et al., 1985) or by in vitro

mutagenesis (Huffaker et al., 1988), cause a cell cycle arrest at large-budded cells with a single nucleus at nonpermissive temperature. Work by Huffaker et al. (1988) correlated the defects in microtubule array with the defects in microtubule functions for various alleles of the TUB2 gene. The results agree with previous work showing that cytoplasmic microtubules are responsible for nuclear migration during the mitotic cell cycle and for nuclear migration and fusion during conjugation (Huffaker et al., 1987, 1988).

There is a group of non-tubulin genes which also affect microtubular functions. The ndc1-1 mutation is shown to be defective in chromosome separation (Thomas and Botstein, 1986). Several cin mutants were isolated by the phenotype of chromosome loss (Huffaker et al., 1987, Hoyt, personal communication).

IV. Signal Transduction

Cells respond to their environment (hormones, growth factors, and neurotransmitters) by means of a wide array of membrane receptors. Signals are generated through these receptor-ligand interactions and transformed into changes in cellular function and metabolism. The signal transduction processes often involve GTP-binding proteins (G proteins) that couple the receptors to the biochemical effector systems that regulate various second messengers (Stryer and Bourne, 1986). A variety of different G proteins are found in different kinds of specialized cells. These can be grouped into at least three effector pathways based on studies mostly in mammals and insects: (1) G_s (stimulatory G protein)

and G_i (inhibitory G protein) regulate the adenylate cyclase, and thus the intracellular levels of cAMP. (2) G proteins regulate the phospholipase C which hydrolyzes phosphatidylinositol 4,5-bisphosphate (PIP_2) to inositol 1,4,5-triphosphate (IP_3, stimulates the intracellular Ca^{++} level) and 1,2-diacyl glycerol (activates the protein kinase C). Ca^{++} and diacylglycerol signals are often synergistic for evoking subsequent cellular processes. (3) Transducin couples the rhodopsin of the outer retina to the cGMP phosphodiesterase in the rod outer segment, regulating the cGMP level.

G proteins are heterotrimeric, consisting of three subunits α, β, and γ. The α-subunits of the different G proteins appear to be characteristic of each G protein, whereas the β-subunit is highly conserved (Stryer and Bourne, 1986). The α subunit binds and hydrolyzes GTP. The G proteins cycle between an inactive GDP state and an active GTP state. In the absence of an extracellular signal, the α-subunit bound to GDP associates with β and γ to form a complex called G-GDP. After binding of ligand to its receptor, the activated receptor stimulates the exchange of GTP for bound GDP. The α-subunit with bound GTP (G_α-GTP) dissociates from the β and γ subunits and interacts with the effector enzyme, regulating the enzyme activity. The interaction is terminated when the bound GTP is hydrolyzed to GDP by the α-subunit.

Whether the signal transduction systems in yeast are analogous to those in mammals and insects is a question of current interest. In Saccharomyces cerevisiae, several GTP-binding proteins are known. For example, RAS1, RAS2, RHO1, RHO2, SEC4, SCG1(GPA1), and YPT1 (Tamanoi et al., 1985, Salminen and Novick, 1987, Schmitt et al., 1986, Dietzel and

Kurjan, 1987, Miyajima et al., 1987) all bind GTP. However, whether these proteins are G proteins that associate receptors with effector pathways is still unproven.

Mating pheromone response in Saccharomyces cerevisiae.

The mating pheromone response in Saccharomyces cerevisiae cells during conjugation is mediated by mating-type-specific receptors. The STE2 and STE3 genes code for α-factor and a-factor receptor, respectively (Burkholder and Hartwell, 1985, Nakayama et al., 1985, Hagen et al., 1986). Recently Dietzel and Kurjan (1987) and Miyajima et al. (1987) have isolated by independent methods an identical gene (SCG1 and GPA1, respectively) which encodes a G_α-like protein implicated in the mating response. The SCG1 gene was isolated by its ability to suppress the pheromone-supersensitive sst2-1 mutation and the GPA1 gene by its hybridization to cDNAs for α-subunits of mammalian G protein. The loss of the SCG1 (GPA1) gene function (by either gene disruption or turning off the gene expression using the galactose inducible GAL1 promoter) leads to G1 arrest and aberrant cell morphology similar to that of the shmoo - phenotypes similar to those seen when cells respond to mating factors. The rat G_α gene complements the growth and morphological defects of the scg1 mutation, indicating that SCG1 is functionally related to mammalian G_α proteins (Kurjan et al., 1987).

The identification of G_α-like proteins and the evidence for their possible association with the mating factor response strongly support the idea that the yeast receptor system may be analogous to the mammalian receptor/signal transduction system (Herskowitz and Marsh,

1987). Yet many questions about the effector system and the intracellular second messenger in the mating factor response are unanswered. Ohsumi and Anraku (1985) observed accumulation of Ca^{++} ion in mating type a cells in response to α-factor. Furthermore, addition of 5mM EGTA decreased the frequency of zygote formation and a Ca^{++} ionophore inhibits shmoo formation of α-factor treated **a** cells. These results suggest that the Ca^{++} uptake induced by α-factor is required for progression of following mating processes. The Ca^{++} ion could be a signaling molecule in the yeast mating factor response. However, the involvement of Ca^{++} ion in conjugation is only correlative.

RAS/adenylate cyclase pathway in Saccharomyces cerevisiae

Wigler's group and the Matsumoto's group have described a regulatory cascade that involves G proteins and cAMP effector systems. In summary, the CDC25 gene products act on the RAS proteins (G proteins) by regulating the guanine nucleotide bound to RAS proteins (Broek et al., 1987). The RAS gene products stimulate the activity of the adenylate cyclase encoded by the CYR1 gene (the effector enzyme), resulting in an increase in the cellular cAMP level (Broek et al., 1985, Kataoka et al, 1985a, Tamanoi et al., 1985, Toda et al., 1985). The level of cAMP modulates the activity of cAMP-dependent protein kinases (TPK1, TPK2, and TPK3) (Toda et al., 1987a) via the regulatory subunit of the protein kinase encoded by the BCY1 gene (Uno et al., 1982, Toda et al., 1987b). In the absence of the BCY1 gene product, the catalytic subunits of the protein kinase are constitutively active independently of the cAMP level.

The yeast RAS1 and RAS2 genes were cloned by their similarities to DNA fragments from mammalian RAS genes and shown to be funtionally homologous to mammalian RAS genes (Powers et al., 1984, Kataoka et al., 1984, 1985b, DeFeo-Jones et al., 1985). The RAS genes were first identified as the oncogene of Harvey (v-H-ras) and Kirsten (v-K-ras) sarcoma viruses (Ellis et al., 1981, Powers et al., 1984). The mutations in genes in the RAS/adenylate cyclase pathway, which cause the increase in the cellular cAMP level or cAMP-dependent protein kinase activity show defects in the cellular responses to both nutritional conditions and heat shock treatment (Broek et al., 1987). These phenotypes are all manifest by strains which have mutations that affect the levels of cAMP or the activity of cAMP-dependent protein kinase; activated form of CDC25 (Broek et al., 1987), RAS2^{val19} (Kataoka et al., 1984), CYR::HIS3 that overexpress the catalytic domain of adenylate cyclase (Kataoka et al., 1985a), bcy1 that encodes a regulatory subunit of the cAMP-dependent protein kinase (Uno et al., 1982, Toda et al., 1987)). These results strongly suggest that the RAS/adenylate cyclase pathway is involved in mediating the cellular responses to external signals. However, what is not clear is whether this response works by the receptor-ligand interaction like those in mammalian signal transduction system.

Chapter 2

Isolation and characterization of *kem* mutations which enhance the nuclear fusion defect of *kar1-1*.

INTRODUCTION

During the conjugation cycle of the yeast Saccharomyces cerevisiae, two parental nuclei fuse immediately after cell fusion to form stable diploids. The sequential events of nuclear fusion in newly formed zygotes have been characterized by electron microscopic studies (Byers and Goetsch, 1974, 1975). The movement of two nuclei toward one another seems to be mediated by the extranuclear microtubules emanating from each spindle pole body embedded within the nuclear envelope. The nuclei appear to fuse at the site of their spindle pole bodies.

Genetic studies support the notion that the microtubules and the spindle pole body play a role in nuclear fusion. There are many mutations that affect nuclear fusion; kar1-1, kar2, kar3, (Conde and Fink, 1976, Fink and Conde, 1976, Polaina and Conde, 1982), tub2 (Thomas, 1984, Huffaker et al., 1988), cdc4, cdc37 (Dutcher and Hartwell, 1982), bik1 (Berlin, personal communication), spa1 (Snyder and Davis, 1986), etc.. Most of these genes appear to be involved in microtubule or spindle pole body function. Rose and Fink (1987) have shown that the KAR1 gene is required for the normal function of the intranuclear and extranuclear microtubules. Recent indirect immunofluorescence experiments have shown that the KAR1::lacz protein fusions are localized at a site near the spindle pole body, suggesting that the KAR1 gene product is likely to be a component of the spindle pole body (Rose, personal communication). The finding that cold-sensitive mutations in the β-tubulin gene TUB2 (Thomas, 1984, Huffaker et al., 1988) or the anti-microtubule drug benomyl (Delgano and Conde,

1984) leads to a failure in nuclear fusion points out the critical role played by microtubules in nuclear fusion.

Because the mechanism of nuclear fusion seems to require both the spindle pole body and microtubules, mutational analysis of genes whose products interact with these structures can be used to investigate the nuclear fusion pathway. I developed a genetic approach to identify genes interacting with KAR1 with the goal of obtaining new genes involved in the nuclear fusion pathway.

Quantitative studies on the frequency of diploids in a mating show that kar1 cells are not completely defective in nuclear fusion. About 5 - 10% of kar1 zygotes in a KAR1 x kar1-1 cross can undergo nuclear fusion to form stable diploids. This low, but measurable frequency of diploid formation is the same regardless of whether both parents are kar1-1 or only one parent is kar1-1 (i.e., the mutant defect is unilateral in its effect). I have isolated mutations called kem (Kar$^-$ enhancing mutations) which reduce or abolish the residual nuclear fusion in Kar$^-$ crosses. The idea of this screen is that a mutation in a gene interacting with KAR1 or a mutation in a gene affecting other steps of the nuclear fusion pathway would intensify the kar1-1 phenotype. This strategy gets around the problem of identifying recessive mutations that affect the mating process.

MATERIALS AND METHODS

Strains, media, and genetic analysis. All yeast strains used in this study are listed in Table 2-1. [ρ^o] strains were derived by growing

Table 2-1. Yeast strains used in this study

Strain	Genotype	Source
JK77	MATa ura3 leu1 ade2 can1 cyh2	This work
JK78	MATa ura3 ade2 can1 cyh2	This work
JK130	MATα ura3-52 his4-29 kem3 kar1-1	This work
JK132	MATα ura3-52 his4-29 kar1-1	This work
JK136	MATα ura3-52 his4-29 kem3	This work
JK137	MATα ura3-52 his4-29	This work
JK156	MATα his4-29 kem1-1	This work
JK158	MATα his4-29 ade2 can1 kem1-1 kar1-1	This work
JK191	MATα ura3-52 his4-29 cyh2 kem1-5	This work
JK217	MATa trp1-1 leu2-3,112 ade2 cyh2 [ρ^o]	This work
JK218	MATa trp1-1 leu2-3,112 ade2 cyh2 kar1-1 [ρ^o]	This work
JK301	MATα ura3-52 his4-29 ade2 cry1 kem2	This work
JK302	MATα his4-29 ade2 kem4	This work
JK303	MATα ura3-52 his4-29 kem5	This work
JK304	MATα ura3 his4-29 kem4 kar1-1	This work
JK306	MATα ura3-52 lys5 kem1-1	This work
JK307	MATa ura3-52 his4-29 kem3	This work
JK308	MATa his4-29 leu2-3 lys5 kem3	This work
JK341	MATα ura3-52 his4-29 cry1 kem1-5	This work
JK342	MATα ura3-52 his4-29 leu1 cry1 kem1-5 kar1-1	This work
5916-6A	MATa his4-29	G. Fink
5916-8A	MATα his4-29	G. Fink

6947-1D	MATa leu2-3 lys1-1 met3	G. Fink
6947-2B	MATα leu2-3 lys1-1 met3	G. Fink
7523-9D	MATa leu2-3 lys1-1 kar1-1	G. Fink
7523-6A	MATα leu2-3 lys1-1 kar1-1	G. Fink
GRF128	MATα leu2-3 lys2	G. Fink
444-1C	MATα met13-25 gln1-37	L. Guarente

respiration-proficient strains in YNB + amino acids containing 10 μg/ml ethidium bromide. After overnight growth, the strains were isolated by plating on solid media and tested for growth on the nonfermentable carbon source, glycerol. A strain that has lost mitochondrial function is unable to grow on glycerol. The loss of mitochondrial DNA in the strains was determined by DAPI staining. Only nonsuppressive [ρ^o] strains were used (Dutcher, 1982). Yeast media and genetic methods are essentially those described by Sherman et al. (1974). YPG + cyh contained 3% glycerol as the sole carbon source and 3 μg/ml cycloheximide (Sigma Chemical Co.). YEPD + cry contained 1 μg/ml cryptopleurine (Chemasea Manufacturing PTY. LTD., Sydney, Australia).

Plate mating. Strains to be tested were patched on YEPD plates. Lawns of strains with an opposite mating type and complementatary auxotrophic markers were cross replica-plated with plates containing patches of the strains to be tested onto fresh YEPD plates for a brief mating. After incubation for 4 hrs at 30°C (or 5 hrs at 24°C or 3.5 hrs at 34°C) , the mating plates were replica-plated to minimal media to select for diploids.

Quantitative mass mating. This assay was performed according to a method developed by Dutcher (1982). Cells were grown to a density of 0.5 - 2 x 10^7 cells/ml. The cross was performed by filtering together 3 x 10^6 cells of each parent onto a Millipore nitrocellulose filter (0.45 μm pore, size 2.5 cm). This filter was then placed onto a YEPD plate. After incubation at 30°C (24°C or 34°C for temperature-sensitive mutations)

for 5 hrs, cells were washed off of the filter into 0.85% saline. Appropriate dilutions were plated onto YEPD plates (to measure the number of total cells), YNB plates (to measure the number of diploids) and YPG + cyh (to measure the number of cytoductants). The ratio of cytoductants to diploids describes the efficiency of nuclear fusion during mating.

Micromanipulation of zygotes. Cells were grown to a density of 0.5 - 2 x 10^7 cells/ml. 2 - 5 x 10^7 cells of each parent were centrifuged and mixed together on a YEPD plate. After incubation for 2 -3 hrs, a mating mixture was spread onto a YEPD plate. Newly formed zygotes were micromanipulated to recorded positions on the YEPD plate. When temperature-sensitive mutations were assayed for mating, the temperature of the plate during micromanipulation was maintained at 34°C by enclosing the microscope in a plastic tent heated by an airflow heater.

Staining of nuclei with DAPI. The DNA staining dye, DAPI (4',6'-diamino-2-phenylindole, Accurate Chemical Co.), was used to reveal the position of the nucleus in newly formed zygotes. Cells were prepared by the following procedure. A sample of 1 x 10^7 cells were suspended in 1 ml of Carnoy fixative (3:1, methanol:glacial acetic acid) and were allowed to fix at room temperature for 30 minutes. The cells were washed twice with 0.85% saline and resuspended in 1 ml of 1 μg/ml DAPI. Staining was performed at room temperature for 45 minutes and DAPI was washed out twice with 0.85% NaCl. The washed cells were sonicated briefly to

disrupt clumps (Dutcher, 1982). The cells were examined under a microscope with optics adjusted for fluorescence.

Isolation of mutants. Ethyl methanesulfonate mutagenesis was carried out as described by Fink (1970). A simple plate mating assay was used to score the efficiency of nuclear fusion in single colonies. Two schemes for isolating mutants are schematically diagramed in Figure 2-1. Mutagenized cells of strain JK77 ($KAR1^+$) were spread on YEPD plates such that about 200 colonies would form on each plate. After incubation at 30°C for 3 days, colonies were mated to a lawn of strain 6947-2B (KAR1) and to a lawn of strain 7523-6A (kar1-1). Mating plates were incubated at 30°C for four hours and then replica-plated onto YNB plates to select for diploids. Colonies which form diploids at the wild type level in KAR1 crosses but no diploids in kar1-1 crosses were considered putative mutants and were characterized further.

A slightly different scheme was used for some of the mutants (see results). Cells of strain JK78 (kar1-1) were mutagenized and allowed to grow up to single colonies on YEPD plates at 23°C. Colonies were mated to a lawn of strain 6947-2B (KAR1) at two different temperatures, 24°C and 34°C, for 4 hrs. After incubation, mating plates were replica-plated onto YNB plates and diploids were allowed to grow at 24°C. Colonies that formed no diploids at 34°C were picked and then screened again by examining the efficiency of zygote formation on the microscope. Only those that formed zygotes in the second screen were considered putative mutants. The percentage of bona fide mutants in this secondary screening is about 5%.

Construction of MATa/MATa or MATα/α diploids. For dominance studies and complementation testing, diploids homozygous at the mating type locus were constructed by a procedure that uses the cry1 mutation to select for mitotic recombinants cry1/cry1 from CRY1/cry1 (Figure 2-4). Crosses were performed in such a way that diploids are heterozygous for the cry1 marker which is tightly linked to the MAT locus. Colonies resistant to cryptopleurine were selected on YEPD + cry plates and then screened for diploids able to mate.

Chromosome gel electrophoresis and hybridization method. The preparation of yeast DNA samples and orthogonal-field-alternation gel electrophoresis for separating chromosomes were performed as described by Carle and Olson (1985). The chromosomal DNA was released from yeast spheroplasts that had been emmbedded in agarose. These DNA molecules were separated on agarose gels in the presence of two alternately applied, approximately orthogonal electrical fields. The agarose gel was run at 55 mW for 18.5 hrs with switching field every 50 sec. Temperature was maintained at 4^{o}C with the pump speed set at 3. The separated DNA was transfered from the agarose gel to a nitrocellulose filter. Hybridization was done at 65^{o}C with probes labelled by nick-translation (Maniatis and et.al., 1982).

RESULTS

Isolation of kem mutants.

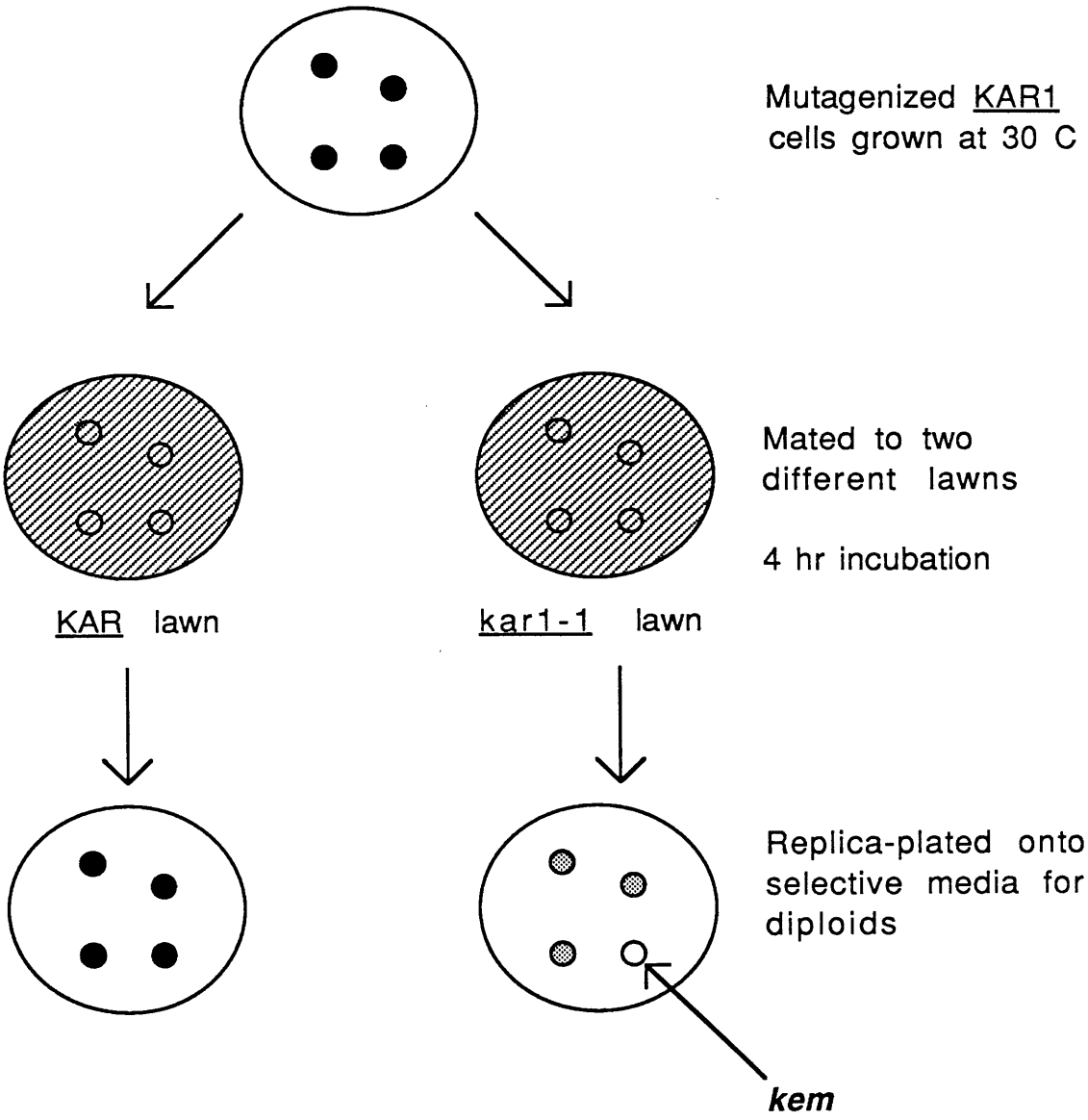
The mutation, kar1-1, prevents nuclear fusion in approximately 90% to 95% of matings. In other words, about 5% to 10% of Kar^- zygotes undergo nuclear fusion to form stable diploids. This residual nuclear fusion is easily assayed by observing the weaker growth of diploids after a four-hour plate mating. In an attempt to investigate genes involved in nuclear fusion, I have isolated new mutations called kem which reduce the residual nuclear fusion in Kar^- crosses. kem mutants were isolated by identifying strains with a partial or complete block in diploid formation in crosses to kar1-1 cells but apparently normal nuclear fusion.

I have used two strategies to isolate mutants. In one the detection lawn is Kar^- and in the other it is Kar^+. In the first scheme, I mutagenized Kar^+ cells and isolated mutants that enhance the nuclear fusion defect of cells when they are crossed to kar1-1 cells (diagrammed in Figure 2-1a). Colonies grown from mutagenized cells were mated to a lawn of Kar^+ cells and to a lawn of kar1-1 cells. After mating for 4 hr, the cells were replica-plated to media selective for diploids. Colonies that showed no diploid formation in a mating by kar1-1 but efficient diploid formation when mated by KAR were picked. In the second scheme, I mutagenized a kar1-1 strain and isolated kem kar1-1 double mutants which enhance Kar^- phenotype when crossed to KAR^+ cells (Figure 2-1b). To increase the chance that I would obtain mutations in genes for vital functions, I looked for temperature-sensitive kem mutations. Colonies

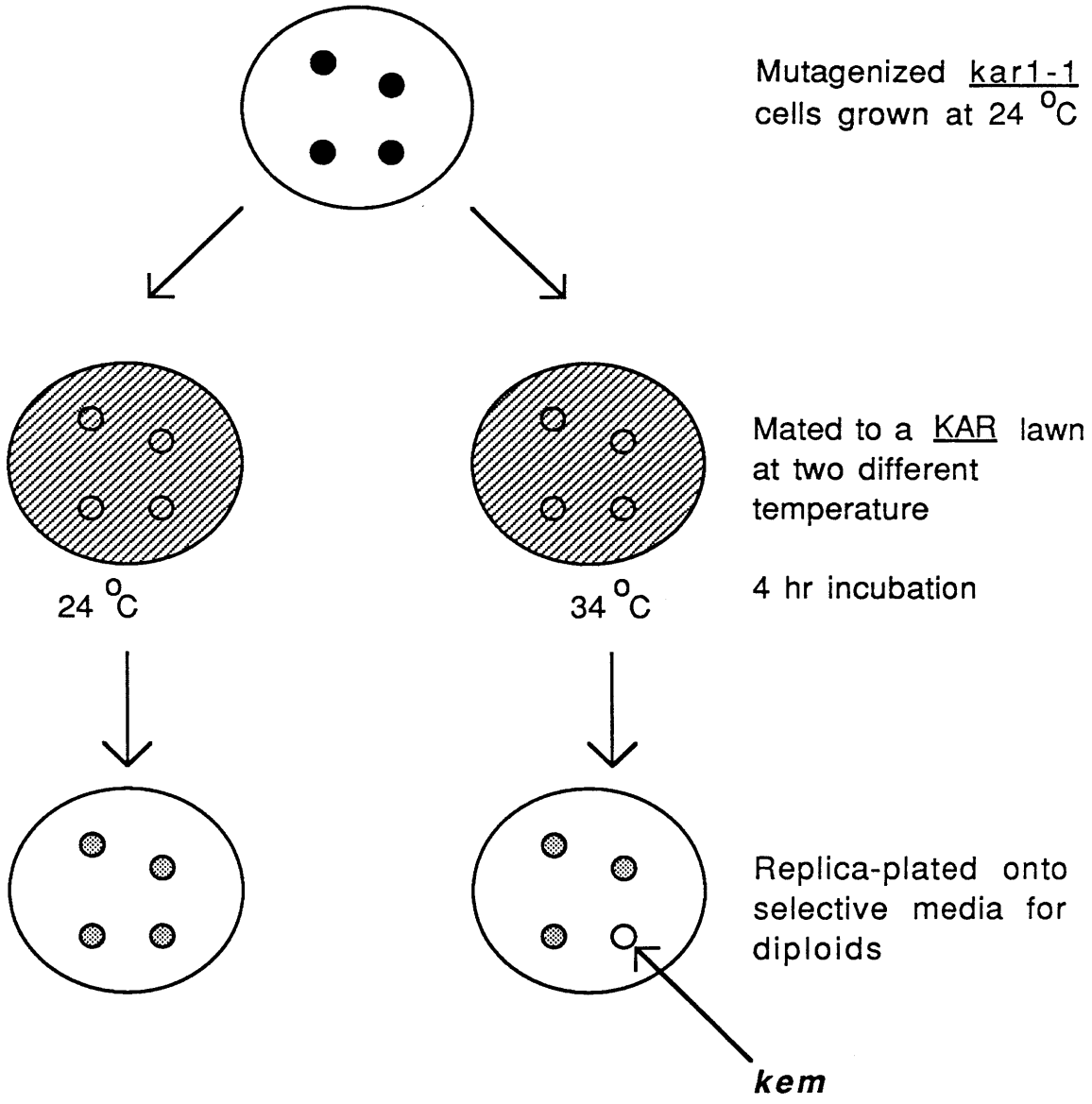
Figure 2-1. Schematic diagram describing two schemes for isolating kem mutants.

(a) Scheme I: Colonies grown from mutagenized Kar^+ cells were mated to a lawn of Kar^+ cells and to a lawn of kar1-1 cells. After mating for 4 hr, plates were replica-plated to media selective for diploids. Colonies which show no diploid formation in a kar1-1 mating but efficient diploid formation in a KAR^+ mating were picked (as indicated by an arrow). (b) Scheme II: Colonies grown from mutagenized kar1-1 cells were mated to a KAR^+ lawn at two different temperature 24°C and 34°C. After mating for 4 hr, diploids were selected by replica-plating on to selective media. Colonies which show no diploid formation only at 34°C were considered putative mutants (as indicated by an arrow).

(a) Scheme I


Mutagenized KAR1 cells grown at 30 C
Mated to two different lawns
4 hr incubation
KAR lawn
kar1-1 lawn
Replica-plated onto selective media for diploids
kem

(b) Scheme II


Mutagenized kar1-1 cells grown at 24 °C
Mated to a KAR lawn at two different temperature
4 hr incubation
24 °C
34 °C
Replica-plated onto selective media for diploids
kem

grown from mutagenized kar1-1 cells were mated to a KAR^+ lawn at two different temperatures 24°C and 34°C. After all were mated for 4 hr, diploids were selected by replica-plating on to selective media. Plates were incubated at 24°C. Colonies which failed to show diploid formation only at 34°C were considered putative mutants.

(1) kem mutations isolated in a KAR^+ strain. I isolated a set of 12 independent kem mutants by screening 18,000 EMS mutagenized cells derived from JK77 (MATa KAR1). To examine the segregation of the Kem^- phenotype of these mutants, I crossed all 12 mutants to wild type strain 5916-8A. Four of the putative mutations (kem1-1, kem1-5, kem2, and kem7) were shown to segregate 2:2 in tetrads for their Kem^- phenotype, indicating that the Kem^- phenotype is due to a single nuclear mutation.

(2) kem mutations isolated in a kar1-1 genetic background. Scheme II gave a set of 7 independent kem mutants after screening 8,000 EMS mutagenized cells derived from JK78 (MATa kar1-1). To examine the segregation of kem, these kem kar1-1 double mutants were crossed to kar1-1 strain GRF128. Four of the putative mutations (kem3, 4, 5,and 6) were shown to segregate 2:2 in tetrads for their Kem^- phenotype, indicating that the Kem^- phenotype is due to a single nuclear mutation. Because the mutations isolated by the second scheme (kem3, 4, 5, and 6) are temperature-sensitive kem, I tested the temperature-sensitive growth phenotype of these mutants. The kem3 strain failed to grow on YEPD at 34°C. The conditional-lethality and the Kem^- phenotype of kem3 cosegregated 2:2 with no recombinants between the two in at least 60 tetrads, suggesting that the temperature-sensitive phenotype of kem3 is

a consequence of the same mutation that leads to the nuclear fusion defect.

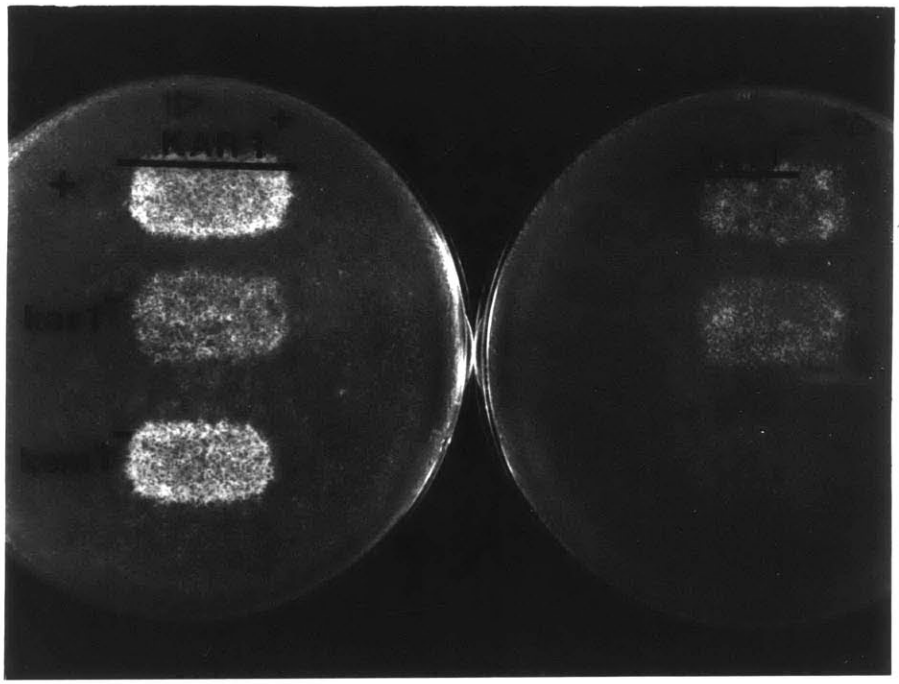
The kem3, 4, 5, and 6 mutants were isolated in a kar1-1 background. In order to assess the phenotype of these kem mutations in Kar^+ background, kem3, 4, 5, and 6 mutants were crossed to the KAR^+ strain, 5916-8A. The resulting tetrads were examined by a plate mating assay for the ability of each spore to form diploids in crosses to both KAR cells and kar1-1 cells. Since the phenotypes of kem kar1-1, KEM kar1-1, or KEM KAR were identifiable and different from each other by this mating assay, a fourth phenotypic class was assumed to be kem KAR. In each case, the kem KAR and the KEM kar1 spores could be identified, suggesting that kem and kar1 are genetically unlinked. Interestingly, the kem KAR spore formed diploids at the wild type level in KAR crosses but failed to form diploids in kar1-1 crosses. This result indicates that mutants isolated by second scheme have the same phenotype as the mutants from the first approach. Figure 2-2 shows the representative Kem^- phenotype revealed by a plate mating assay. The weak diploid formation in a KEM KAR x kar1-1 cross is drastically reduced in a kem x kar1-1 cross. The diploid formation in a kem x KAR1 cross is as efficient as that in a wild type cross.

kem enhances the nuclear fusion defect of kar1-1.

The Kar^- enhancing phenotype in screening of mutants was based on diploid formation. To verify that decreased diploid formation in kem x kar1-1 crosses is due mainly to the enhanced block in nuclear fusion rather than a defect in zygote formation or zygote viability, I

Figure 2-2. Diploid formation in crosses of kar1-1 and kem mutants as measured by a plate mating assay.

Patches of strains grown on a YEPD plate were mated to a lawn of KAR or kar1-1 cells. After incubation at 30°C for 4 hr, plates were replica-plated onto YNB plates to select for diploids. From the top, the patches are KEM,KAR (JK137), kar1-1 (JK132), and kem1-5 (JK191). The left plate is mated with a KAR lawn (6947-1D) and the right plate is mated with a kar1-1 lawn (7523-9D).



performed various assays for the Kar^- phenotype.

Failure to complete nuclear fusion would result in the formation of cytoductants, haploid progeny which contain the nuclear genotype of one parent and the cytoplasmic components of both parents. The quantitative mass mating assay measures the frequency of cytoductant formation and diploid formation in a cross. The ratio of cytoductants to diploids would indicate the efficiency of nuclear fusion during mating. As diagrammed in Figure 2-3 the cross involves a mating between a $Cyh^s[\rho^+]$ strain and a $Cyh^r[\rho^o]$ strain with selection for $Cyh^r[\rho^+]$ cytoductants on media that contain a non-fermentable carbon source and cycloheximide. Cyh^r/Cyh^s diploids do not grow on cycloheximide because Cyh^r allele is recessive. Diploids are monitored by using the complementing auxotrophic markers. Table 2-2 summarizes the results of mass mating experiments with a set of kem strains, which confirm that kem reduces the residual diploid formation of the kar1-1 mutation mainly by inhibiting nuclear fusion. The ratio of cytoductants to diploids in kar1-1 crosses is 5 - 6 (line 1,2 in Table 2-2), which is consistent with the previous report (Dutcher, 1981, Dutcher and Hartwell, 1982). In crosses of kem x kar1-1 or kem kar1-1 x KAR^+ the ratio was increased 5 - 40 fold (line 3 - 5, 8 - 11), suggesting that the kem mutations intensify the nuclear fusion defect of kar1-1. The kem strains in crosses to a wild type strain gave the same ratio as the wild type strain. Based on the data with the kem kar1-1 double mutants presented in Table 2-2, kem mutations fall into two groups; (I) those whose phenotype is the same whether the kem and kar1-1 mutations are present in the same parent or in a different parent (i.e. the ratio in kem x kar1-1 is the same as that in kem kar1-1

Figure 2-3. Diagram describing quantitative mass mating assay for measuring the frequency of cytoductant and diploid formation.

The nucleus is genetically marked with either Cyh^S or Cyh^R alleles. A cross is carried out between a Cyh^S [ρ^+] parent and a Cyh^R [ρ^o] parent. A successful nuclear fusion in a zygote produces a Cyh^S [ρ^+] diploid. A failure of nuclear fusion produces two kinds of cytoductants, Cyh^S [ρ^+] and Cyh^R [ρ^+]. YPG + Cyh plates can select for the the Cyh^R [ρ^+] cytoductants.

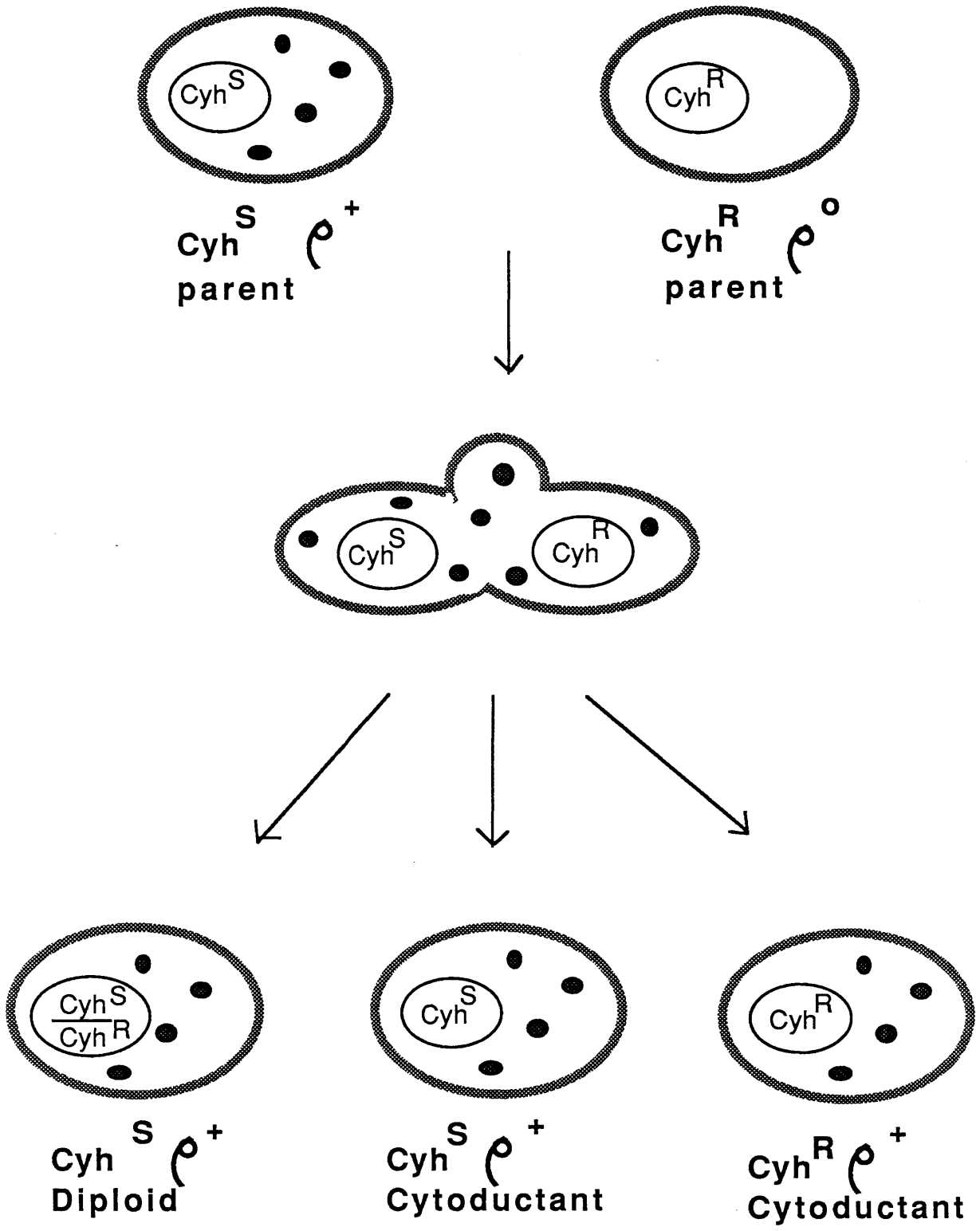

Cyh^S
Cyh^R
Cyh^S ρ+
parent
Cyh^R ρo
parent
Cyh^S
Cyh^R
Cyh^S/Cyh^R
Cyh^S ρ+
Diploid
Cyh^S ρ+
Cytoductant
Cyh^R ρ+
Cytoductant

Table 2-2. The ratio of cytoductants to diploids produced in crosses of kem and kar1-1 mutants as measured by quantitative mass matings. The frequency of cytoductant formation/the frequency of diploid formation is shown in parentheses.

	a Cyh^r [ρ^o] parent			
α Cyh^s [ρ^+] parent	KAR$^+$ (JK217)		kar1-1 (JK218)	
1. KEM KAR (JK137)	0.001	(0.0006/0.6)	5.0	(0.10/0.02)
2. kar1-1 (JK132)	5.0	(0.15/0.03)	6.3	(0.19/0.03)
3. kem1-1 (JK156)	0.005	(0.0009/0.19)	200	(0.10/0.0005)
4. kem2 (JK301)	0.001	(0.0003/0.25)	40	(0.10/0.0025)
5. kem3 (JK136)	0.007	(0.002/0.28)	26	(0.18/0.007)
6. kem4 (JK302)	0.001	(0.0005/0.50)	11	(0.22/0.02)
7. kem5 (JK303)	0.005	(0.0009/0.20)	3	(0.02/0.006)
8. kem1-1 kar1-1 (JK158)	180	(0.09/0.0005)	800	(0.08/0.00001)
9. kem3 kar1-1 (JK130)	28	(0.11/0.004)	32	(0.16/0.005)
10. kem4 kar1-1 (JK304)	60	(0.03/0.0005)	38	(0.15/0.004)
11. kem5 kar1-1 (JK305)	13	(0.013/0.001)	60	(0.06/0.001)

x KAR^+) (kem1, kem3), (II) those whose phenotype is stronger when kem kar1-1 mutations are present in the same parent (kem4, kem5). For kem5 the pheotype is observed only with kem5 kar1-1 strain.

Microscopic observation of DAPI-stained nuclei in zygotes supports the contention that kem mutations affect the nuclear fusion. Zygote formation in kem x kar1-1 or kem kar1-1 x KAR crosses was as efficient as in a wild type cross (about 15 - 20% for kem1-1, kem3, kem4, and kem5). After mating for 3 - 4 hr, cells were fixed, stained with DAPI, and observed in the fluorescence microscope. The number of zygotes with a single nucleus and the number of zygotes with two nuclei unfused were counted. The results shown in Table 2 -3 suggest that the residual nuclear fusion of kar1-1 crosses is reduced in kem x kar1-1 or kem kar1-1 x KAR crosses.

Another way of assaying the Kar^- phenotype is to isolate individual zygotes from a mating mixture by micromanipulation. The resulting zygotic clones formed on YEPD rich media are then analyzed for the genotype of the constituent cells. Micromanipulation permits the investigation of the results of individual conjugation events and confirmation that the heterocaryons observed on the microscope give rise to cytoductant clones after subsequent mitotic growth. Results from micromanipulation with strains carrying kem1-1, kem1-5, and kem3 are shown in Table 2-4. All of the zygotes in crosses kem x kar1-1 or kem kar1-1 x KAR resulted in the formation of cytoductant clones, supporting the conclusion that the kem mutations (kem1 and kem3) eliminate the residual nuclear fusion present in kar1-1 crosses. A certain portion of the micromanipulated zygotes gave rise to a diploid sector in

Table 2-3. Efficiency of nuclear fusion in crosses of kem and karl-1 mutants as measured by DAPI-staining of zygotes. Numbers indicate the percentage of zygotes with a single nucleus. The number of total zygotes examined are shown in parentheses.

	MATa [ρ^o] parent	
MATα [ρ^o] parent	KAR^+ (JK217)	karl-1 (JK218)
KEM KAR (JK137)	98 (197)	16 (118)
karl-1 (JK132)	15 (213)	14 (79)
kem1-1 (JK156)	90 (136)	0 (205)
kem3 (JK136)	100 (125)	1 (139)
kem1-1 karl-1 (JK158)	0 (139)	0 (62)
kem3 karl-1 (JK130)	0 (109)	0 (48)
kem4 karl-1 (JK304)	0 (52)	-
kem5 karl-1 (JK306)	0 (75)	-

Table 2-4. Efficiency of diploid formation in crosses of kem and kar1-1 mutants measured by micromanipulation of zygotes. Numbers indicate the percentage of diploid zygotic clones. The total number of viable zygotes analyzed is shown in parentheses.

	MATa Cyh^r [ρ^o] parent	
MATα Cyh^s [ρ^+] parent	KAR$^+$ (JK217)	kar1-1 (JK218)
KEM KAR (JK137)	98 (57)	2 (138)
kar1-1 (JK132)	7 (125)	3 (71)
kem1-1 (JK156)	90 (79)	0 (178)
kem1-5 (JK341)	100 (75)	0 (56)
kem3 (JK136)	100 (40)	0 (55)
kem1-5 kar1-1 (JK342)	0 (74)	
kem3 kar1-1 (JK130)	0 (48)	

cytoductant colonies. These diploids were probably a result of mating events between progeny cytoductants that grew out of the original zygote.

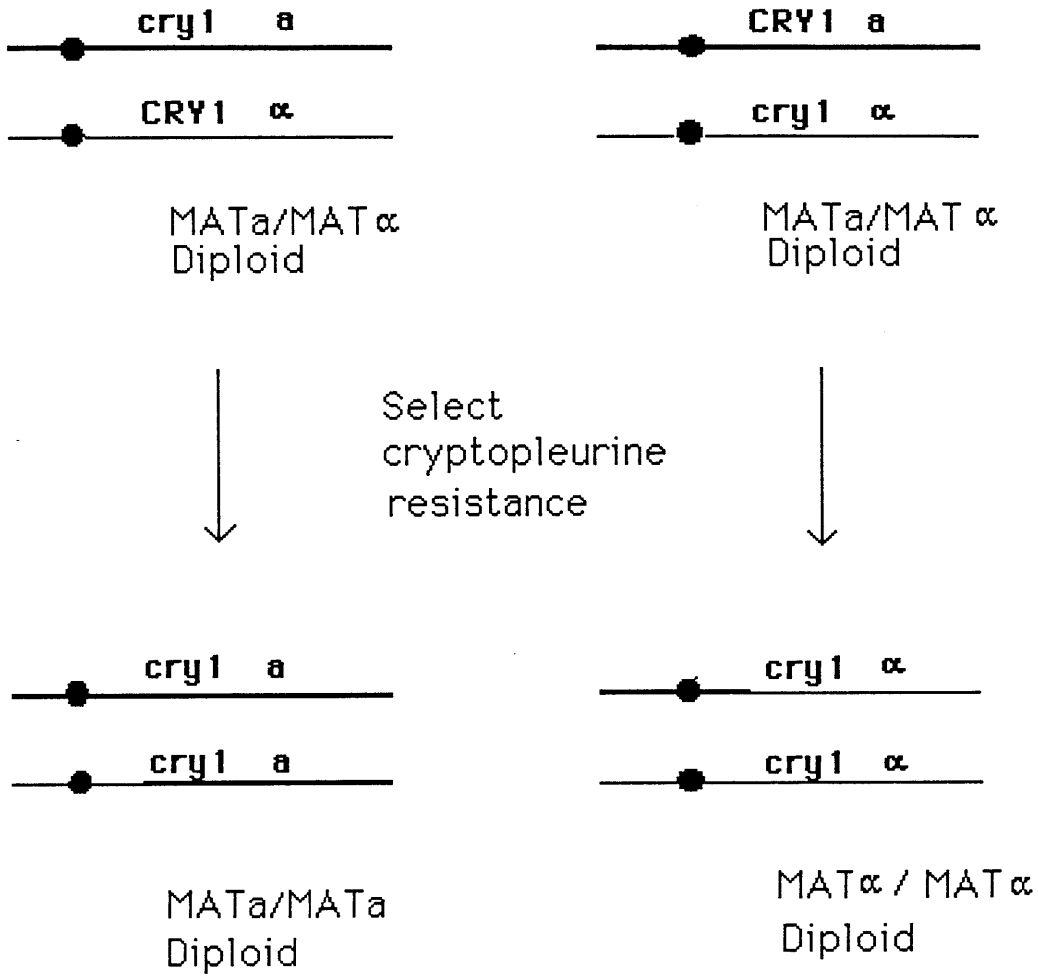
Dominance-recessiveness and complementation test.

To assess the dominance-recessiveness relationships for each of the kem mutations, I carried out crosses between a set of kem mutants and a KEM strain harboring a cry1 allele. The cry1 marker, which is tightly linked to the MAT locus, was used to construct diploids homozygous for the mating locus. In a cross of CRY1 x cry1, MATa/MATα diploids isolated are heterozygous for the cry1 marker. Mitotic recombinants (cry1/cry1) which are resistant to cryptopleurine were selected on YEPD + cry (1 μg/ml) plates and subsequently screened for diploids homozygous at the MAT locus (see Figure 2-4 for details). The Kem$^-$ phenotype of each of these diploids was determined by plate mating assay. 7 strains (kem1-1, kem1-5, kem2, kem3, kem4, kem5, and kem6) tested showed recessiveness.

Complementation tests were performed among four recessive mutations (kem1-1, kem1-5, kem2, and kem3) to define complementation groups. For each of these mutations, mutant strains carrying a cry1 allele were constructed by crosses. The kem strains were intercrossed in such a way that resulting diploids would be heterozygous for the cry1 marker. Diploids homozygous at the MAT locus were isolated as mitotic segregants as described earlier. In this test kem1-1 and kem1-5 failed to complement each other for the Kem$^-$ phenotype and kem2 and kem3 complemented kem1-1, kem1-5, and each other, suggesting that there are

Figure 2-4. Genetic method for constructing diploids homozygous for the mating type locus.

To construct a MATa/MATa diploid, a strain whose genotype is MATa cry1 is crossed to a MATα strain. This diploid heterozygous for both cry1 and MAT is sensitive to cryptopleurine. Cells resistant to cryptopleurine are often recombinants of the genotype, MATa/MATa. Because the cry1 locus is tightly linked to the MAT locus, the frequency of coconversion of two loci among crypropleurine resistant cells is high. MATα/MATα diploids are constructed by selecting for Cry^r in diploids obtained from a cross of MATα cry1 x MATa CRY1.


cry1 a
CRY1 α
MATa/MATα
Diploid
CRY1 a
cry1 α
MATa/MATα
Diploid
Select
cryptopleurine
resistance
cry1 a
cry1 a
MATa/MATa
Diploid
cry1 α
cry1 α
MATα / MATα
Diploid

at least three complementation groups and kem1-1 and kem1-5 are functionally identical.

Mapping of KEM1 and KEM3.

Both KEM1 and KEM3 were mapped to the left arm of chromosome VII by hybridization to whole yeast chromosomes separated by electrophoresis (Carle and Olson, 1985). Full length chromosome DNA molecules from yeast cells are separated by an orthogonal-field-alteration electrophoresis, transfered to a nitrocellulose filter, and hybridized with a radioactively labeled probe specific to KEM1 or KEM3, respectively. I used a 3.0-Kb PvuII fragment containing a part of KEM1 gene and a 2.0-Kb ClaI-PvuII fragment containing KEM3 gene for making probes for this study (cloning of KEM1 is described in detail in Chapter 3 and KEM3 in Appendix I). For gels of intact yeast chromosomes, I used a set of yeast strains carrying a fragment of chromosome VII (chromosome VII was fragmented at the centromere) so that I could determine to which arm of chromosome VII these genes are located.

To confirm this assignment genetically and to determine the map location of these genes more precisely, I carried out crosses involving known markers on the left arm of chromosome VII and analyzed the resulting tetrads. Mapping data presented in Table 2-5 establish the gene order and map distances (centimorgans) as follows: Cen V - Met 13 - (16 cM) - KEM3 - (18 cM) - Lys 5 - (13 cM) - KEM1 (Figure 2-5). KEM1 and KEM3 are genetically linked, but they are independent KEM genes as suggested by complementation tests.

Table 2-5. Mapping Data

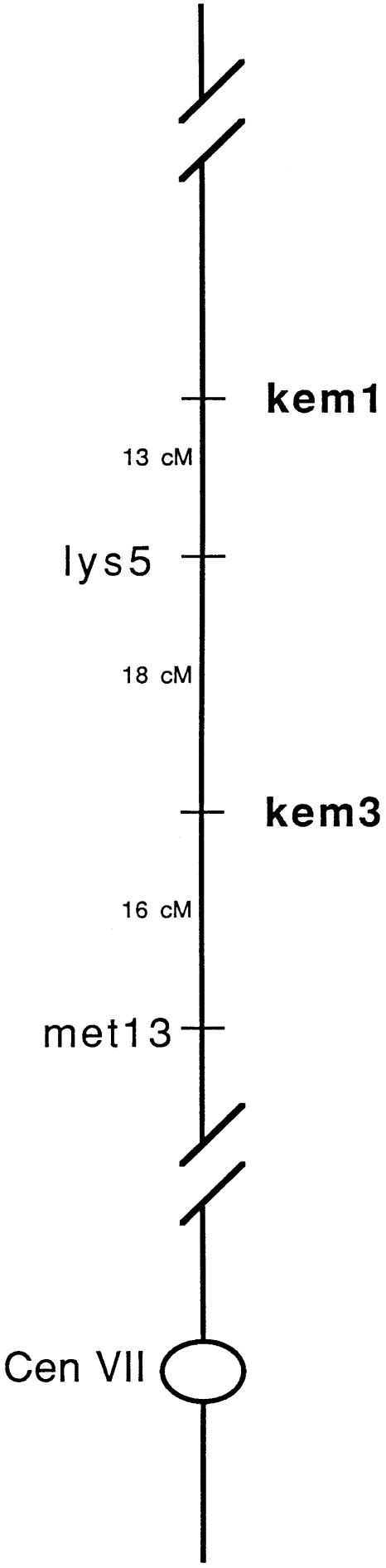
Gene pair	Segregation (no. of tetrads)[a]			Map distance[b]
	PD	NPD	TT	
kem1 - *lys5*	25	0	9	13
lys5 - *kem3*	82	1	38	18
kem1 - *kem3*	8	1	7	40
kem3 - *met13*	32	0	15	16

a. PD, parental ditype; NPD, nonparental ditype; TT, tetratype

b. The map distances were calculated according to Mortimer and Shild (1981).

Figure 2-5. Map location of KEM genes.

KEM1 and KEM3 are located on the left arm of the chromosome VII.


kem1
13 cM
lys5
18 cM
kem3
16 cM
met13
Cen VII

DISCUSSION

Eight kem mutations were isolated that reduce the residual nuclear fusion in kar1-1 crosses. These mutations define at least three genes KEM1, 2, and 3. The residual nuclear fusion occurring in 5 - 10% of kar1-1 zygotes is an interesting and provoking characteristic. I propose several explanations for this question. First, the simplest explanation would be that the kar1-1 mutation is leaky. The finding that KAR1 is an essential gene (Rose and Fink, 1987) favors this interpretation because kar1-1 cells are perfectly viable without any detectable defect in the mitotic cell cycle. However, temperature-sensitive alleles of KAR1 constructed by in vitro mutagenesis show that the Kar^- phenotype of these mutations at the nonpermissive temperature is less severe than that of the kar1-1 mutation (Rose, personal communication). Since the original scheme for isolating kar mutations demands normal mitotic division of the mutated nucleus (Conde and Fink, 1976), the kar1-1 mutation is likely to be a missense allele with a defect limited to the nuclear fusion.

A second explanation is that perhaps there are parallel pathways for nuclear fusion. A cooperative action of these pathways facilitates a successful nuclear fusion event. As an example for this model, I postulate that several different structures around the spindle pole body region serve as the initial fusion site. The kar1-1 mutation destroys one of these and leaves the other structures still functional. Based on electron microscopic observations, Byers group (Byers and Goetsch., 1974, 1975) have pointed out the essential roles of the spindle pole

body during nuclear fusion including being the initial fusion site. Evidence has been accumulated for the possibility that the KAR1 gene encodes a component of the spindle pole body. Work of Rose and Fink (1987) indicates that KAR1 gene products are required for the spindle pole body function. The KAR1::lacz protein fusions stain a specific structure near the spindle pole body in indirect immunofluorescence experiments (Rose et al., 1987).

A third explanation for the residual nuclear fusion in kar1-1 crosses is that the KAR1 gene products function as a regulatory component of nuclear fusion processes. In the absence of KAR1 function, nuclei may fuse at a basal level but the process is not as efficient. Rose et al. (1986) have shown that nuclear fusion is not a passive process nor a constitutive function of the nucleus, but requires activation by mating factors. The cell cycle block by α-factor is at the point prior to spindle pole body duplication in G1 phase (Byers and Goetsch, 1975). This spindle pole body structure persists during conjugation. The regulatory function of KAR1 protein could be for maintaining the appropriate arrangement of the spindle pole body during fusion processes.

The nuclear fusion of kem mutants in crosses to Kar^+ strains is as efficient as that in wild type crosses. The effects of kem mutations on nuclear fusion is seen in crosses involving kar1-1 cells. A preliminary analysis with kem1 and kem3 mutants indicate that these kem mutation do not enhance the nuclear fusion defect in kar2 crosses. A group of mutations other than kar1-1 have been identified to cause the Kar^- phenotype. These include kar2, kar3, a few cdcs, tub2, and bik1. Whether

kem mtations isolated are specific to the kar1-1 mutation or they affect other Kar$^-$ mutations as well remains as an interesting question. Allele specificity is also worth investigating.

Another interesting feature of kem mutations is that they are, like kar1-1, unilateral in their effects; when one parent in a kar1-1 cross carries a kem mutation (for example, kem KAR1 x KEM kar1-1 or kem kar1-1 x KEM KAR1), the kem mutation enhances the Kar$^-$ phenotype of kar1-1. As for the unilateral pattern of kar1-1, Fink and Conde (1976) suggested a "catena" model, according to which the KAR1 gene acts prior to cell fusion to construct a functional nucleus. Once the chain of developmental events leading to the functional nucleus is completed, the presence of the KAR1$^+$ gene product is unable to rectify the kar1-1 defect. This model has been supported by the subsequent work of Dutcher and Hartwell (1983). The KEM genes, like KAR1, may act prior to cell fusion.

The interaction of kem mutations with the kar1-1 mutation showed two patterns (based on the results of quantitative mass mating analysis of kem mutants and kem kar1-1 double mutants). The criterion is whether kem and kar1-1 mutations need to be in the same parent or not in order to generate the phenotype. In type I (kem1 and kem3) the effect was independent of the kar1-1 parent, i.e. the Kem$^-$ phenotype was the same whether the cross was kem x kar1-1 or kem kar1-1 x KAR$^+$. In type II (kem4 and kem5) the effect was dependent on kar1-1 parent, i.e. the phenotype was stronger in a kem kar1-1 x KAR$^+$ cross than in a kem x kar1-1 cross. I propose various models to interpret the interactions of kem mutations with kar1-1; both type I and type II are considered. The

first model is that the KEM gene products interact with the KAR1 proteins and modulate their proper function or organization. Mutations in the KEM genes affect these interactions leading to the formation of the altered KAR1 proteins. The defect of kem mutations in type I affects both wild type KAR1 proteins and defective kar1-1 proteins (assuming that the kar1-1 proteins are produced and present in cell). Either the altered KAR1 proteins together with kar1-1 proteins from the other parent (in kem x kar1-1 crosses) or the altered kar1-1 proteins (in kem kar1-1 x KEM KAR1 crosses) generate a stronger nuclear fusion defect. The altered KAR1 proteins with the wild type KAR1 proteins such as in kem x KAR^+ crosses would lead to normal fusion. In case of type II the kem mutation only affect kar1-1 proteins. Therefore, kem and kar1-1 need to be in the same parent to produce the effect. Alternatively the KEM gene products themselves are components of the nuclear fusion apparatus. The kem defect leads to a failure of nuclear fusion that is additive to that of kar1-1. In the presence of the functional KAR1-mediated step, the kem defect is not detected (in kem x KAR crosses, nuclear fusion is normal).

The interpretations concerning the interaction of the kem mutations with kar1-1 or the effects of kem mutations on nuclear fusion could be very informative and useful for investigation of the KEM genes. In following chapters, charaterization of KEM genes will be described in order to understand their roles in nuclear fusion pathway or in other cellular processes.

Chapter 3

keml mutations cause a defect in microtubule and spindle pole body function and in the cellular response to nutritional conditions.

INTRODUCTION

I have described the isolation of a set of Kar$^-$ enhancing mutations (kem) in chapter 2. The genetic interaction of these mutations with the kar1-1 mutation, which produces a more severe defect in nuclear fusion during conjugation opens a series of questions on the cellular functions of KEM genes independent of KAR1. The KAR1 gene which was originally identified as the kar1-1 mutation is required for both nuclear fusion and the mitotic cell cycle (Conde and Fink, 1976, Rose and Fink, 1987). The analysis on various kar1 mutations using electron microscopy and indirect immunofluorescence suggests that KAR1 is required for normal function of microtubules and spindle pole bodies during these processes (Rose and Fink, 1987). Therefore, it is of interest to investigate KEM genes with regard to microtubule, microtubule-associated protein, or spindle pole body function during conjugation or the mitotic cycle.

In Saccharomyces cerevisiae, the conjugation cycle is coordinated with the mitotic cell cycle. When mitotically growing haploid cells of opposite mating types are mixed, cells become arrested at the G1 phase of the cell cycle by the mating pheromone a- or α-factor and then proceed sequentially through cell fusion followed by nuclear fusion (see review by Thorner, 1981). Immediately after nuclear fusion, the resulting zygotic nucleus begins to divide entering the mitotic cell cycle. Efficient switching between the mitotic and the conjugation cycle appears to be correlated with the temporal organization of major structural components participating in these cycles such as microtubules and spindle pole body. The organization of microtubules and spindle pole

body during the cell cycle and the conjugation cycle has been extensively studied using electron microscopy and indirect immunofluorescence (Byers and Goetsch, 1974, 1975, Adams and Pringle, 1984, Kilmartin and Adams, 1984). These studies suggest that microtubules and spindle pole body affect both the mitotic and the conjugation cycle.

In the electron microscope, the spindle pole body appears as a dense structure embedded in the nuclear envelope (Robinow and Mark, 1966). During mitosis, the spindle pole body is duplicated, separated, and transmitted to two daughter nuclei. The spindle pole body functions as a microtubule organizing center (Pickett-Heaps, 1969). The spindle pole body appears to control the microtubules which radiate from its surface. This apparent control has some experimental support. In vitro studies show that dynamic assembly of microtubules is initiated at the spindle pole body (Byers et al., 1978). Microtubules emanate from the spindle pole body into the nucleus (intranuclear) and into the cytoplasm (cytoplasmic). Cold-sensitive mutations in the β-tubulin gene TUB2 cause a defect in microtubule array. The analysis on these mutations suggests that intranuclear microtubules are required for chromosome segregation and cytoplasmic microtubules are required for nuclear migration during the mitotic cell cycle and nuclear fusion during conjugation (Thomas, 1981, Huffaker et al., 1988). Studies using anti-microtubule drug benomyl or nocodazole have also shown that microtubules are invovled in nuclear fusion during conjugation (Delgano and Conde, 1984) and nuclear migration/division during mitosis (Pringle et al., 1986).

This chapter focuses on the phenotypes caused by mutations in KEM1 as a route to understanding functions of the KEM1 gene. Their effects on cellular processes involving microtubule or spindle pole body function have been investigated.

MATERIALS AND METHODS

Strains. All the yeast strains used in this study are listed in Table 3-1. Isogenic KEM1 and kem1-1 strains (JK204 and JK205) were derived from kem1-1 strain JK336 by the method of integration/popout on 5-fluoro-orotic acid medium as described by Boeke et al. (1985). In this method a segment of DNA on a plasmid is used to replace the homologous segment resident on the chromosome. The integrating plasmid pJI61 (Figure 3-4) containing the URA3 marker and the KEM1 gene was transformed into JK336 so that KEM1 could be integrated at the kem1-1 locus and popouts were isolated on 5-fluoro-orotic acid medium. Since kem1-1 is hypersensitive to benomyl, the KEM1 colonies could be identified by their relative benomyl resistances. Isogenic KEM1 and kem1-5 strains (JK190 and JK191) were derived from kem1-5 strain JK335 by the same method. Even though each pair of KEM1 and kem1 strains are isogenic, the kem1-1 and kem1-5 strains (JK205 and JK191) resulting from these constructions are not isogenic. Isogenic KEM1 and kem1 null (kem1::URA3) strains were derived by replacing the wild type KEM1 segment on the chromosome with a kem1 disrupted copy by gene replacement (Rothstein, 1983). A linear BamHI-XhoI DNA fragment of pJI90 (Figure 3-4) carrying a disrupted gene was transformed into KEM^+ strain

Table 3-1. Yeast strains used in this study

Strain	Genotype	Source
JK147	MATa ura3-52 leu2-3,112 trp1-1 ade2 cyh2	This work
JK161	MATa ura3-52 trp1-1 leu2-3,112 kem1-1	This work
JK190	MATα ura3-52 his4-29 cyh2	This work
JK191	MATα ura3-52 his4-29 cyh2 kem1-5	This work
JK196	MATα ura3-52 his4-29 cyh2 [ρ^o]	This work
JK197	MATα ura3-52 his4-29 cyh2 kem1-5 [ρ^o]	This work
JK200	MATa/MATα ura3-52/ura3-52 trp1-1/trp1-1 lys2-801/lys2-801	This work
JK204	MATα ura3-52 his4-29	This work
JK205	MATα ura3-52 his4-29 kem1-1	This work
JK219	MATα trp1-1 ade2 cyh2 [ρ^o]	This work
JK237	MATα ura3-52 his4-29 leu2 kem1-1 bcy1	This work
JK245	MATα ura3-52 his4-34 leu2-3,112 kem1::URA3	This work
JK248	MATa ura3-52 leu2-3,112 trp1-1 ade2 cyh2 kem1::URA3	This work
JK251	MATα ura3-52 his4-34 leu2-3,112	This work
JK310	MATα his4-29 cyh2 kem1-1 [ρ^o]	This work
JK311	MATa his4-29 cyh2	This work
JK312	MATa his4-29 cyh2 kem1-1	This work
JK313	MATα his4-29 cyh2 kem1-5 [ρ^o]	This work
JK314	MATa leu1 ade2 kem1-5	This work
JK315	MATa leu2-3,112 his1 can1	This work

JK316	MATa leu2-3,112 his1 can1 kem1-5	This work
JK326	JK334/F762	This work
JK327	JK333/F762	This work
JK328	JK332/F762	This work
JK329	JK333/JK161	This work
JK330	JK335/JK316	This work
JK331	JK332/JK161	This work
JK332	MATα leu2-3,112 his1 can1 kem1-5	This work
JK333	MATα leu2-3,112 his1 can1 kem1-1	This work
JK334	MATα leu2-3,112 his1 can1	This work
JK335	MATα ura3-52 his4-29 cyh2 kem1-5	This work
JK336	MATα ura3-52 his4-29 kem1-1	This work
JK340	MATα his4-29 cyh2 kem1-1	This work
5916-6A	MATa his4-29	G. Fink
F760	MATa ura3-52 trp1-1 lys2-801	J. Thomas
F762	MATa ura3-52 trp1-1	J. Thomas
RA1-13D-R	MATa ura3 leu2 his3 trp1 bcy1	K. Matsumoto

JK147 to construct kem1::URA3 strain JK248. Strain JK251 was transformed with the same DNA fragment to construct strain JK245.

[ρ^o] strains were derived by growing of respiration-proficient strains in YNB + amino acids containing 10 μg/ml ethidium bromide. After overnight growth the strains were isolated by plating on solid media and tested for growth on the nonfermentable carbon source, glycerol. The loss of mitochondrial DNA in [ρ^o] strains was determined by DAPI staining. Only nonsuppressive [ρ^o] strains were used (Dutcher, 1982). Escherichia coli HB101 (Boyer and Roulland-Dussoix, 1969) was used for bacterial transformation and plasmid growth.

Media and genetic analysis. Yeast media, methods of crosses and tetrad analysis were essentially as described by Sherman et al. (1974). YPG + cyh contained 3% glycerol as the sole carbon source and 3 μg/ml cycloheximide (Sigma Chemical Co.). Benomyl plates were made by adding slowly measured amounts of the benomyl stock solution (10 mg/ml in dimethyl sulfoxide, stored at -20°C) to warm YEPD medium with vigorous swirling to prevent precipitation. Benomyl was a generous gift from E. I. Dupont deMours and Co. (Inc.). Synthetic complete medium (SC) consisted of YNB media with addition of all amino acids. Canavanine medium is SC minus arginine plus canavanine sulfate (60 μg/ml). SC - His is SC medium without histidine. SC - Ura is SC medium without uracil. Nitrogen starvation media contained 0.17% Difco yeast nitrogen base w/o amino acids and ammonium sulfate plus 2% glucose. YPA is the same as YEPD except that it contained 2% potassium acetate instead of 2% glucose. Bacterial media were made as described Davis et al. (1980).

Transformation and DNA manipulation techniques. Yeast transformation was carried out by the lithium acetate method developed by Ito et al. (1983) using 50 μg per transformation of sonicated calf thymus DNA (Sigma Inc.) as carrier. Transformants were plated on SC - Ura to select plasmids. E. coli transformation was performed by the calcium chloride procedure of Mandel and Higa (1970). Rapid isolation of plasmid DNA from E. coli was done by the boiling lysis method (Holmes and Quigley, 1981). Yeast DNA was prepared essentially same as described by Boeke et al. (1985). Restriction endonuclease analysis and agarose gel electrophoresis were as described in Maniatis et al. (1982).

Plasmid constructions. Plasmids pJI43 and pJI44 were isolated from a yeast genomic library contained on YCp50, a vector carrying the URA3 gene, a yeast centromere (CEN4), and PBR322 sequences. Yeast inserts prepared by Sau3A partial digestion were inserted at BamHI site of YCp50 (This YCp50 genomic library was made and generously given by M. Rose). Construction of the plasmid pJI74 involved several steps of subcloning as follows: the 9 Kb BamHI-NruI fragment of pJI44 was inserted to the BamHI site and the NruI site of YCp50 to make pJI60. pJI60 was first digested with BamHI and the recessed 5′ ends were filled with Klenow enzyme. This linear plasmid was digested partially with PvuII and ligated to create pJI74 which now has a deletion of a 2.0 kB BamHI-PvuII fragment. A BamHI site was regenerated by this ligation. The plasmid pJI82 was constructed by inserting a 5.5 Kb BamHI-HindIII fragment from pJI74 to the BamHI site and the HindIII site of YCp50.

Plasmid pJI73 was constructed by digesting pJI60 with BstEII, filling the recessed 3′ end with Klenow, and ligating the blunt ends. The plasmid pJI91 was constructed by digesting pJI74 partially with NcoI, filling the recessed 3′ ends, and ligating the blunt ends. Plasmid pJI93 was constructed by deleting a 1.6 Kb BglII internal fragment of pJI74 after partial digestion with BglII. The integrating plasmid, pJI61, was constructed by inserting the 9 Kb BamHI-NruI fragment of pJI60 at the BamHI and NruI sites of the integrating vector, YIp5 (Botstein et al., 1979).

I constructed the gene disruption plasmid pJI90 carrying a kem1::URA3 insertion-deletion mutation: a 1.1 Kb HindIII fragment containing the URA3 gene (the 5′ overhangs were filled with Klenow enzyme) was inserted between the PvuII site and the BstEII site of pJI74 (the 5′ overhangs of BstEII-cut was filled with Klenow enzyme).

Quantitative mass mating, micromanipulation of zygotes, and staining nuclei with DAPI. See chapter 2.

Immunofluorescence. Indirect immunofluorescence was performed by the method of Adams et al. (1984) with a few modifications. A mating mixture (1 - 5 x 10^7 cells/ml) was resuspended in 10 ml of 0.1 M potassium phosphate, pH 6.5 ("P buffer") and fixed by adding 1 ml of 37% formaldehyde. After incubation at room temperature for 2 hrs, cells were centrifuged (4,000g) , washed twice with 0.1 M P buffer, washed once with 1.2 M sorbitol/0.1 M P buffer, and resuspended in 1 ml of 1.2 M sorbitol/0.1 M P buffer. 5 μl of β-mercaptoethanol and 30 μl of

zymolyase (10 mg/ml, 60K activity, from Kirin co. Japan) were added to the cell suspension to digest off the cell wall. After 1.5 hr incubation at 30°C with gentle shaking, cells were centrifuged, washed once with 1.2 M sorbitol/0.1 M P buffer, and resuspended in 3ml of 1.2 M sorbitol/0.1 M P buffer. 15μl of cell suspension was applied to a well on a polylysine coated slide (8 well Flow-labs slide). The slide was immersed in cold methanol (-20°C) for 6 minutes and into cold acetone (-20°C) for 30 seconds. The antibody reaction was carried out by adding 15 μl of 1:40 dilution of YOL1/34 (anti-tubulin antibody purchased from Accurate Chemical Co.) in BSA/ sorbitol/ P buffer (10 mg/ml BSA, 1.2 M sorbitol, 0.1M potassium phosphate, pH 6.5) to each well and incubating in a moist chamber at room temperature for 1 hr. Antibodies were washed off three times with BSA/ sorbitol/ P buffer and secondary antibody reaction was carried out by adding 15 μl of Rhodamine-conjugated anti-rat antibodies (1:500 dilution, Boehringer Mannheim Biochemicals) to each well. After incubation at room temperature in dark for 1 hr, antibodies were washed off four times with BSA/ sorbitol/ P buffer and twice with sorbitol/ P buffer. 15 μl of 1 μg/ml DAPI was added for 5 minutes to stain nuclear DNA. After a wash with sorbitol/ P buffer, slides were mounted with p-phenylenediamine/90% glycerol and examined on the fluorescent microscope.

Determination of frequencies of chromosome loss and mitotic recombination. The frequency of chromosome loss and mitotic recombination was measured in diploids by the method of Hartwell and Smith (1985). In Figure 3-3, a schematic diagram describes the assay for

chromosome loss and mitotic recombination. The configuration of genetic markers on chromosome V of each parent is indicated. Chromosome loss or recombination was signaled by the appearance of recessive resistance markers in diploids. The ura3-52 marker was included for the purpose of maintaining both chromosomes in a diploid on minimal media. Crosses were made between appropriate MATa and MATα strains, diploids homozygous or heterozugous for kem1 were isolated by streaking on minimal media. Three clones of each diploid strain from minimal media were streaked on synthetic complete medium plates and grown at 30°C to a colony of about 10^6 cells. Six to eight colonies were assayed for each diploid strain. Individual colonies were cut from the plate, resuspended in 1 ml of 0.85% saline and sonicated to disrup clumps of cells. Appropriate dilutions were made and plated onto SC media to determine the total number of viable cells and onto SC - arginine plus canavanine sulfate (60 μg/ml) to select cells that expressed the recessive can1 marker. The colonies that grew up on canavanine plate were replica-plated to SC - his plates to score His^- (chromosome loss) and His^+ (mitotic recombination).

Nitrogen starvation. Cells grown to a log phase in YEPD rich medium were centrifuged, washed, and resuspended in yeast minimal media lacking nitrogen (0.17% of Difco yeast nitrogen base w/o amino acids and ammonium sulfate plus 2% glucose). The final cell density was 1×10^6 cells/ml. After various incubation periods, samples were removed from cultures and sonicated to disperse clumps. The total number of cells as well as budded and unbudded cells were counted on the microscope. For

determination of cell viability, cells were diluted in 0.85% saline and plated on YEPD plates. Colonies were counted after incubation for 3 - 4 days at 30°C.

RESULTS

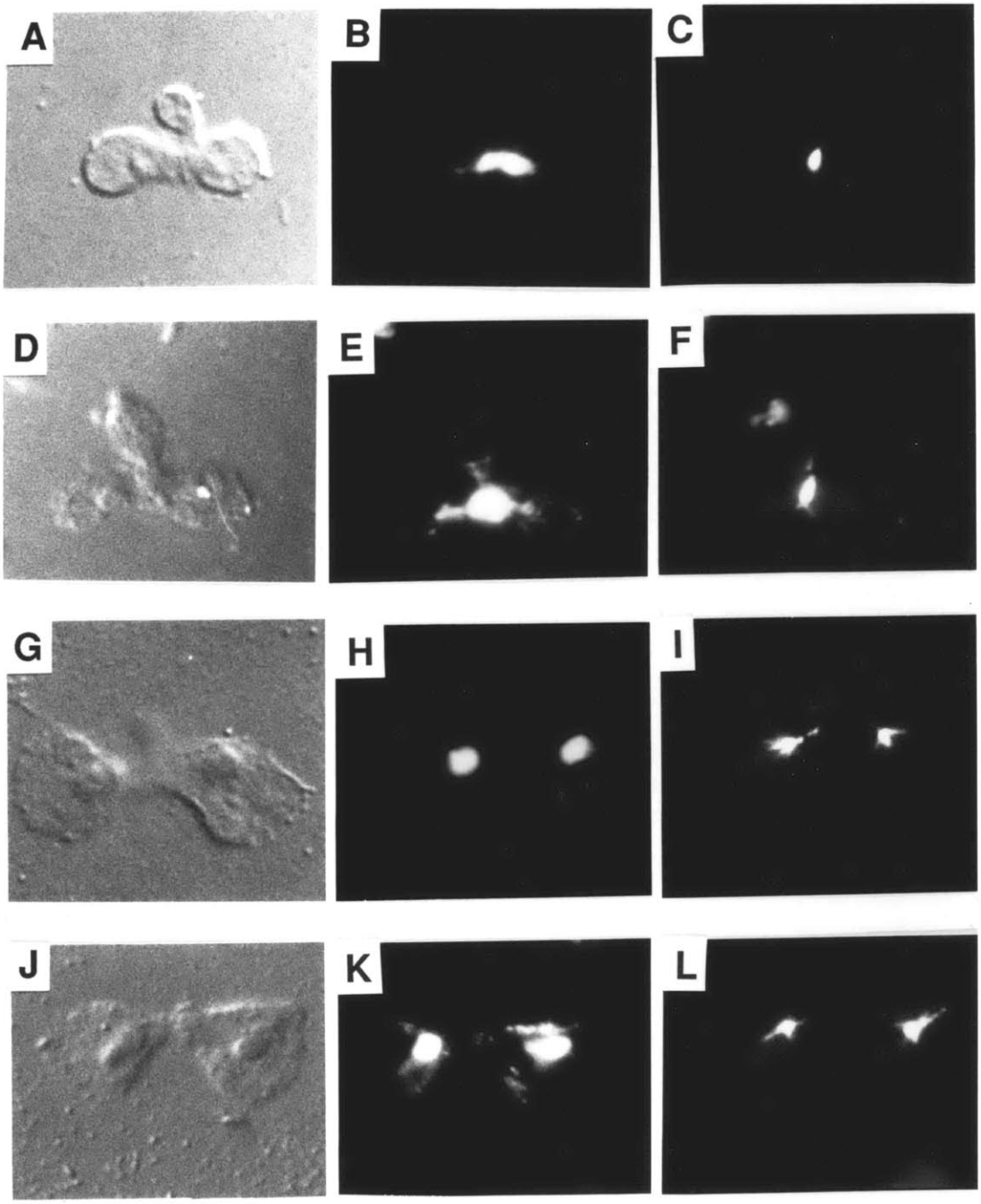
kem1 has a bilateral nuclear fusion defect.

I have investigated the effect of kem1 mutations on nuclear fusion where both parents are Kar^+. Since crosses KAR kem1 x wild type have normal nuclear fusion (see chapter 2), matings between KAR kem1 and KAR kem1 were examined. Nuclear fusion defects are characterized as one of two types: either both parents of the cross must be mutant for nuclear fusion to fail (a bilateral defect in nuclear fusion), or only one parent need be mutant for nuclear fusion to fail (a unilateral defect). The strains carrying kar1-1 show a unilateral defect and β-tubulin mutants a bilateral defect.

Light microscope observations of the nuclear DNA and microtubules in zygotes suggest that nuclear fusion is defective in a kem1 x kem1 cross, whereas nuclear fusion is normal in crosses of KEM1 x KEM1 and kem1 x KEM1. Zygotes from crosses of KEM1 x KEM1, kem1-5 x KEM1, and kem1-5 x kem1-5 were fixed, their nuclear DNA were visualized by DAPI-staining, and their microtubules visualized by indirect immunofluorescence using anti-tubulin antibody (Figure 3-1). Zygotes from the cross kem1-5 x KEM1 (panels D, E, and F) appeared similar to those from the wild type cross KEM1 x KEM1 (panels A, B, and C). Matings in these crosses resulted in a zygote with a single bright DAPI staining

Figure 3-1. Nuclear fusion defect in kem1 x kem1 crosses as revealed by DAPI-staining and antitubulin immunofluorescence.

Each three panels represent the same zygote revealed by Nomarsky optics, DAPI staining, and antitubulin staining. A - C zygote from a KEM x KEM cross (JK219 x JK311); D - F zygote from a kem1-5 x KEM1 (JK313 x JK311) cross; G - L zygotes from a kem1-5 x kem1-5 (JK313 x JK314) cross.


A
B
C
D
E
F
G
H
I
J
K
L

region and single spindle pole body (presumed to be the diploid nucleus). However, in kem1-5 x kem1-5 crosses a large number of zygotes appeared have unfused nuclei (panels G - L). Cytoplasmic microtubules often pointed toward the zygotic bud instead of toward the opposing nucleus. These results suggest that kem1 has a bilateral nuclear fusion defect. The severity of this defect was analyzed quantitatively using KEM, kem1-1, and kem1-5 strains. In each cross, a MATα [ρ^0] strain was mated to a MATa [ρ^+] strain on a Millipore nitrocellulose filter at 30°C for 3 hrs. Cells were washed off the filter, fixed, and stained with DAPI (see materials and methods). The number of zygotes with two unfused nuclei and the total number of zygotes were determined. The presence of mitochondrial DNA revealed by DAPI staining indicated that the cytoplasms mix efficiently in the zygotes. As shown in Table 3-2, approximately 20 - 30% of kem1 x kem1 zygotes fail to fuse nuclei. A few percentage of kem1 x KEM1 zygotes have two unfused nuclei. However, this was not considered to be significant since there will be a slight fluctuation in a number due to a small sample size.

Genetic evidence confirms my cytological observations of nuclear fusion defect in kem1 x kem1 crosses. Quantitative mass matings were carried out to measure the production of cytoductants versus diploids. This assay is diagramed in Figure 2-3 (see Chapter 2). A cytoductant is a haploid progeny with the nuclear genotype of one parent and the cytoplasms contributed by both parents. The cytoductant formation in a cross gives an indication that cell fusion and cytoplasmic mixing are efficient but concommitant nuclear fusion is defective. The ratio of cytoductant to diploid in kar1-1 crosses is usually in the range of

Table 3-2. Failure of nuclear fusion in crosses of kem1 mutants as measured by examining DAPI-stained nuclear DNA in zygotes.

	MATa [ρ^+] parent		
MATα [ρ^o] parent	KEM$^+$ (JK311)	kem1-5 (JK314)	kem1-1 (JK312)
KEM (JK219)	0.6 (159)	5 (56)	9 (52)
kem1-5 (JK313)	1.5 (63)	26 (54)	20 (57)
kem1-1 (JK310)	6.0 (48)	18 (72)	23 (24)

Numbers indicate the percentage of zygotes with two unfused nuclei in each cross (the number in parentheses shows the total number of zygotes examined).

2 - 5. The ratio of cytoductant to diploid was measured in crosses of KEM1 x KEM1, kem1-5 x KEM1, and kem1-5 x kem1-5 and the data are summarized in Table 3-3. In a kem1-5 x kem1-5 cross, the ratio is significantly increased, confirming our conclusion that kem1 has a bilateral nuclear fusion defect without major defects in cell fusion or cytoplasmic mixing.

kem1 mutants are hypersensitive to the antimicrotubule drug benomyl.

Yeast strains in a wild type background are resistant to benomyl up to a concentration of 20 μg/ml at 26°C on YEPD medium, but are inhibited for growth at a concentration of 40 μg/ml (Thomas and et.al., 1985). This growth inhibition is due to the fact that benomyl binds to tubulin and depolymerizes microtubules. To ask whether kem1 affects the microtubules, I examined the growth of kem1 mutants at various concentrations of benomyl in compared to KEM1 wild type strains. The results shown in Figure 3-2 indicate that kem1 mutants are hypersensitive to benomyl even at a concentration of 10 μg/ml. This hypersensitive phenotype and the kem1 mutation cosegregate 2:2 in the kem1 x KEM cross (Figure 3-2b).

kem1 cause a defect in mitotic chromosome transmission.

To study effects of kem1 mutations on microtubule function, I measured the frequency of chromosome loss in mitotically growing cells of diploid strains KEM1/KEM1, KEM1/kem1, and kem1/kem1. Chromosome V was marked with can1 conferring resistance to canavanine and a recessive auxotrophic marker his1 as shown in Figure 3-3. Each diploid strain was

Table 3-3. Ratio of cytoductant to diploid in crosses of kem1-5 mutants as measured by quantitative mass mating

Cross[a]	Relevant[b] Genotype	Cytoductant frequency	Diploid frequency	Ratio of[c] cyto/dip
JK196 x JK315	KEM x KEM	0.0008	0.45	0.002
JK196 x JK316	KEM x kem1-5	0.0009	0.28	0.003
JK197 x JK315	kem1-5 x KEM	0.001	0.31	0.005
JK197 x JK316	kem1-5 x kem1-5	0.02	0.18	0.11

a. Strain JK196 and JK197 are isogenic pairs.
Strain JK315 and JK316 are sister spores from the same cross.

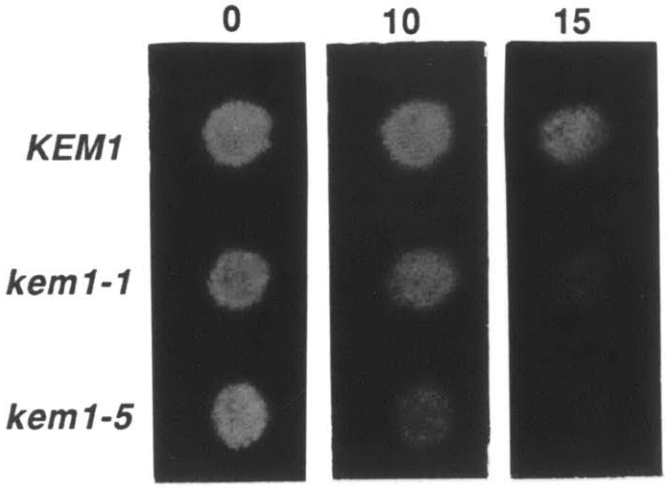
b. The cross is α Cyh^R [ρ^o] x a Cyh^S [ρ^+].

c. Numbers indicate the ratio of cytoductants to diploids in each cross.

Figure 3-2. Benomyl-hypersensitivity of kem1 strains.

(a) The growth of KEM1 (JK204), kem1-1 (JK205), and kem1-5 (JK191) strains was examined at various concentrations of benomyl (0, 10, and 15 μg/ml). (b) Segregation of benomyl-hypersensitivity in a kem1-1 x KEM1 (JK340 x 5916-6A) cross was examined. Cells were suspended in 0.85% saline solution in multi-well plate. A multi-pronged inoculating device was usedto place cell suspensions on a YEPD plate and a benomyl plate (15 μg/ml). Pictures were taken after 2 days. Tetrads arranged from top to bottom show 2:2 segregation of benomyl sensitivity.

(a)



(b)

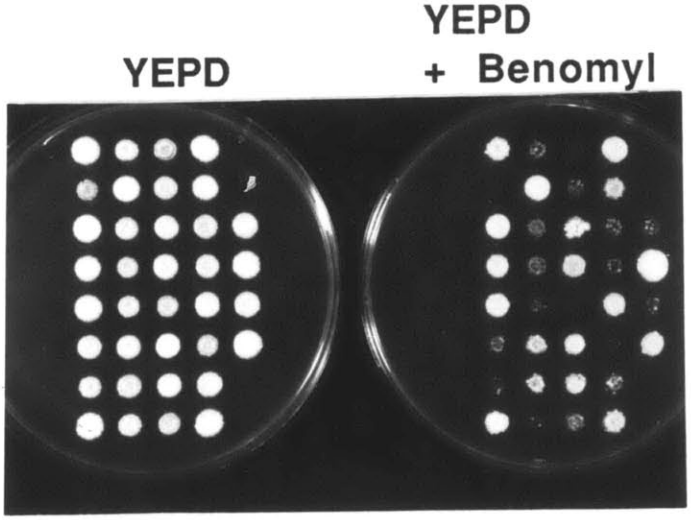
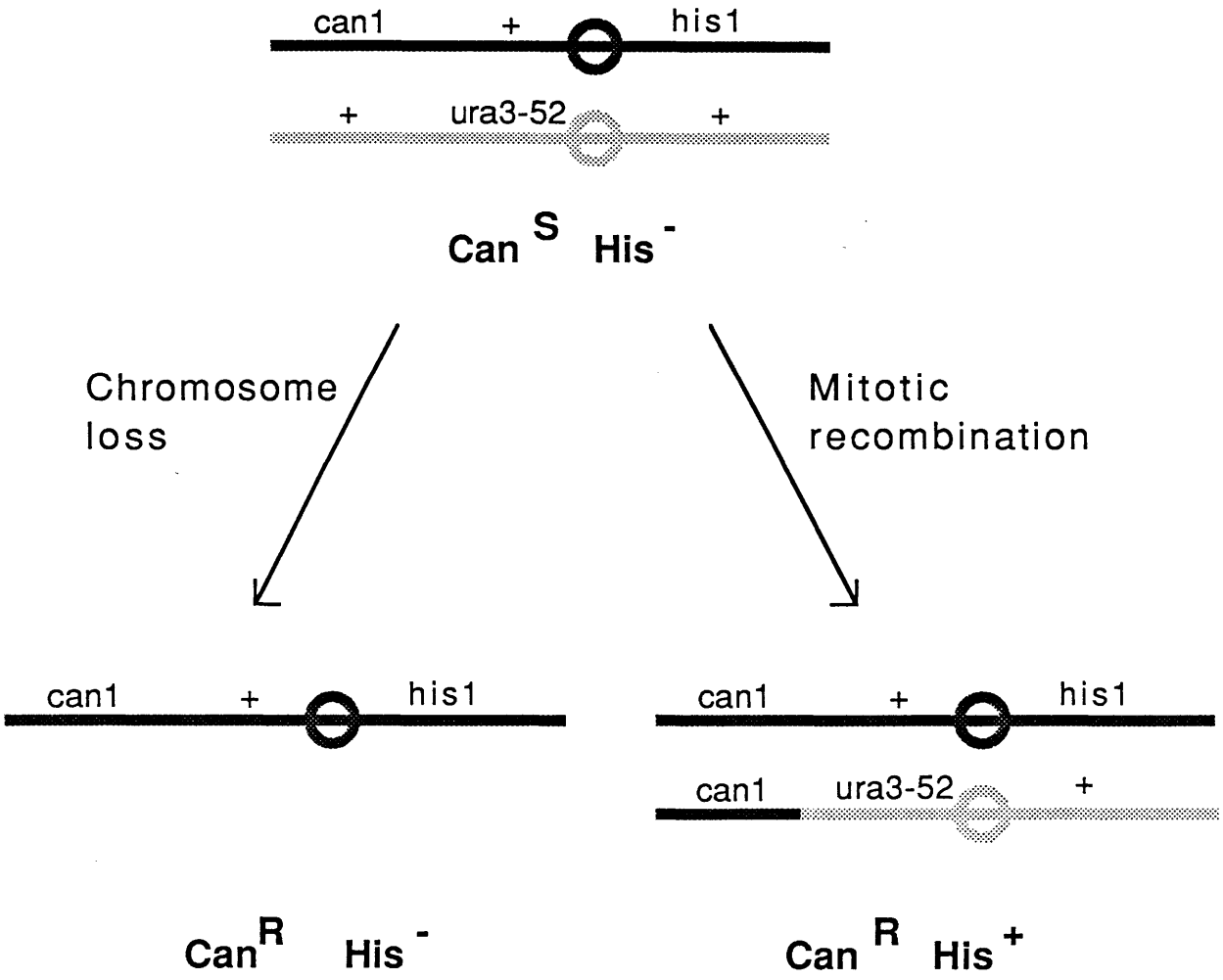


Figure 3-3. Diagram describing an assay for chromosome loss.

Chromosome V in the diploid is marked with *can1* and *his1*. *can1* is a recessive allele conferring resistance to canavanine sulfate. *his1* is a recessive histidine auxotroph marker located on the opposite arm from *can1* locus. Starting diploid strain is Can^S His^+. Loss of one homolog makes cells Can^R His^-. Mitotic recombination results in Can^R His^+ cells.


can1
+
his1
+
ura3-52
+
Can S His -
Chromosome loss
Mitotic recombination
can1
+
his1
can1
+
his1
can1
ura3-52
+
Can R His -
Can R His +

streaked out on synthetic complete medium and allowed to grow mitotically without any selection. Cells that are canavanine resistant were selected on a SC - arg + canavanine plate. A cell that is monosomic resulting from the loss of one chromosome V homologue or one that is recombinant for one arm of chromosome V will form a colony on this plate. Details of the experimental procedures are described in materials and methods. The frequency of chromosome loss and mitotic recombination was determined by an analysis of the frequency of Can^r His^- cells and Can^r His^+ cells (Table 3-4). KEM1/KEM1, KEM1/kem1-1, and KEM1/kem1-5 diploids lose chromosome V at a frequency of 1 - 3 x 10^{-5}. kem1-1/kem1-1, kem1-1/kem1-5, and kem1-5/kem1-5 diploids lose chromosome V at a frequency of 20 - 30 x 10^{-5}. These results indicate that there is about 10 -20 fold increase in the frequency of the chromosome loss in kem1 homozygous diploids and that this phenotype is recessive. The frequency of mitotic recombination in kem1/kem1 strains is almost the same as in KEM1/KEM1.

Cloning of KEM1

Since the exact nature of the kem1-1 or kem1-5 allele is not known, I decided to investigate the phenotype of a kem1 null allele constructed by gene disruption (Rothstein, 1983). For this purpose, first, I cloned the KEM1 gene. The KEM1 gene was isolated by its ability to complement the kem1-1 mutation. I examined both benomyl-hypersensitivity and the Kem^- phenotype of kem1-1 transformants for complementation. The strain JK336 (ura3-52, his4-29, leu1, kem1-1) was transformed with DNA from a

Table 3-4. Frequency of chromosome loss and mitotic recombination in kem1/kem1 diploids

Diploid	Chromosome loss[a]	Mitotic recombination[b]
KEM1/KEM1 (JK326)	1.2	2.30
KEM1/kem1-1 (JK327)	1.1	0.93
KEM1/kem1-5 (JK328)	3.2	1.61
kem1-1/kem1-1 (JK329)	22.9	1.18
kem1-5/kem1-5 (JK330)	16.4	1.87
kem1-1/kem1-5 (JK331)	27.7	1.51

Each number represents an average derived from 6 - 8 independent assays.

a. Frequency of Can^R His^- cells appearing in a single colony. Numbers indicate (the number of Can^R His^- cells)/(the total number of diploid cells) x 10^5.

b. Frequency of Can^R His^+ cells appearing in a single colony. Numbers indicate (the number of Can^R His^+ cells)/(the total number of diploid cells) x 10^4.

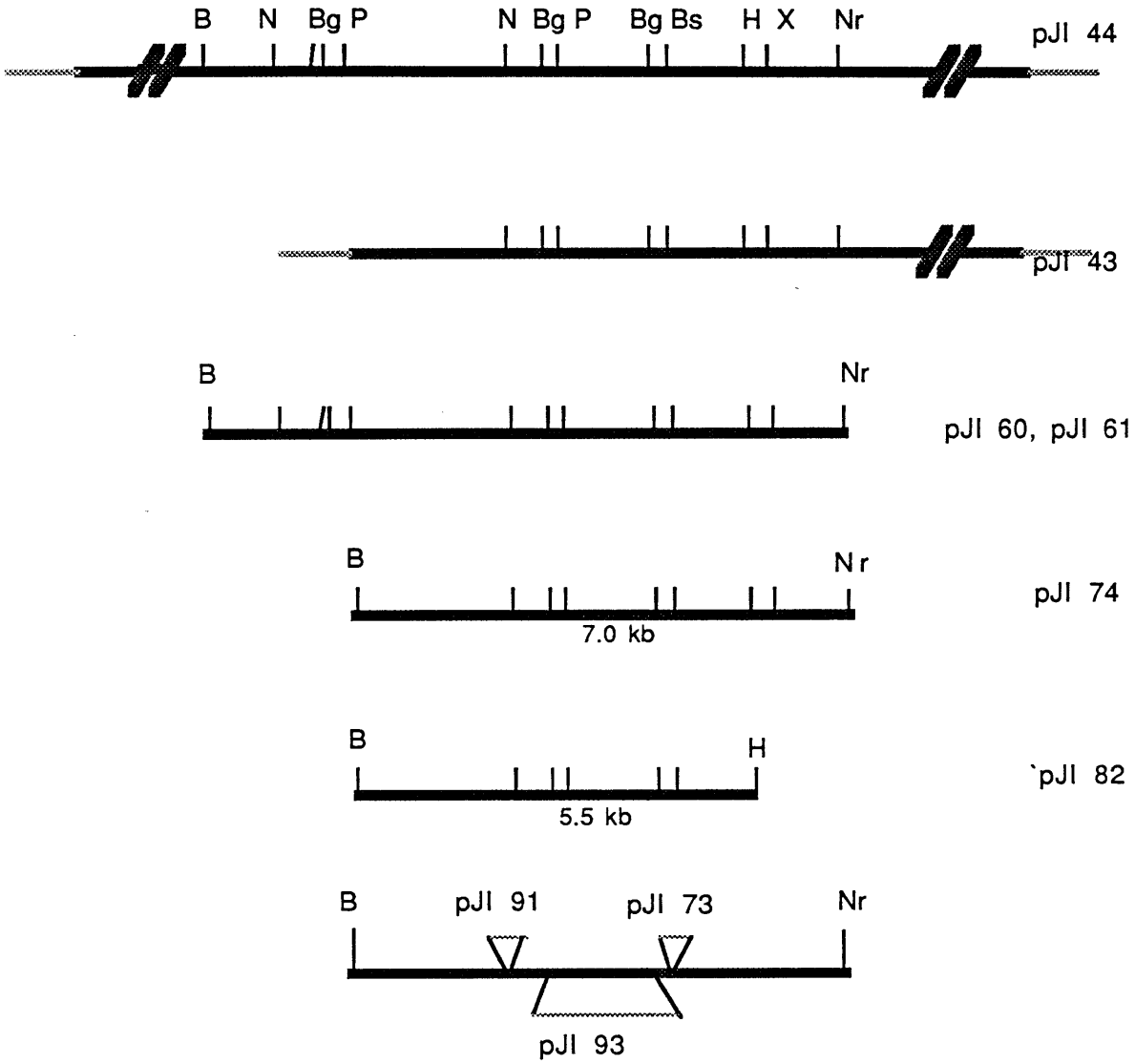
yeast genomic library contained on the YCp50 vector carrying the URA3 gene and a yeast centromere (CEN3). Ura^+ transformants were selected at 30°C and colonies were replica-plated on benomyl plates (10 μg/ml benomyl). After overnight incubation of the plates at 26°C, benomyl-resistant colonies were picked and tested for the ability to form diploids in crosses to a kar1-1 strain by a plate mating assay (examining the Kem^+ phenotype). Two of 16,000 transformants were identified as benomyl-resistant and Kem^+. Plasmids from these strains were recovered in E. coli and purified. These two isolated plasmids, pJI43 and pJI44, complemented both alleles of kem1 when used to transform kem1-1 and kem1-5 strains. Restriction endonuclease maps of pJI43 and pJI44 (Figure 3-4) show that there are about 9 Kb overlapping yeast DNA sequences. I subcloned portions of the insert into the YCp50 vector and tested for complementation of the kem1-1 mutation. The smallest fragment of DNA tested that contains full complementing acitivity is a 5.5 Kb PvuII-HindIII fragment (pJI82, Figure 3-4). Construction of frameshift mutations at a NcoI site and a BstEII site within this fragment (pJI91 and pJI73, Figure 3-4) destroyed complementing activity, as did deletion of the 1.6 Kb BglII fragment (pJI93, Figure 3-4). Therefore, NcoI, BglII, and BstEII sites are internal to the complementing gene.

To demonstrate that the cloned sequence contains the KEM1 gene, I determined whether this DNA sequence could integrate along with the plasmid vector at the KEM1 chromosomal locus by homologous recombination. A BamHI-NruI fragment was subcloned into the integrating vector YIp5 (pJI61). This vector carries the URA3 marker as well as the

Figure 3-4. DNA inserts of the plasmid vectors used in this study.

pJI44 and pJI43 are isolates from a YCp50 genomic library. The vector sequence is indicated as a light thin line at both sides of the insert. The Sau3A insert fragment is inserted at the BamHI site of YCp50. pJI74; the 7.0 kb PvuII - NruI fragment was inserted at the BamHI and NruI sites of the YCp50. The BamHI site is regenerated. pJI82; the 5.5 kb BamHI - HindIII fragment was inserted at the BamHI and HindIII sites of YCp50. pJI91 and pJI73 contain NcoI and BstEII sites filled in respectively. pJI93 contains a 1.6 kb BglII deletion.

pJI61; the 9.0 kb BamHI-NruI fragment of KEM1 is inserted at the BamHI and the NruI sites of the integrating vector YIp5 (URA3). pJI90; The boxed region corresponds to the 1.1 kb HindIII fragment containing the URA3 gene which replaces the 1.3 kb PvuII - BstEII fragment internal to KEM1.


B N Bg P N Bg P Bg Bs H X Nr
pJI 44
pJI 43
B Nr
pJI 60, pJI 61
B Nr
pJI 74
7.0 kb
B H
pJI 82
5.5 kb
B pJI 91 pJI 73 Nr
pJI 93
KEM1 (3.5 kb)
1 kb
B BamHI
Bg BglII
Bs BstEII
H HindIII
N NcoI
Nr NruI
P PvuII
X XhoI
B N Bg H X Nr
URA3
pJI 90

pBR322 sequence and can only give stable transformants by intergration into the genome. A Ura^+ transformant obtained by transforming a strain of genotype KEM1 ura3-52 (F760) with the pJI61 plasmid DNA were crossed to a strain of genotype kem1-1, ura3-52 (JK336) and to a strain of genotype kem1-5 ura3-52 (JK337). Diploids from each cross were selected and sporulated. In 20 tetrads from each cross, the Ura^+ phenotype and the benomyl-hypersensitive phenotype segregated 2:2 and all Ura^+ spores were benomyl-resistant. These results demonstrate that the cloned sequence complementing the kem1-1 mutation has been integrated at the KEM1 locus by homologous recombination and is the authentic KEM1 gene.

Disruption of KEM1 affects the mitotic cell division.

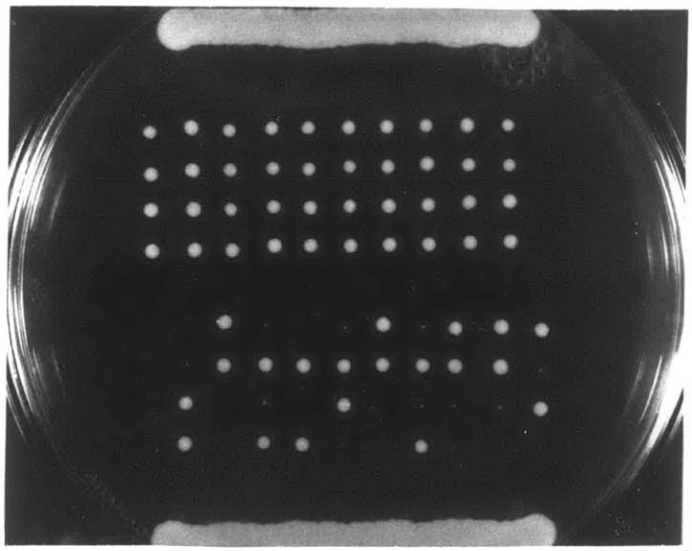
To disrupt the KEM1 gene, a simultaneous insertion-deletion mutation was created. A 1.4 Kb PvuII-BstEII internal fragment of th KEM1 gene was replaced with a 1.1 Kb HindIII fragment carrying the yeast URA3 gene (Figure 3-4, pJI90). A linear BamHI-XhoI fragment carrying the disrupted gene was used to disrupt one copy of the KEM1 gene in a diploid strain homozygous for the ura3-52 mutation (JK200). After transformations the Ura^+ diploid transformants were sporulated and tetrads dissected. All four spores derived from this diploid are viable. However, two spores in each tetrad are very slow growing. The bottom array in Figure 3-5 shows the 2:2 segregation of this slow-growth phenotype. The original Ura^- parent strain was compared as a control (upper array in Figure 3-5). The disruption marker URA3 and the slow-growth phenotype cosegregated 2:2, indicating that the slow-growth phenotype is due to the kem1 disruption. This result was confirmed by

Figure 3-5. 2:2 segregation of the slow-growth phenotype in the tetrads from +/kem1::URA3 diploids.

Tetrads from the parent diploid strain (JK200) is shown in upper array and the Ura^+ transformant in bottom array. The plate was incubated for 2 days at 30^oC.

+/+

+/*kem1::URA3*



Southern blot analysis. DNA was prepared from a parent diploid strain (JK200), a Ura^+ diploid transformant, and four spores from a tetrad and digested with BglII. The blot, probed with the 5 Kb PstI-HindIII fragment of the KEM1 gene, gave a predicted pattern (Figure 3-6). Gene disruption alters two (1.6 kb and 4.4 kb fragments) of the three BglII fragments of KEM1 present in a parent strain generating a disrupted 5.7 kb BglII fragment. The 3.0 kb BglII fragment of KEM1 remains the same. Southern blot experiments with genomic yeast DNA at high or low stringency indicate that the KEM1 gene is present as a single copy in a haploid yeast genome (data not shown). From these results we conclude that the KEM1 gene is not essential but plays an important role in spore germination and mitotic cell growth.

kem1 null mutation affects the spindle pole body duplication.

Strains carrying a kem1 null allele, kem1::URA3, exhibit altered cell morphology during mitotic cell growth. Microscopic examination of the culture shows that about 80% of kem1::URA3 cells have an elongated rod-shape and that the size of cells tends to be as twice large as wild type cells (Figure 3-7). The morphology of microtubules of mitotically growing kem1::URA3 cells was investigated in comparison to wild type cells by indirect immunofluorescence using anti-tubulin antibodies. In wild type strains, when the bud becomes half the size of the mother cell, duplicated spindle pole bodies begin to separate developing intranuclear microtubules in between. At the stage of large-budded cells, the nucleus elongates and divides into two daughter cells and long intranuclear microtubules are observed (Figure 3-8 (a)).

Figure 3-6. Southern blot analysis of total yeast DNA from a parent strain (JK200), a Ura^+ transformant, and four spores from a resulting tetrad.

The DNA was digested with BglII, separated on an agarose gel, and transferred to nitrocellulose filter. The DNA probe used for hybridization was made from a 5.0 kb PstI - HindIII fragment containing KEM1. The size and origin of the hybridizing fragments are indicated.

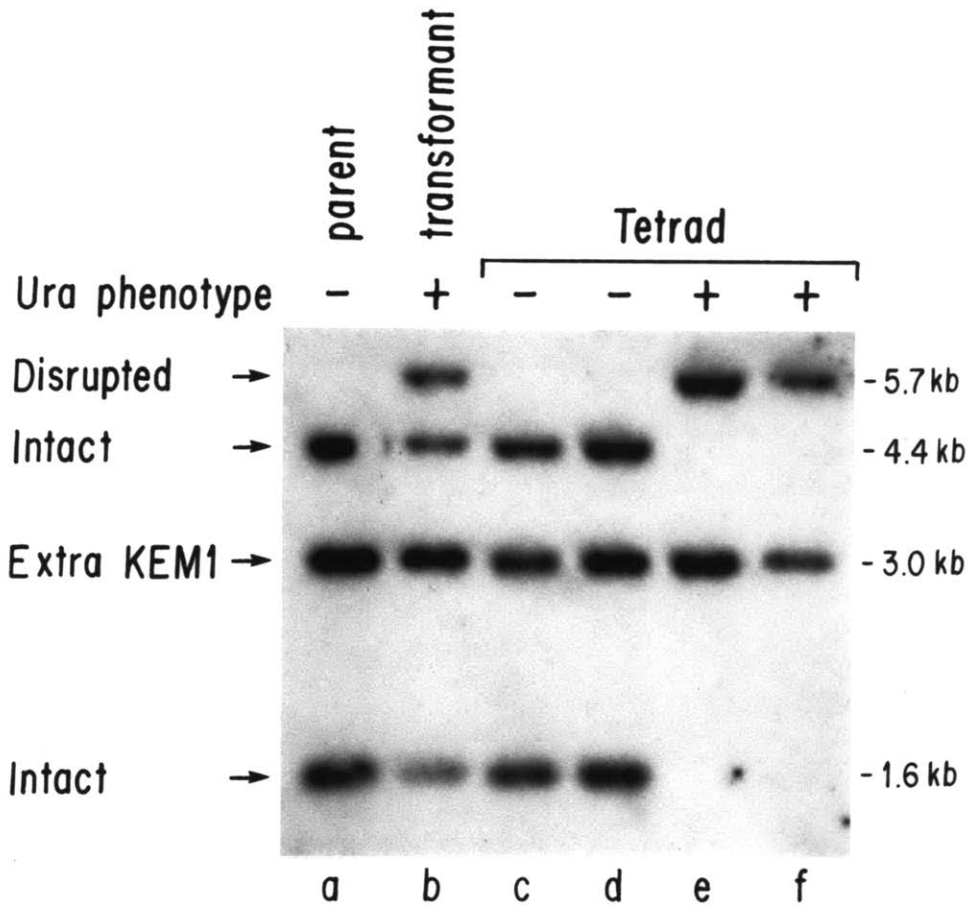
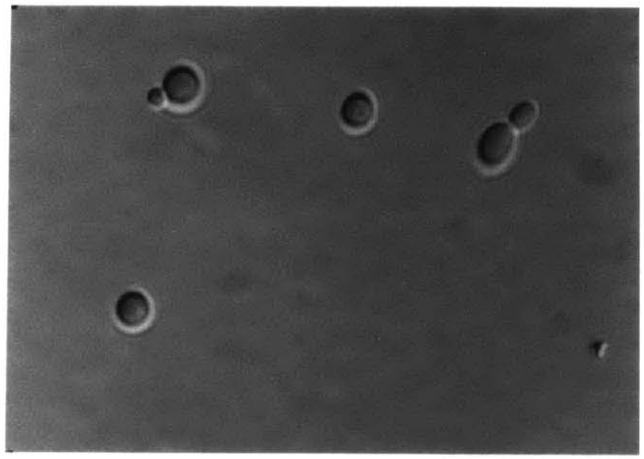

parent
transformant
Tetrad
Ura phenotype
- + - - + +
Disrupted
Intact
Extra KEM1
Intact
5.7 kb
4.4 kb
3.0 kb
1.6 kb
a b c d e f

Figure 3-7. Morphology of mitotically growing kem1::URA3 cells compared with KEM1 cells.

(a) KEM1 strain (JK251) (b) kem1::URA3 strain (JK245)

(a) *KEM1*



(b) *kem1::URA3*

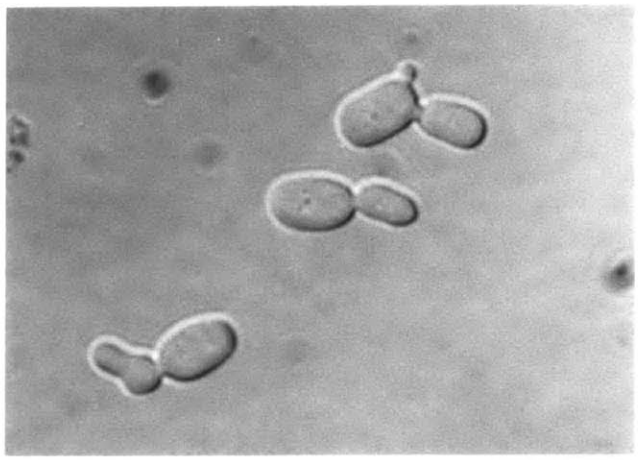
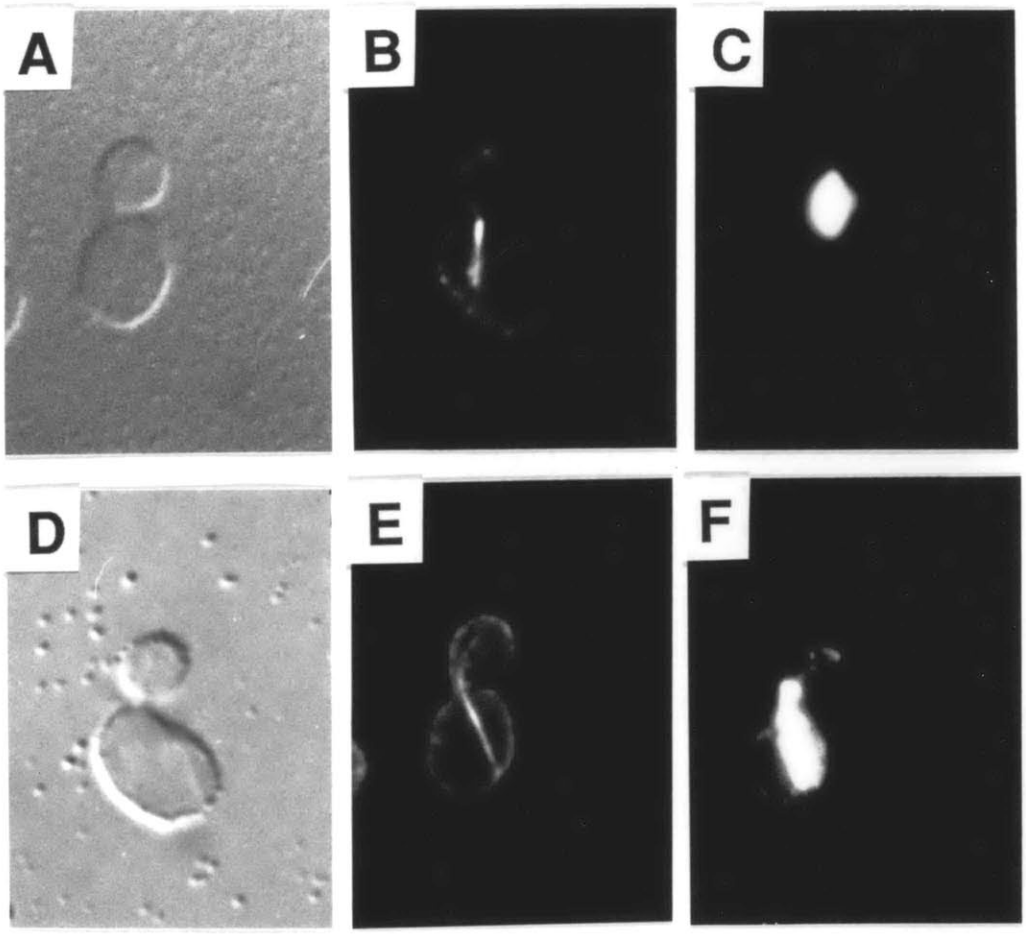




Figure 3-8(a). Nuclear and microtubular staining of large-budded cells of KEM1 strain.

Exponentially growing KEM1 (JK251) cells were fixed and stained with the fluorescent dye DAPI for nuclear DNA and with anti-tubulin antibody / rhodamine-conjugated secondary antibody for microtubules. Each three panels represent the same cell revealed by Nomarsky optics, anti-tubulin staining, and DAPI staining.


A
B
C
D
E
F

In kem1::URA3 strains, however, a great number of large-budded cells contained a single focus of anti-tubulin staining (Figure 3-8 (b), A - C). This stained region presumably represents a single unduplicated spindle pole body or duplicated but unseparated spindle pole bodies without progression to the stage where the intranuclear spindles being developed. Ten percent of cells contain two nuclei (Figure 3-8 (b), D - I) which is probably due to the nuclear division in a mother cell without migration into a daughter cell (Figure 3-8 (b), D - F). Quantitative analysis of these large budded cells are summarized in Table 3-5 with a diagram showing the relavant nuclear structure. These results suggest that the kem1 null mutation affects the spindle pole body duplication. The cordination of the nuclear division and cell division is sometimes defective to produce binuclear cells.

kem1/kem1 diploids fail to sporulate.

In response to certain conditions such as nutrient starvation, wild type yeast diploid cells undergo G1 arrest, meiosis, and sporulation. I constructed kem1/kem1 homozygous diploids and tested cells of this genotype for their ability to sporulate. Diploid strains were patched on pre-sporulation plates and grown to thick patches. A large portion of cells was transfered to SPOR (containing 1% potassium acetate and 0.1% glucose) or NGS (containing potassium acetate w/o glucose) plates by replica-plating. I followed sporulation for a period of days by observing cell morphology and DAPI-stained nuclear DNA in the microscope. For each diploid strain, at least 200 cells were examined.

Figure 3-8(b). Defects in nuclear division and spindle pole body separation of kem1::URA3 cells as revealed by nuclear and microtubular staining.

Exponentially growing kem1 (JK245) cells were fixed and stained with the fluorescent dye DAPI for nuclear DNA and with anti-tubulin antibody / rhodamine-conjugated secondary antibody for microtubules. Each set of three panels represents the same cell revealed successively by 1) Nomarsky optics, 2) anti-tubulin staining, and 3) DAPI staining.

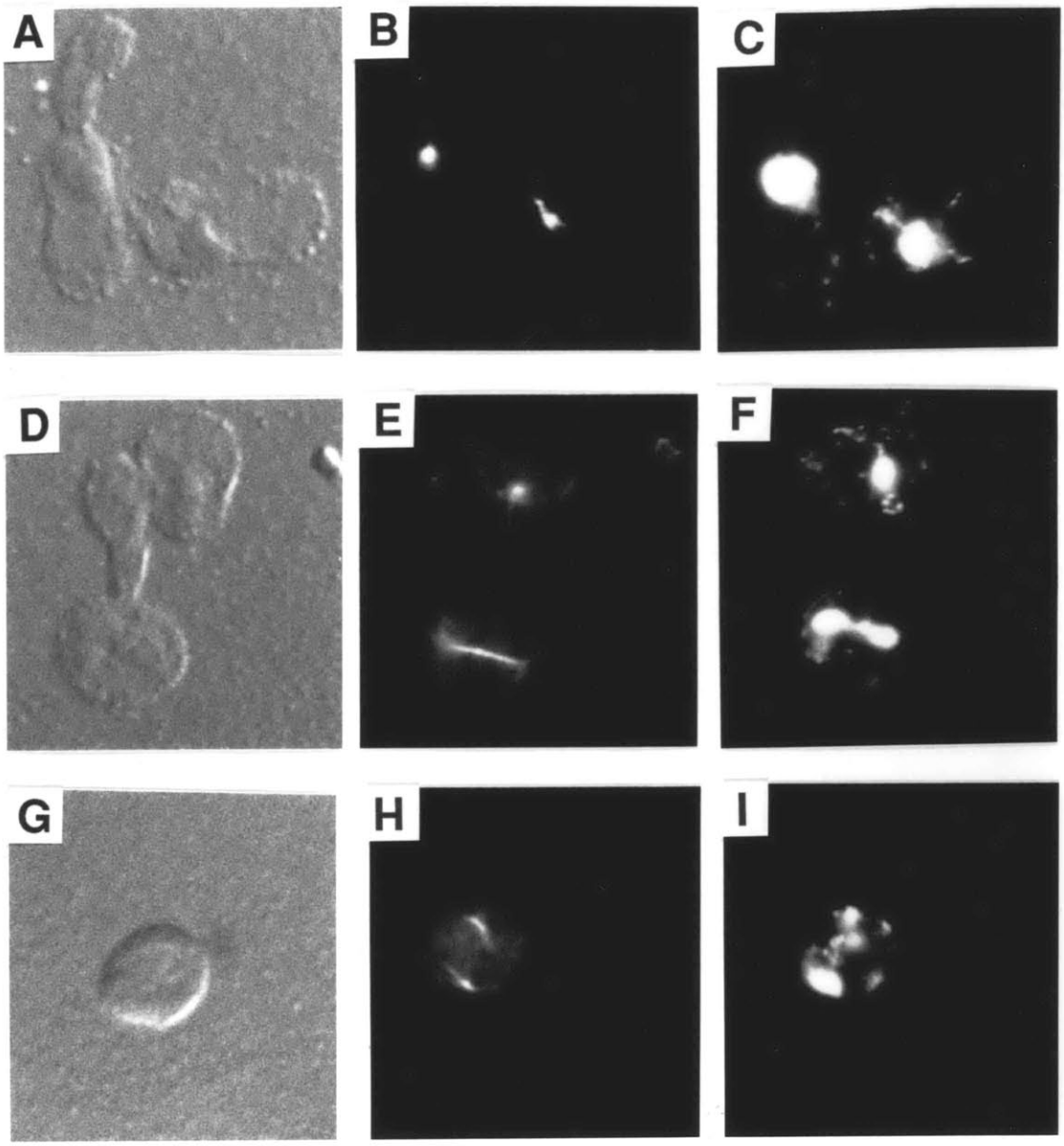
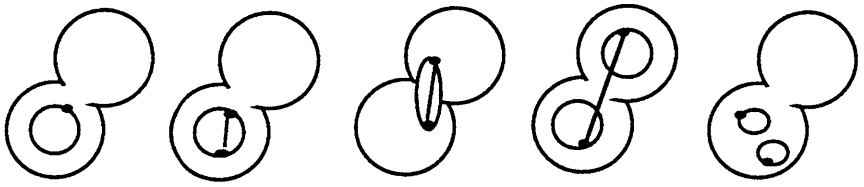

A
B
C
D
E
F
G
H
I

Table 3-5. Nuclear division and spindle pole body separation in large budded cells of KEM1 and kem1::URA3 strains.



a

						b
KEM1	0	34	11	41	0	(74)
kem1::URA3	27	17	15	32	10	(133)

a. The diagram shows the large budded cells; nuclei, spindle pole bodies, and intranuclear spindles are shown.

b. Numbers indicate the percentage of cells with a diagramed structure (the number in parentheses is the total number of cells examined).

Under this conditions 40 - 60% of wild type diploid cells sporulated (Figure 3-9, A, B). Diploids homozygous for kem1-1, kem1-5, or kem1::URA3 failed to sporulate under the same sporulation conditions (Figure 3-9, C, D). Diploids heterozygous for kem1 sporulated as efficiently as wild type strains, indicating that this sporulation defect is recessive. The sporulation phenotype cosegregates 2:2 with the kem1 mutation.

kem1 mutants lose viability upon nutritional starvation.

I have observed that kem1 mutant cells die very rapidly when stored at room temperature on YEPD plates. This observation together with the previous finding that kem1/kem1 homozygous diploids do not sporulate prompted an examination of the sensitivity of kem1 mutant cells to starvation conditions. kem1 mutant cells (kem1::URA3, kem1-1, and kem1-5) lose viability upon prolonged incubation on minimal media lacking nitrogen and YPA media containing nonfermentable carbon source (acetate). These viability phenotypes cosegregated 2:2 with the kem1 mutation (Figure 3-10). The response of kem1 mutant cells to nitrogen starvation was examined quantitatively. Cells were grown to log phase and shifted from YEPD rich medium to minimal media lacking nitrogen. Under this regime, wild type cells complete their cell cycle, arrest uniformly as unbudded cells, and remain viable for a long period of time. The initial response of the kem1 mutants to nitrogen starvation was the same as wild type cells: 90 - 95% of the cells arrested as unbudded cells after 20 hrs of the shift. However, upon continuing starvation the kem1 mutants lost viability. Figure 3-11 shows that after

Figure 3-9. Sporulation defect in kem1/kem1 diploids as revealed by cell morphology and DAPI-staining.

Each pair of panels represents the same cells revealed by phase optics and DAPI staining. A - B KEM1/KEM1 diploid cells on the sporulation media after incubation for 5 days at 23°C; C - D kem1/kem1 diploid cells on the sporulation media after incubation for 5 days at 23°C.

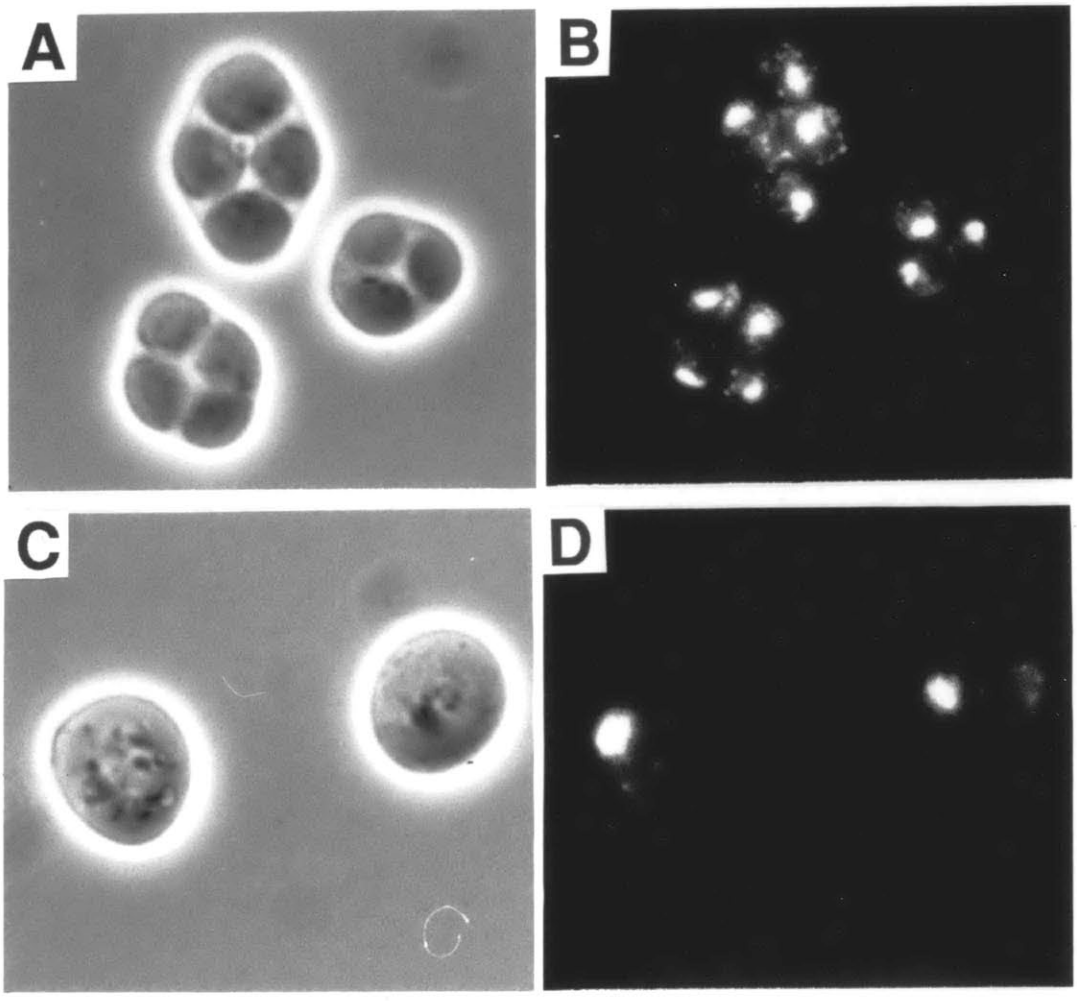
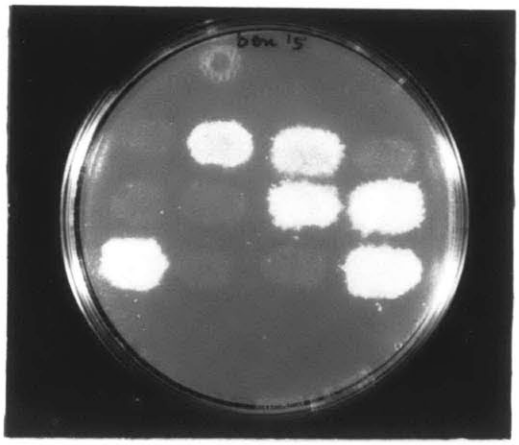

A
B
C
D

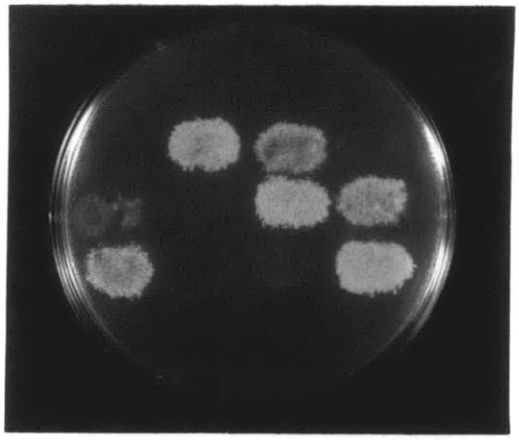
Figure 3-10. Sensitivity of the keml mutants to the nutritional starvation.

Spores from a keml x KEM1 cross were patched on a YEPD plate and grown over night. This master plate was replica-plated onto benomyl (15 μg/ml in YEPD), YNB w/o nitrogen, and YPA plates. (a) The benomyl plate was incubated at 24°C for 1 day. (b) The YNB w/o nitrogen plate was incubated at 30°C for 5 days and replica-plated back onto a YEPD plate. The picture was taken after incubation for one day at 30°C. (c) The YPA plate was incubated at 30°C for 7 days and replica-plated on a YEPD plate. The picture was taken after incubation for one day at 30°C.

(a) Benomyl



(b) YNB w/o nitrogen



(c) YPA

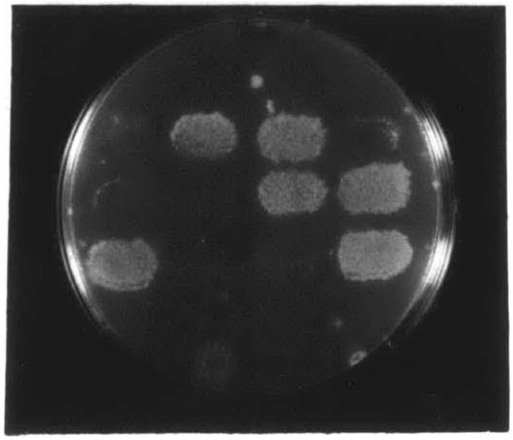
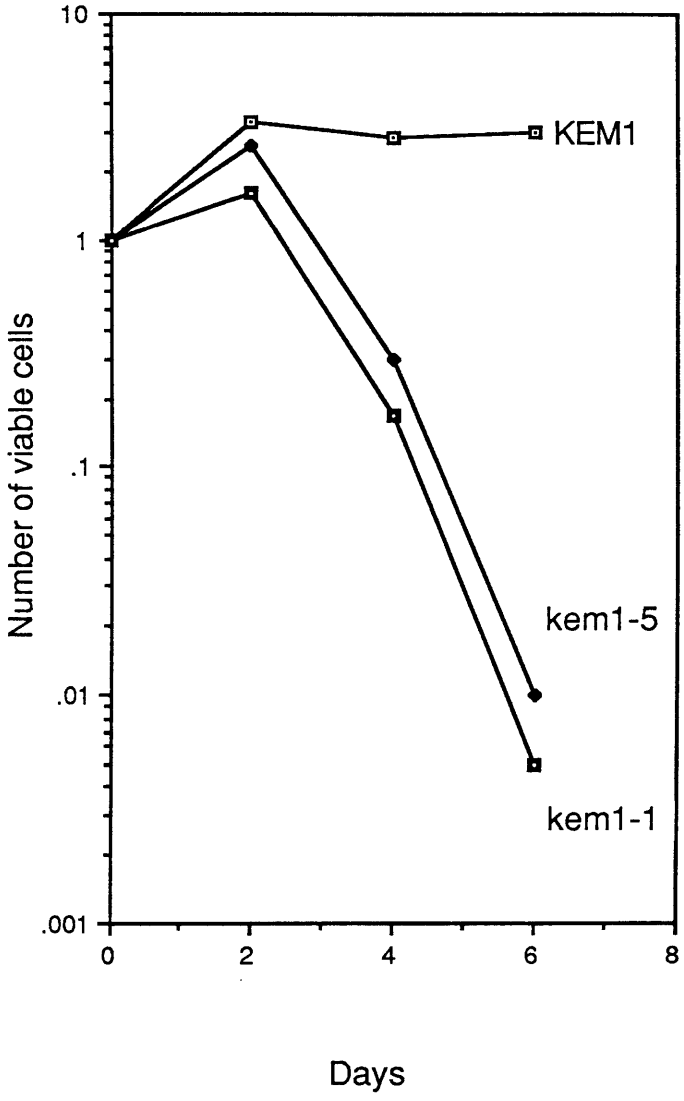


Figure 3-11. Viability of kem1 mutants after nitrogen starvation

Exponentially growing cultures of KEM1 (JK204), kem1-1 (JK205), and kem1-5 (JK191) were shifted from YEPD to SD media lacking nitrogen. Viability was measured after various incubation periods.


10
1
.1
.01
.001
0
2
4
6
8
Number of viable cells
Days
KEM1
kem1-5
kem1-1

4 days only 5% of both kem1-1 and kem1-5 cells were viable and after 6 days most of these cells were dead.

The recovery of starved kem1 cells upon addition of rich medium is different from that of KEM1. After 40 hrs of starvation (when most of the kem1 and KEM1 cells were blocked in the cell cycle but still viable) cells were shifted back to YEPD medium. After 3 hrs in YEPD medium, wild type cells restarted the cell division and 30 - 50% of cells were budded whereas most of kem1 cells remained arrested in the unbudded state. After 6 hrs in YEPD medium, 50 - 60% of wild type cells and 20 - 30% of kem1 cells were budded. Upon continuing incubation, the percentage of budded cells in kem1 culture increased to 50 - 60%.

These observations support an explanation that strains carrying kem1 mutations show a defect in a proper response to the nutritional changes in the medium. The inability to respond probably leads to cell death under nutritional starvation conditions.

kem interaction with the RAS/adenylate cyclase pathway.

The set of phenotypes observed in kem1 mutants such as sensitivity to nitrogen starvation and failure of sporulation closely resembles the phenotypes of certain mutations in genes encoding regulatory components of the RAS/adenylate cyclase pathway. $RAS2^{val19}$ (Kataoka et al., 1984; Toda et al., 1985), CYR1::HIS3 (Kataoka et al., 1985), bcy1 (Toda et al., 1987), and $CDC25^{HS}$ (Broek et al., 1987) have either elevated cellular levels of cAMP or activated cAMP-dependent protein kinase, resulting in a syndrome of phenotypes similar to those described above.

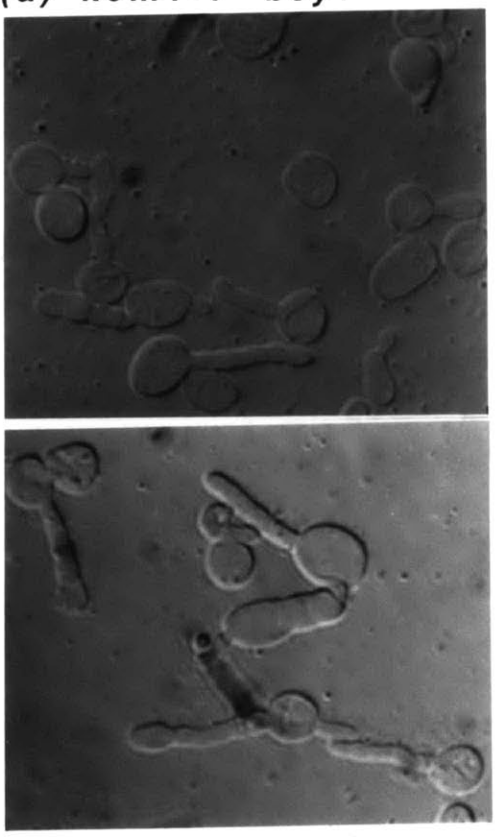
To test whether the KEM1 gene is also involved in this pathway, I crossed the kem1-1 mutant to cdc25 and cyr1-1. cdc25 is a mutation in a gene encoding a positive regulator of RAS2 protein and cyr1-1 is a mutation in a structural gene of adenylate cyclase. Both mutations cause decreased levels of adenylate cyclase activity. Analysis of phenotypes of double mutants from these crosses indicates that kem1 does not suppress the conditional lethal phenotype of either cdc25 or cyr1-1 and neither cdc25 nor cyr1-1 suppresses kem1. These results imply that the kem1 mutation may not affect the cellular level of cAMP.

I carried out a cross between kem1 and bcy1 in order to investigate the genetic interaction between the two. bcy1 is a mutation in the structural gene for the regulatory subunit of the cAMP-dependent protein kinase, resulting in an activated form of this enzyme. kem1 bcy1 double mutants were identified and they showed both sensitivity to nitrogen starvation and the Kem^- phenotype. The budding pattern of the kem1 bcy1 double mutant is greatly altered. The double mutant produces long tubular cells (Figure 3-12). This result suggests that bcy1 and kem1, both showing sensitivity to nitrogen starvation, act synergistically to generate a more severe phenotype in kem1 bcy1 double mutants. But kem1 does not seem to affect the RAS/Adenylate cyclase pathway in which bcy1 is involved. Therefore, I feel that there may be an alternative pathway mediated by KEM1 by which cells sense the nutritional conditions in the medium.

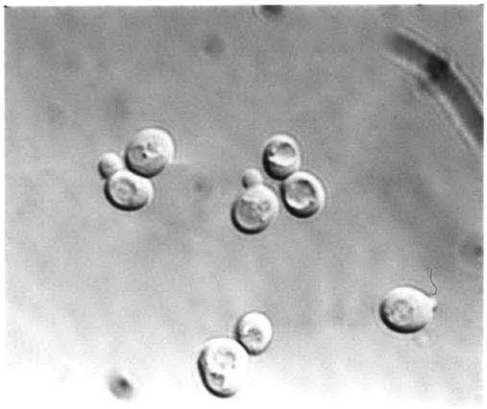
Figure 3-12. Budding pattern of kem1 bcy1 double mutants

Mitotically growing cells of (a) kem1 bcy1 (JK237), (b) kem1 bcy1 [KEM1 on Ycp50], (c) kem1 (JK205), and (d) bcy1 (RA1-13D-R) are shown by Nomarsky optics.

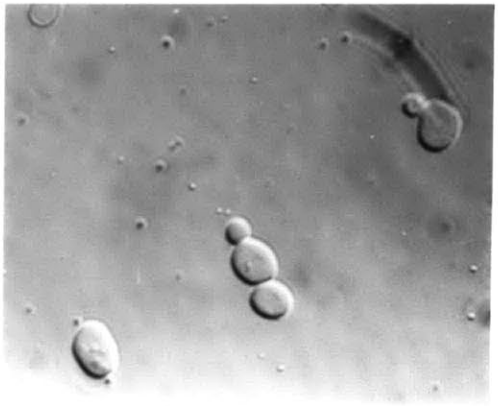
(a) kem1-1 bcy1



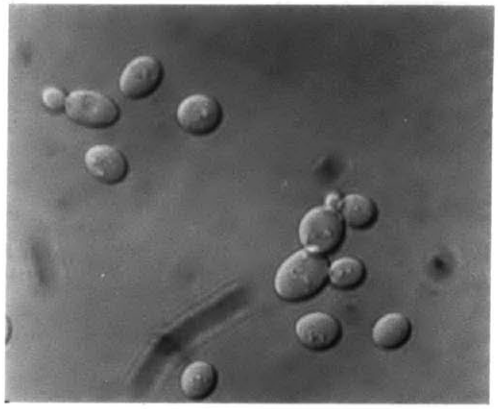
(b) kem1-1 bcy1
[KEM1 on Cen]



(c) kem1-1



(d) bcy1



keml mutants are sensitive to EGTA.

Ca^{++} ion is an essential nutrient of cells and is known to be an important regulatory molecule in cellular processes including motility, cytoskeletal restructuring, and ion fluxes (Ohya et al., 1984, Davis and Thorner, 1986). EGTA, when added into culture media, binds Ca^{++} ion as well as Mg^{++} ion making them unavailable to the cell. I have investigated the effects of EGTA on growth of keml mutants. Cells grown to log phase (1 - 2 x 10^7 cells/ml) were plated out on YEPD and YEPD containing various concentrations of EGTA. As shown in Figure 3-13, growth of keml mutants are inhibited in 1 mM EGTA whereas growth of a wild type strain is not. This sensitivity indicates that the cellular state concerning ion level is altered in keml mutants.

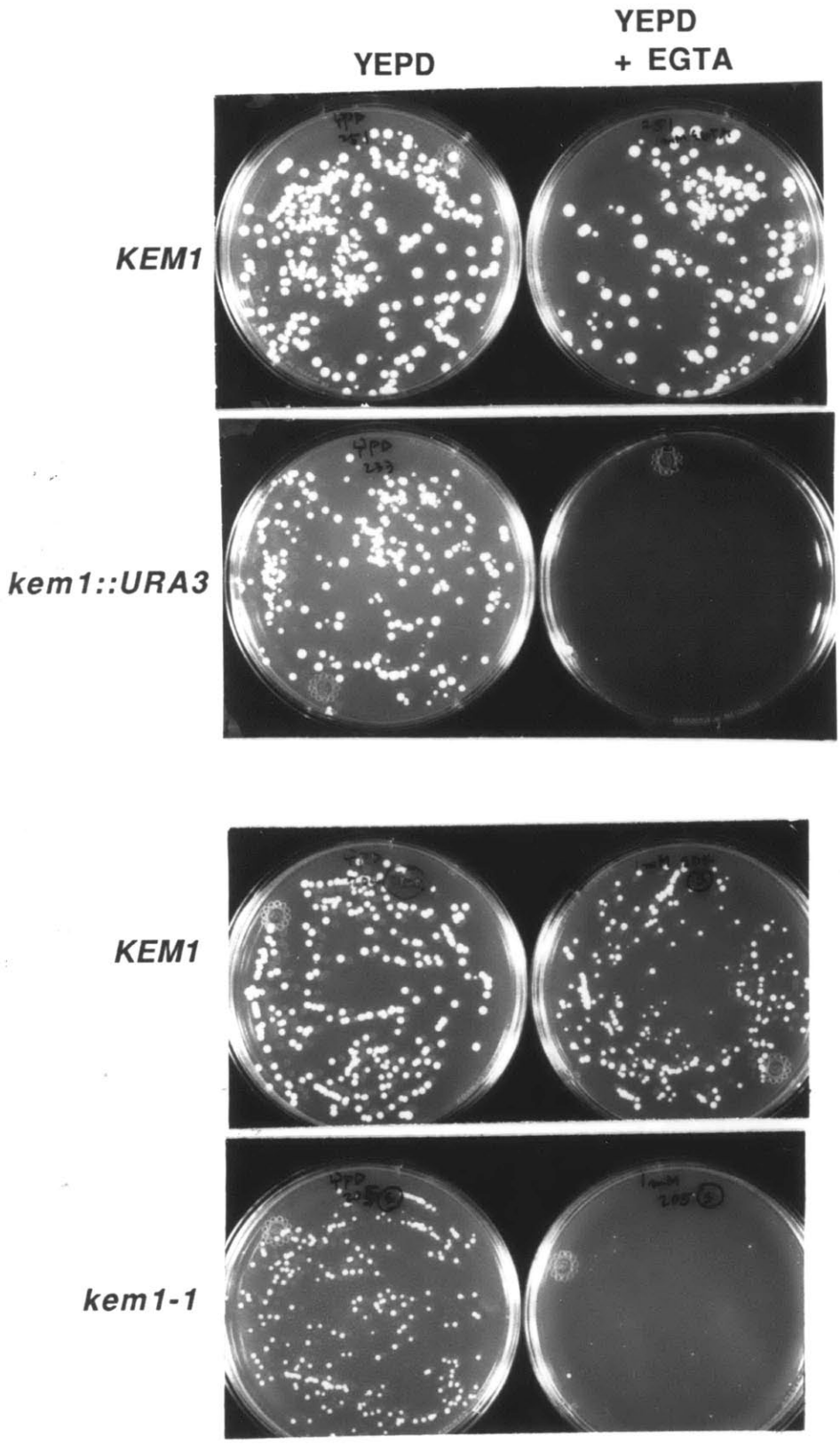
DISCUSSION

The main conclusion from this chapter is that mutations in KEM1 cause defects in several cellular functions including nuclear fusion during conjugation, chromosome transmission, spindle pole body duplication, and the proper response to nutritional conditions. These pleiotropic effects suggest that the KEM1 gene is involved in a regulatory process that controls the functions of the spindle pole body or microtubules during conjugation as well as mitotic cell cycle.

I have shown that keml mutations cause a bilateral nuclear fusion defect. In crosses where both parents are keml, about 30% of the zygotes fail to fuse nuclei with the result that cytoductants are produced at

Figure 3-13. Sensitivity of kem mutants to EGTA

Mitotically growing cultures of isogenic strains KEM1 and kem1 were plated out on YEPD plates and YEPD plates containing 1 mM EGTA.


YEPD
YEPD
+ EGTA
KEM1
kem1::URA3
KEM1
kem1-1

high frequency. The nuclear fusion defect of kem1 mutants was somewhat expected because kem1 mutations were isolated by the Kem$^-$ phenotype - enhancement of the nuclear fusion defect of the kar1-1 mutation (see Chapter 2).

Several phenotypes of kem1 mutants lead me to suggest that the KEM1 gene affects microtubules. The kem1 mutants are hypersensitive to anti-microtubule drug benomyl. In S.cerevisiae, mutations conferring resistance to benomyl at a concentration of 40 μg/ml are found almost exclusively in the TUB2 β-tubulin gene (Thomas et al., 1985). Mutations in α-tubulin genes (cold-sensitive mutations in TUB1 or a null allele of TUB3) also cause hypersensitivity to benomyl (Schatz et.al., 1986, Stearns, personal communication). In Aspergillus nidulans, mutations in the β-tubulin gene were isolated by selecting resistance to benomyl (Sheirr-Neiss, 1978) and mutations to hypersensitivity were found in an α-tubulin gene (Oakley and Morris, 1974). This specific relationship between a benomyl phenotype and mutations in tubulin genes imply that the KEM1 gene (not related to any known tubulin genes in S. cerevisiae) may be required for controlling normal function of microtubules. Yeast microtubules form two structures: intranuclear spindles and cytoplasmic microtubules. Intranuclear spindles function probably in chromosome separation and nuclear division during mitosis and meiosis (Byers, 1981, Thomas et al., 1986, Huffaker et al., 1988). Cytoplasmic microtubules are thought to be involved in nuclear fusion during conjugation (Byers and Goetsch, 1974, 1975). Some defects caused by the kem1 mutations appear to be associated with these processes. In kem1 mutants, the frequency of chromosome loss during mitotic cell division was increased

10 - 20 fold and nuclear fusion was blocked in about 30% of kem1 x kem1 zygotes. These phenotypes imply that the KEM1 gene affects both intranuclear spindles and extranuclear microtubules.

The effects of the KEM1 gene on microtubule function could be rather indirect. When the kem1-1 mutants were crossed to either tub2-104 (Thomas et al., 1985) or tub1-1 (Stearns, personal cmmunication) strains, the double mutants (kem1-1 tub) arising from these crosses gave no evidence for a genetic interaction between the genes. Studies with the kem1 null mutation relate the KEM1 gene to the spindle pole body function. In the absence of KEM1 function cell division is significantly slowed down and is accompanied by altered cell morphology. The crucial defect causing this slow growth appears to be in the spindle pole body duplication/separation during the cell cycle. Because the spindle pole body is associated with the organization of microtubule arrays during yeast life cycle (Robinow and Mark, 1966, Byers and Goetsch, 1974, 1975, Byers, 1981, Kilmartin and Adams, 1984), the spindle pole body function and the microtubule function are closely linked to each other generating coherent effects on cellular processes. This notion is likely to explain the phenotypes observed in kem1 mutant strains concerning microtubule and spindle pole body function.

I have shown that kem1 strains are defective in cellular response to the nutritional conditions. Their inability to sporulate and the sensitivity to nitrogen starvation closely resemble those of some mutants implicated in the RAS/adenylate cyclase pathway (RAS2^{val19} and bcy1) (Kataoka et al., 1984, Uno et al., 1982, Toda et al., 1987) and the ypt1 mutant (Segev and Botstein, 1987). Several lines of evidence

suggest that the KEM1 gene does not act through the cAMP-mediated effector system. First, upon nitrogen starvation kem1 mutant cells arrest at G1 as unbudded cells, whereas the RAS2^{val19} and bcy1 cells fail to arrest in G1 phase. The kem1 mutants appear to be defective in restoring the cell cycle from G1 arrest caused by nitrogen starvation. Second, genetic analysis using cyr1-1, cdc25, and bcy1 mutations indicate that there is no apparent suppression activity between kem1 and these mutations. The cyr1-1 encodes the adenylate cyclase (Kataoka et al., 1985b) and the CDC25 gene product appears to act as a positive regulator of RAS2 proteins which controls the adenylate cyclase (Toda et al., 1985, Broek et al., 1987). The long tubular cells observed in the kem1 bcy1 culture indicate that cell growth and cell division are uncoupled in kem1 bcy1 double mutant cells. It is possible that the KEM1 gene affects the processes downstream of cAMP-dependent protein kinase in the RAS/adenylate cyclase pathway in such a way that the effects of kem1 and bcy1 are additive producing a more severe phenotype. Another explanation would be that the KEM1 is involved in an alternative regulatory pathway which affects the cellular response to the nutritional conditions in the similar way as the RAS/adenylate pathway. Considering other phenotypes of kem1 mutants, I infer that the regulatory function involving KEM1 is specific or directed to the spindle pole body or the microtubule function, that is, the KEM1 gene specifies a signaling or sensing function that transfers the message concerning the nutritional state of cell to the spindle pole body or microtubules.

The possible existence of a regulatory mechanism on the spindle pole body duplication in response to the nutritional conditions has been already implicated partly by studies with the CDC31 gene. The CDC31 gene is suggested to control the spindle pole body duplication in response to the cellular level of Ca^{++} ion at the specific stage of the cell cycle (Baum et al., 1986a, 1986b). The YPT1 gene (related to the mammalian ras genes) was shown to bind to GTP and, like KEM1, to be involved in sporulation and nitrogen starvation (Segev and Botstein, 1987). The cold-sensitive mutation in YPT1 (Segev and Botstein, 1987) and the loss of the YPT1 function derived by galactose-inducible promotor (Schmitt et al., 1986) cause the aberrant arrangement of microtubules in arrested cells. These findings support the notion that the spindle pole body or microtubule function is influenced by the transferred signals concerning cellular nutritional conditions. These structures may be responsive as well to the signals concerning conjugation and mitotic cycle. The KEM1 gene is likely to be involved in these regulatory processes relaying the nutritional or may be developmental signals to the spindle pole body or microtubules during conjugation and the mitotic cell cycle.

Chapter 4

Transposon insertions in *KEM1* and localization of *KEM1*::*lacz* fusion proteins

INTRODUCTION

The mutation kem enhances the Kar$^-$ phenotype of kar1-1 in Saccharomyces cerevisiae. The Kar$^-$ phenotype results from a failure of nuclear fusion during conjugation. The analysis of kem1 mutations (kem1-1, kem1-5, and kem1 null) have suggested that KEM1 controls the spindle pole body or microtubule function, probably in response to the cellular nutritional conditions. This notion was based on the observations that the kem1 mutations cause a defect in following processes; (1) nuclear fusion during conjugation (2) mitotic chromosome transmission (3) spindle pole body duplication/separation during the cell division cycle (4) response to nutritional conditions. In an attempt to identify and elucidate the functions of KEM1 defined by mutational analysis, I have taken an alternative approach utilizing current molecular genetic techniques available in yeast. I expect that the information on the structure or intracellular localization of gene products would provide useful clues to the identification of gene functions.

The structure-function analysis has been greatly assisted by development of indirect immunofluorescence techniques in yeast. The arrangement of cytoskeletal proteins such as microtubules, actins, and intermediate filaments have been investigated by visualizing the structures with protein specific antibodies (Adams and Pringle, 1984, Kilmartin and Adams, 1984, Haarer and Pringle, 1987). Antibodies raised to the native proteins encoded by known genes have been very useful in revealing the intracellular localization of the gene products.

β-galactosidase protein fusions often allow to localize the gene products with β-galactosidase specific antibodies supporting the functions predicted for the gene products. In this chapter, I will describe the insertion mutagenesis in KEM1 and the intracellular localization of the KEM1 gene product.

MATERIALS AND METHODS

Strains, media, and genetic analysis. Yeast strain JK191 is MATα, ura3-52, his4-29, cyh2, kem1-5. Strain JK147 is MATa, ura3-52, leu2-3,112, trp1-1, ade2, cyh2. Strain JK336 is MATα, ura3-52, his4-29, kem1-1. Yeast media was essentially as described by Sherman et al. (1974). Benomyl plates were made by adding slowly the benomyl stock solution (10 mg/ml in dimethyl sulfoxide, stored at -20°C) to warm YEPD medium with vigorous swirling to prevent precipitation. Benomyl was a generous gift from E. I. Dupont deMours and Co., Inc. Sc - Ura or SC - Ura - Leu plates consisted of YNB with all amino acids added except uracil or except uracil and leucine.

Escherichia coli HB101 (Boyer and Roulland-Dussoix, 1969) was used for bacterial transformation and plasmid growth. Escherichia coli DB1329 is recA56, arg^-, Δlac-proXIII, Nal^R, Rif^R, ara^-/F′ $laci^Q$ (pro^+) and carries pNK629 (Huisman et al., 1987). Escherichia coli DB1328 is spontaneous λ-resistant mutant of HB101. Bacterial media were made as described by Davis et al. (1980).

Transformation and DNA manipulation techniques. Yeast transformation was carried out by the lithium acetate method developed by Ito et al. (1983) using 50 μg per transformation of sonicated calf thymus DNA (Sigma Inc.) as carrier. Transformants were plated on SC - Ura or Sc - Ura - Leu plates to select for plasmids. E. coli transformation was performed by the calcium chloride procedure of Mandel and Higa (1970). Rapid isolation of plasmid DNA from E. coli was done by the boiling lysis method (Holmes and Quigley, 1981). Yeast DNA was prepared essentially same as described by Boeke et al. (1985). Restriction endonuclease analysis and agarose gel electrophoresis were as described in Maniatis et al. (1982).

Plasmid constructions. Plasmid pJI103 was constructed by inserting 5.5 Kb BamH1-HindIII fragment carrying KEM1 sequence between a BamHI site and a HindIII site of YCp402. YCp402 (Ma et al., 1987) is a vector containing the LEU2 marker and Cen4, which is derived from YCp50 by replacing URA3 with LEU2. Plasmids pJI116 or pJI117 was constructed by isolating 9.5 Kb BamHI-HindIII fragment (contains KEM1 sequence with a part of mini-Tn10-LUK sequence, HindIII cuts in kanR gene) from T67 or T79 and inserting between BamHI and HindIII sites of YEp13, a high copy vector carrying the LEU2 marker and a 2μ sequence for origin of replication. The construction of frameshift plasmid pJI126 was done by digesting pJI116 partially with NcoI, filling 3'recessed ends with Klenow, and ligating blunt ends. The deletion plasmid pJI128 was constructed by partial digstion of T67 with BglII and ligation.

Mini-Tn10-LUK transposon mutagenesis. Transposon mutagenesis was peformed essentially same as described by Huisman et al. (1987) except that I followed the protocol revised by Andy Hoyt. The E. coli strain DB1329 carrying pNK629 (containing Tn10 transposase with an IPTG inducible promoter) was transformed with a target plasmid pJI103 and transformants were selected on LB + Tet + Amp plates to maintain both pNK629 (Tet^R) and pJI103 (Amp^R). A transformant BJ80 was grown overnight in LB + Tet + Amp liquid medium at 37°C , diluted into LB + 0.2% maltose + 1 mM IPTG + Tet + Amp and grown to log phase (Klett 50). 40 ml of culture was centrifuged and resuspended in 4 ml of LB + maltose + IPTG + 10 mM $MgCl_2$. λLUK lysates were added to an m.o.i. of 0.4, which was incubated at room temperature for 30 min to allow phage infection. This culture was diluted with 36 ml of LB + IPTG and incubated at 37°C for 1.5 hr. After cells were centrifuged and resuspended in LB, appropriate dilutions were made and plated on LB + Na pyrophosphate (1.25 mM) + kan (50 μg/ml) + Amp. Plates were incubated overnight at 39 - 42°C. We prepared DNA from a pool of about 10,000 colonies, which was transformed into the E. coli strain DB1328 selecting for Kan^R and Amp^R colonies.

Plate mating. Strains to be tested were patched on YEPD plates. Lawns of strains with an opposite mating type and complementatary auxotrophic markers were cross replica-plated with plates containing patches of the strains to be tested onto fresh YEPD plates for a brief mating. After 4 hr incubation at 30°C (or 5 hr at 24°C or 3.5 hr at 34°C) , the mating plates were replica-plated to minimal media to select for diploids.

A quick β-galactosidase assay. Cells were grown to log phase ($O.D._{600}$= 1.0). 1 ml of culture was centrifuged, washed once with dH_2O, and resuspended in 0.8 ml of Z-buffer (Miller, 1972) supplemented with 0.0075% sodium dodecyl sulfate. Cells were permealized by adding 60μl of chloroform followed by vigorous agitation. The assay was started by adding 0.2 ml of ONPG (4 mg/ml) at 28°C and stopped by adding 0.45 ml of 1M Na_2CO_3 (Miller, 1972). This reaction mixture was centrifuged and measured at $O.D._{420}$. Units of β-galactosidase are expressed by the formula (1,000 x $O.D._{420}$)/($O.D._{600}$ x volume of culture x minutes of assay).

Western blots. Total protein was isolated from yeast cells by the following procedure. 5 ml of cell culture grown to log phase ($O.D._{600}$= 1.0) was centrifuged, washed once with dH_2O, and resuspended in 50 μl of dH_2O. Cells were lysed by agitation for 90 seconds on the vortex mixer in the presence of 10 μl of 100% trichloroacetic acid and 0.2 mg of glass beads. 500 μl of cold 5% trichloroacetic acid was added to this mixture, which was centrifuged at 13K for 20 minutes. The pellet was washed once with 1.5 ml of cold H_2O and centrifuged for 3 - 5 minutes. Pellets were resuspended in 150 μl of sample buffer (12.5% glycerol, 2% sodium dodecyl sulfate, 80 mM Tris-hydrochloride, 2.5% β-mercaptoethanol, and 0.12% bromophenol blue), neutralized by adding 3 μl of 2 M Tris base, and boiled for 5 minutes. After centrifugation at room temperature, 25μl of supernatant of each sample was loaded onto a 7.5% polyacrylamide gel, subjected to electrophoresis, and transfered to nitrocellulose filter (Towbin et al., 1979). The filter was placed in a

blocking solution (5% instant milk, 150 mM NaCl, 50 mM Tris hydrochloride pH 7.5, 0.5% azide, and 0.5% TWEEN20) for 30 minutes with shaking. β-galactosidase antibodies (generously given by Tom Mason) were added (1 ml/10 ml) and incubated for 3 hours. The filter was washed three times in blocking solution without milk and incubated in bloking solution with the $[I_{125}]$-labeled anti-protein A for 2 hrs. The filter was washed three times as above and exposed to X-ray film.

Immunofluorescence. Indirect immunofluorescence was peformed by the method of Adams et al. (1984) with a few modifications. 10 ml of yeast culture grown to early log phase ($< 1 \times 10^7$ cells/ml) was fixed by adding 1 ml of 1 M potassium phosphate, pH 6.5 ("P buffer") and 1 ml of 37% formaldehyde. After incubation at room temperature for 2 hrs, cells were centrifuged (4,000g) , washed twice with 0.1 M P buffer, washed once with 1.2 M sorbitol/0.1 M P buffer, and resuspended in 1 ml of 1.2 M sorbitol/0.1 M P buffer. 5 μl of β-mercaptoethanol and 30 μl of zymolyase (10 mg/ml, 60K activity, from Kirin co. Japan) were added to the cell suspension to digest off the cell wall. After 1.5 hr incubation at 30^{o}C with gentle rocking, cells were centrifuged, washed once with 1.2 M sorbitol/0.1 M P buffer, and resuspended in 3ml of 1.2 M sorbitol/0.1 M P buffer. 15μl of cell suspension was applied to a well on a polylysine coated slide (8 well Flow-labs slide). The slide was immersed in cold methanol (-20^{o}C) for 6 minutes and into cold acetone (-20^{o}C) for 30 seconds. The antibody reaction was carried out by adding 15 μl of 1:40 dilution of β-galactosidase antiserum in BSA/ sorbitol/ P buffer (10 mg/ml BSA, 1.2 M sorbitol, 0.1M potassium phosphate, pH 6.5)

to each well and incubating in a moist chamber at room temperature for 1 hr. Antibodies were washed off three times with BSA/ sorbitol/ P buffer and secondary antibody reaction was carried out by adding 15 μl of Rhodamine-conjugated anti-mouse antibodies (1:500 dilution, Boehringer Mannheim Biochemicals) to each well. After incubation at room temperature in dark for 1 hr, antibodies were washed off four times with BSA/ sorbitol/ P buffer and twice with sorbitol/ P buffer. 15 μl of 1 μg/ml DAPI was added for 5 minutes to stain nuclear DNA. After a wash with sorbitol/ P buffer, slides were mounted with p-phenylenediamine/90% glycerol and examined on the fluorescent microscope.

RESULTS

Transposon insertions in KEM1 using mini-Tn10-LUK.

To make insertion mutations in the cloned KEM1 gene, I performed transposon mutagenesis using mini-Tn10-LUK system developed by Huisman et al. (1987). For the analysis of KEM1, this system has several useful features. (i) The random sites and the high frequency of transposition events allow definition of the functional boundaries of the KEM1 gene. (ii) The expression of the lacZ gene, possibly resulting from in-frame fusion with KEM1 provides information about the orientation of the KEM1 message. (iii) KEM1::lacZ protein fusions, if they are stable, can be used to localize the KEM1 gene products.

Transposon insertions into the KEM1 gene were isolated as follows. E. coli strain DB1329 harboring a plasmid that gives an IPTG-inducible production of Tn10 transposase function was transformed with the target

plasmid pJI103 (Figure 4-1) which contains a 5.5 Kb fragment of the KEM1 gene on YCp402. YCp402 is a pBR322 derivative carrying the yeast LEU2 gene and a yeast centromere, CEN4 (Ma et al., 1987). After induction of transposase function in the transformants BJ80, I introduced the mini-Tn10-LUK carried on λ-phage into this strain. Mini-Tn10-LUK consists of the two termini of Tn10, the E. coli lacZ gene, the kanR gene, and the yeast URA3 gene (Figure 4-1). Transposition of the mini-Tn10-LUK element into the plasmid pJI103 was selected on kanamycin plates. Plasmid DNAs were prepared from a pool of Kan^R colonies and introduced into a E. coli strain DB1328 by transformation for individual analysis. A total of 85 transformants were examined by restriction analysis after rapid plasmid preparations and all shown to have insertions. Of those, 43 plasmids contained insertions in the KEM1 sequence, which were analyzed further for more precise restriction mapping. Figure 4-1 demonstrates the structure of mini-Tn10-LUK and its insertion sites in the KEM1 gene with regard to the known restriction sites. The arrow indicates the orientation of mini-Tn10-LUK, directing from lacZ to kanR.

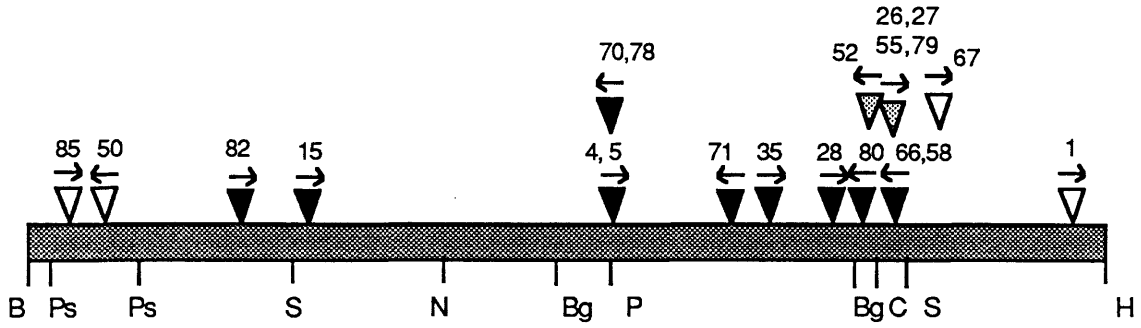
Insertion mutations define a 3.5 Kb region required for KEM1 function.

To test the complementing activity of each plasmid carrying a mini-Tn10-LUK insertion in KEM1, I transformed strain JK191 (kem1-5) with these plasmids. Patches of transformant strains were made and tested for benomyl hypersensitivity by replica-plating onto benomyl plates (10 or 15 μg/ml benomyl in YEPD medium). The Kem^- phenotype was also examined by a plate mating assay. The master plates with patches of strains to be

Figure 4-1. Restriction map of the plasmid vector used for transposon insertion analysis as well as the structure of mini-Tn10-LUK element.

(a) The DNA insert of pJI103 is shown as a filled-in box. The 5.5 kb BamHI - HindIII fragment is inserted at the BamHI and HindIII sites of Ycp402 (a derivative of Ycp50 with LEU2 replacing URA3, Ma et al., 1987). The site of insertions is indicated with a triangle. Numbers indicate the insertion plasmids. The fill of the triangle describes the complementing activity of the insertion plasmids; white (fully complementing acitivity), black (no complementing activity), gray (partially complementing acitvity). The arrow on top indicates the orientation of the mini-Tn10-LUK element from lacZ toward kanR. The predicted region of KEM1 function is shown. (b) The structure of mini-Tn10-LUK element. Numbers represent the distance in nucleotide of each junction from the left end of the Tn-LUK element. lacZ transcription is from left to right. The lacZ structural gene segment begins at codon eight of the protein coding sequence.

(a)

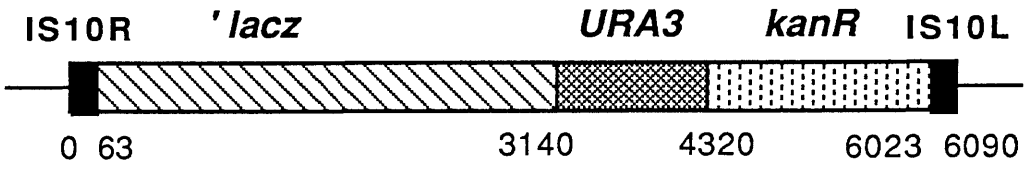


KEM1 **(3.5 kb)**

1 Kb

B BamHI
Bg Bgl II
C ClaI
H Hind III
N NcoI
P Pvu II
S SnaB I
X Xho I

(b)



tested were replica-plated onto a lawn of KAR1 cells and onto a lawn of kar1-1 cells. After mating for 4 hrs at 30°C, plates were replica-plated onto SC plates to select diploids.

The results are summarized in Table 4-1. The plasmid with insertion T50 has full KEM1 complementing activity, indicating that T50 lies outside of the KEM1 gene boundary. The insertion T82 destroys the complementing activity, indicating that it is internal to the KEM1 gene. Starting from T82, a continuous region of 3.5 Kb is shown to be required for KEM1 function. Plasmids with insertions T27, T52, T55, or T79 are partially functional. They complement the benomyl-hypersensitive phenotype but not the Kem$^-$ phenotype. This partial activity implies that T27, T52, T55, and T79 lie internal to the KEM1 gene and they define a boundary of KEM1 function. Insertion T67 which lies right next to those insertions with partial activity (within 100 bps) shows full complementing activity. The conclusion from these results is that a 3.5 Kb region defined by insertion mutations is required for KEM1 function.

KEM1::LACZ protein fusion.

The lacZ gene of mini-Tn10-LUK element (Figure 4-1) lacks the first seven amino acids and both transcriptional and translational initiation signals. Therefore, insertion in the proper orientation and reading frame within the target gene will create a protein fusion. This fusion extends from the target gene, across the 70 bp terminus of the transposon, and into the lacZ gene.

Table 4-1. Complementing acivity of transposon insertion plasmids.

Plasmid #[a]	Benomyl sensitivity[b]	Diploid formation[c]	β-galactosidase activity[d]
T85	+	+	-
T50	+	+	-
T82	-	-	-
T15	-	-	-
T4,5,38,39,49,63	-	-	-
T70,78	-	-	-
T71	-	-	-
T35	-	-	-
T28	-	-	-
T80	-	-	-
T52	+/-	+/-	-
T26	+	+	+
T27	+/-	-	+
T55	++/-	-	+
T79	++/-	-	+
T58,66	-	-	-
T67	+	+	+
T1	+	+	-

a. Strain JK191 (kem1-5) was transformed with the plasmids indicated.

b. Complementation of benomyl-hypersensitivity of kem1-5 is indicated. +; full complementation, ++/- and +/-; partial complementation, -; no complementation.

c. Complementation of Kem^--phenotype (diploid formation in crosses to a kar1-1 strain) of kem1-5 is indicated. +; full complementation, -; no complementation.

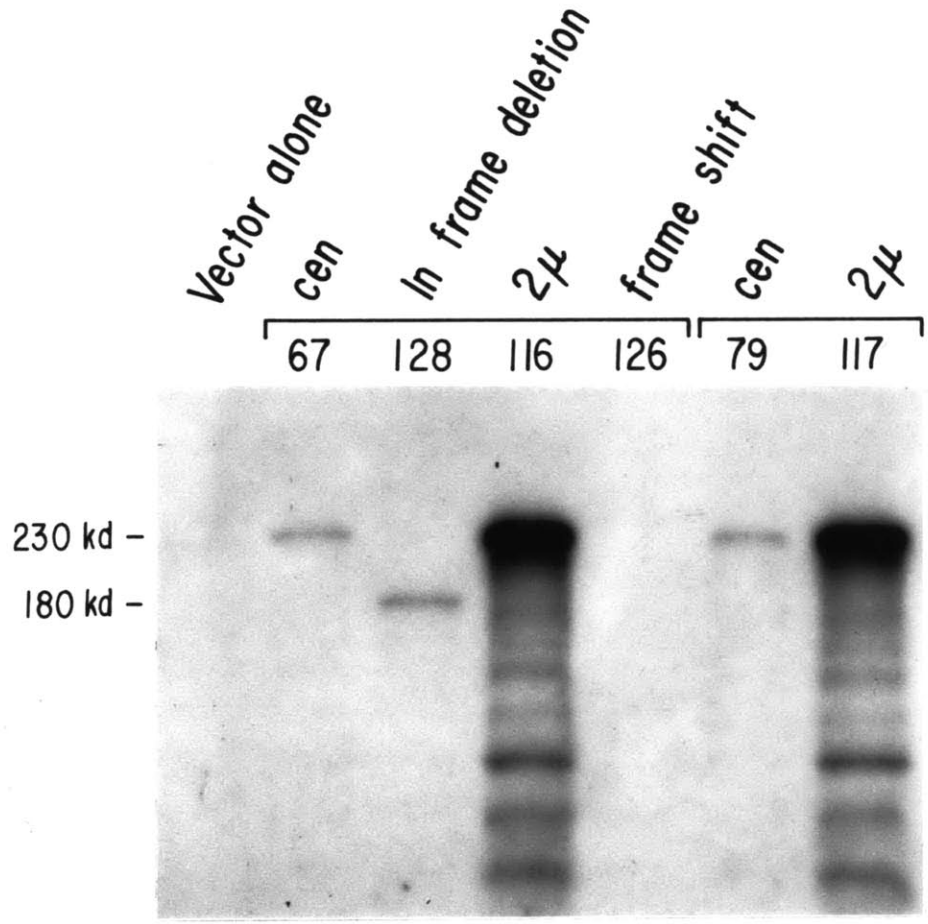
d. β-galactosidase activity determined by using X-gal indicator plates. +; blue patches -; white patches.

To identify KEM1::lacz fusion plasmids, I tested the strains haboring plasmids with mini-Tn10-LUK insertions in KEM1 for β-galactosidase activity on X-Gal indicator plates. Five plasmids (T26, T27, T55, T79, and T67) gave blue colonies, indicating efficient production of β-galactosidase. This result was confirmed by an β-galactosidase assay using chloroform-permeabilized cells. As shown in Figure 4-1, all of five insertions showing β-galactosidase activity are in the same orientation, strongly suggesting that the reading frame of the KEM1 gene proceeds in the direction from a PstI site toward a HindIII site. If this is the correct direction of the reading frame, insertions T26, T27, T55, T79, and T67 are located at the C-terminus of the KEM1 polypeptide. These locations probably explain full KEM1 complementing activity of plasmids T26 and T67 and partial activity of T27, T55, and T79. A frame shift mutation at the upstream NcoI site in the KEM1 sequence (pJI126) destroys the KEM1 complementing activity as well as β-galctosidase acivity of plasmid T67. These results suggest that in-frame insertion T67 is internal to a coding sequence of the KEM1 gene and creates a functional KEM1::lacz fusion.

To demonstrate that in-frame insertion of mini-Tn10-LUK in the KEM1 gene generates the expected KEM1::lacz fusion protein, I peformed western blot analysis using antibodies to β-galactosidase. Extracts of yeast cells carrying different plasmids were resolved by SDS-polyacrylamide gel electrophoresis, transfered to nitrocellulose filter, and hybrid proteins were identified by β-galcatosidase antibodies and [I^{125}]-lableled protein A. Fusions T67 and T79 produce hybrid proteins with approximate molecular weight of 230 Kd (lane 67, 79 in Figure 4-2),

Figure 4-2. Western blot analysis of KEM1::lacz fusion proteins.

The yeast strain JK147 was transformed with various plasmids carrying KEM1::lacz protein fusions. Protein extracts were prepared from whole cells, resolved on SDS - 7.5 % polyacrylamide gel, and transferred onto nitrocellulose filter. β-galactosidase was identified by using anti-β-galactosidase antibodies and [I^{125}]-protein A. Lane 67; plasmid T67 carrying KEM1::lacz fusion on a Cen-vector, lane 128; plasmid pJI128 carrying KEM1::lacz fusion with 1.6 kb BglII in-frame deletion in KEM1, lane 116; plasmid pJI116 carrying KEM1::lacz on 2μ-vector, lane 128; plasmid pJI126 carrying KEM1::lacz fusion with a NcoI site filled generating a frame shift mutation in KEM1, lane 79; plasmid 79 carrying KEM1::lacz fusion on a Cen-vector, lane 117; plasmid pJI117 carrying KEM1::lacz on 2μ-vector.


Vector alone
cen
In frame deletion
2μ
frame shift
cen
2μ
67
128
116
126
79
117
230 kd –
180 kd –

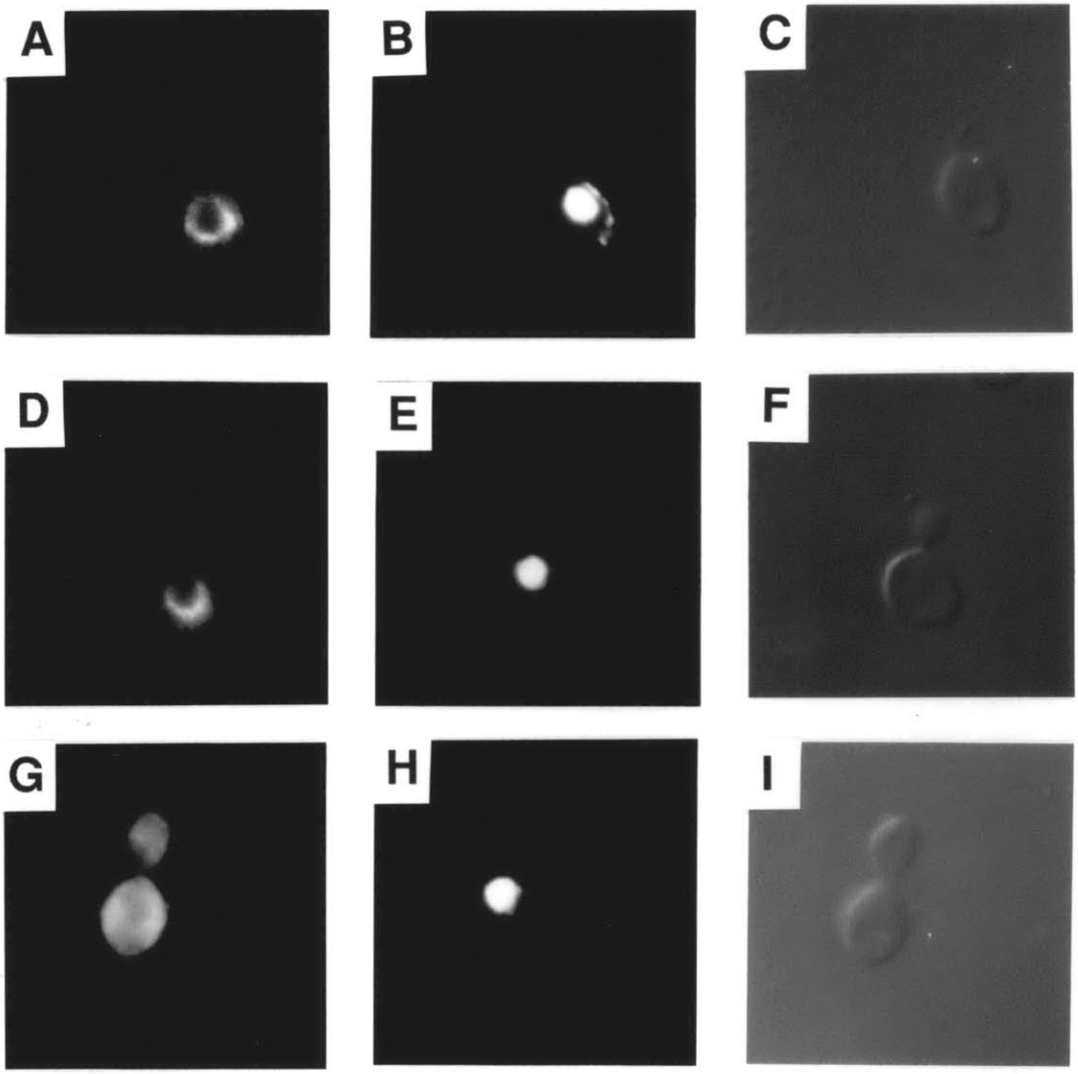
which is expected from the location of these insertion at the C-terminus of KEM1. In cells with plasmids pJI116 and pJI117 (insertion T67 and T79 on 2μ high copy plasmid) hyprid proteins were produced at the increased level (Figure 4-2). In-frame deletion of a 1.6 Kb BglII fragment in the KEM1 sequence of fusion T67 (pJI128) reduces the molecular weight of hybrid proteins by the size of the deleted fragmet (lane 128 in Figure 4-2). pJI128 is nonfunctional in complemetation of kem1 mutation. The plasmid pJI126 carrying a frame shift mutation at the upstream NcoI site does not produce hybrid proteins (lane 126 in Figure 4-2). These results confirm the conclusion that in-frame insertions of mini-Tn10-LUK in KEM1 sequence generated funtional KEM1::lacz protein fusions.

Localization of KEM::LACZ protein fusions

To determine the cellular location of the KEM1 gene product, I performed immunofluorescence microscopy on cells carrying KEM1::lacz functional protein fusion on a high copy vector. Formaldhyde-fixed cells were treated with anti-β-galactosidase antibody which was visualized using rhodamine-conjugated antibodies. The KEM1::lacz fusions give bright staining around the nucleus (Figure 4-3, panels A - F) whereas a HTS1::lacz fusion (generously given by Chiu, personal communication) as a cytoplasmic control stains the whole cytoplasm (panels G - I). The HTS1 gene encodes the histidine-tRNA synthetase (Natsoulis et al., 1986). Cells treated with mating pheromones or zygotes in mating culture also show staining around the nucleus (not shown). These data suggest

Figure 4-3. Intracellular localization of KEM1::lacz fusion proteins revealed by indirect immunofluorescence.

The yeast strain JK147 was transformed with plasmids carrying KEM1::lacz or HTS1::lacz protein fusions. Each set of three panels represents the same cell revealed by 1) anti-β-galactosidase staining, 2) DAPI staining, and 3) Nomarsky optics. A - F cells carrying KEM1::lacz fusion on 2μ-vector (pJI116); G - I a cell carrying HTS1::lacz fusion on 2μ-vector (pIC 231).


A
B
C
D
E
F
G
H
I

that the KEM1::lacz fusion proteins are localized to the nuclear periphery.

DISCUSSION

In this chapter I have described transposon insertion analysis of KEM1 and intracellular localization of KEM1::lacz hybrid proteins. A collection of random insertions of mini-Tn10-LUK element (Huisman et al., 1987) in KEM1 defined an approximately 3.5 kb region required for the KEM1 function and gave functional KEM1::lacz protein fusions. Indirect immunofluorescence using anti-β-galactosidase antibodies localized the KEM1::lacz hybrid proteins to the nuclear periphery.

The cellular location of the KEM1::LACZ fusion proteins at the nuclear periphery suggests to me that the native KEM1 proteins are localized to the same region. The nucleus of a eucaryotic cell is enclosed by a double membrane structure called nuclear envelope (Byers, 1981, Alberts et al., 1983). Inner and outer membranes of the nuclear envelope is separated by the perinuclear space. The outer membrane is continuous with the endoplasmic reticulum (ER) membrane. In indirect immunofluorescence microscopy with KEM1::LACZ, the staining around the nucleus was bright and faded out into the cytoplasm suggesting that these hybrid proteins are presumably present in the nuclear envelope and may be in ER membranes as well.

In previous chapters I have shown that the KEM1 gene affects nuclear fusion during conjugation as well as spindle pole body function. Nuclear fusion would require the fusion of two nuclear envelopes

followed by the reorganization of membrane structure. Although the mechanism by which membranes fuse is not understood, it is very likely that a majority of the participating proteins are present at or near the nucleus. The spindle pole body that is also affected by KEM1 is embedded in the nuclear envelope participating in nuclear fusion processes as well as in organization of microtubules (Robinow and Mark, 1966, Byers and Goetsch, 1974, 1975). The functions of the KEM1 gene defined by mutational analysis appear to be in good agreement with the predicted cellular location of the KEM1 proteins.

Studies on the cellular localization of the gene products are often hindered by a number of reasons. An approach using indirect immunofluorescence requires an abundance of stable proteins in the cell for visualization in the light microscope. Efficient and stable antibody-antigen interaction is another critical factor. The use of anti-β-galacosidase antibodies to stain the β-galactosidase hybrid proteins often gives an informative signal which the antibodies against native proteins can not. However, the large size of β-galactosidase proteins may lead to mislocalization. I have tried to use functional KEM1::LACZ protein fusions on a high-copy vector. The KEM1 on a high-copy vector does not seem to affect mitotic growth nor the diploid formation in mating. The investigation on the cellular localization of the KEM1 proteins should be checked by using KEM1-specific antibodies and cell fractionation techniques to verify the results with KEM1::LACZ protein fusions.

Kaiser (1987) constructed gene fusions between the yeast SUC2 gene and the E. coli β-galactosidase gene. The SUC2 gene encodes invertase,

the secreted form of which is produced in cytoplasm and transfered to cell surface via the secretory pathway. The hybrid protein containing 19 amino acids of the invertase signal sequence showed the immunofluorescent staining around the nucleus. With an analysis of this fusion in sec18 strain that has greatly altered ER structure, Kaiser claimed that the staining pattern is indicative of ER localization. This conclusion is based on the idea that entry into the ER is an early step of the secretory pathway. Because the KEM1::lacz fusion proteins are localized to the nuclear periphery, it is possibile that the location of a majority of the hybrid proteins at this region is a reflection of the same block in secretion shown for SUC2::lacz. As mentioned earlier in this discussion, the only way to be certain about the cellular location of the KEM1 protein is to study it using KEM1 specific antibodies.

Appendix I

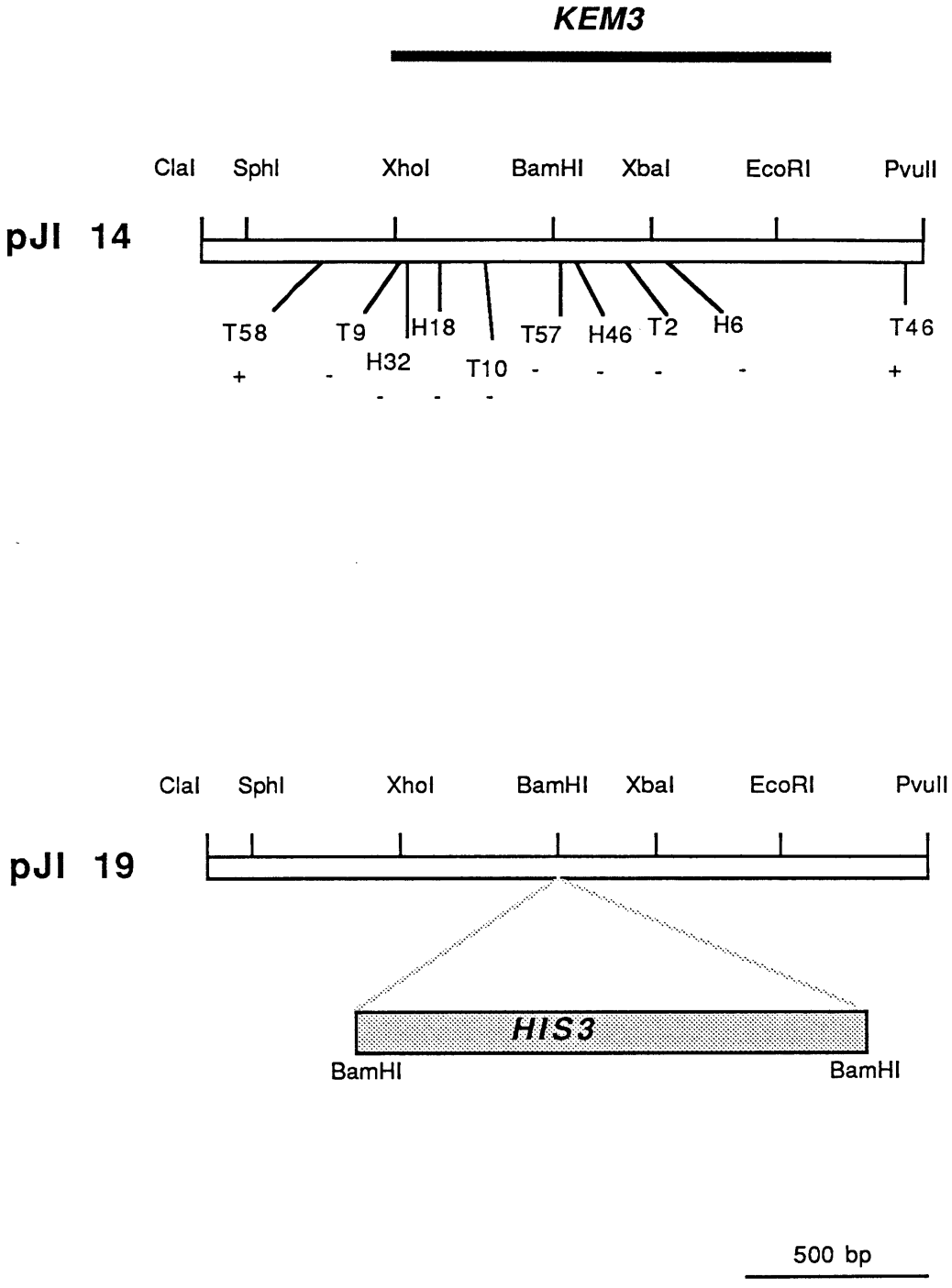
Cloning and disruption of KEM3

As described in chapter 2, kem3 mutant strains are temperature sensitive for growth, which is the secondary phenotype acquired along with the Kem$^-$ phenotype. I isolated the KEM3 gene by its ability to complement this growth defect of the kem3 mutation. The strain JM111-17C (ura3-52, his4-29, kem3) was transformed with DNA from a yeast genomic library contained on the YCp50 vector carrying the URA3 gene and a yeast centromere (CEN3). Ura$^+$ transformants were selected at 24^{o}C, replica-plated onto YEPD plates, and plates were incubated at 34^{o}C. Temperature-resistant colonies were picked and tested for plasmid dependence. Two strains after screening 5,000 transformants were identified, and their plasmid DNAs were isolated by transforming E. coli. Retransformation of the kem3 strain with the isolated plasmids (pJI1 and pJI2) confirmed that two plasmids carry the complementing activity; both ts for growth and the Kem$^-$ phenotype. Restriction map analysis with pJI1 and pJI2 identified 4.5 Kb overlapping region of yeast DNA. Subcloning experiments demonstrated that the complementing region was localized to a 2 Kb ClaI-PvuII fragment (pJI14, Figure 5-1). A deletion of a 400 bp EcoRI-PvuII fragment (pJI4) destroys complementing activity, indicating that this EcoRI site is internal to the KEM3 gene.

The boundaries of the KEM3 gene were defined by linker insertion mutations. A plasmid pJI14 was partially digested with either TaqI or HinFI and ligated with synthetic HindIII linkers (details of the

Figure 5-1. Restriction map of the plasmid inserts containing KEM3 and kem3 disruption.

pJI14 carries a 2.0 kb ClaI - PvuII fragment of KEM3 at the ClaI and SalI sites of Ycp50. The site of linker insertions is shown with indication of the complementing activity; + (complementation of temperature-sensitivity of kem3), - (no complementation). pJI19 carries the same 2.0 kb ClaI - PvuII fragment as pJI14 with the 1.8 kb BamHI HIS3 fragment inserted at the BamHI site within KEM3.


KEM3
ClaI
SphI
XhoI
BamHI
XbaI
EcoRI
PvuII
pJI 14
T58
T9
H18
H32
T10
T57
H46
T2
H6
T46
+
-
-
-
-
-
-
-
-
+
pJI 19
HIS3
BamHI
BamHI
500 bp

procedures are under Linker insertion mutagenesis in this appendix). Plasmids carrying the linker insertions were tested for their ability to complement the kem3 mutation. As shown in Figure 5-1, results from these linker insertions along with subcloning experiments define a region of approximately 1.2 Kb required for complementing activity.

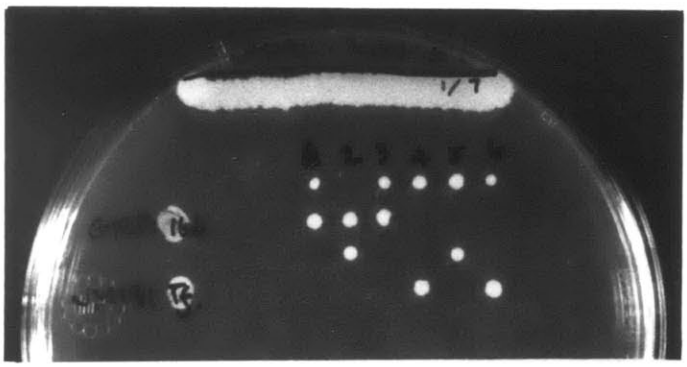
To test that the cloned sequence is indeed the KEM3 gene, I integrated this DNA sequence into the chromosome by homologous recombination and examined its linkage to the kem3 mutation. A ClaI-PvuII fragment was subcloned into the integrating vector YIp5 carrying the URA3 marker to make plasmid pJI21. pJI21 plasmid DNA was degested with XhoI to stimulate the recombination into the chromosomal locus homologous with the insert sequence and used to transform a KEM, ura3-52 strain (TD28). A Ura^+ transformant was crossed to a kem3, ura3-52 strain (JM88-13C), diploids were selected and sporulated. In 20 tetrads analyzed, Ura^+ and Ts^+ cosegregated 2:2. indicating that the site of integration is tightly linked to the KEM3 gene. This results show that the cloned sequence is the authentic KEM3 gene.

The conditional-lethal phenotype of the kem3 mutation strongly suggests that the KEM3 gene is essential. To verify this, I disrupted the KEM3 gene with a selectable yeast gene. A 1.8 Kb BamHI fragment containing the yeast HIS3 gene was inserted into the BamHI site of pJI14, which is internal to the KEM3 gene (pJI19, Figure 5-1). A diploid strain homozygous for his3-200 (JM191) was transformed with a linear ClaI-PvuII fragment containing the disrupted gene to disrupt one copy of the KEM3 gene (Rothstein, 1983). The His^+ transformants were selected,

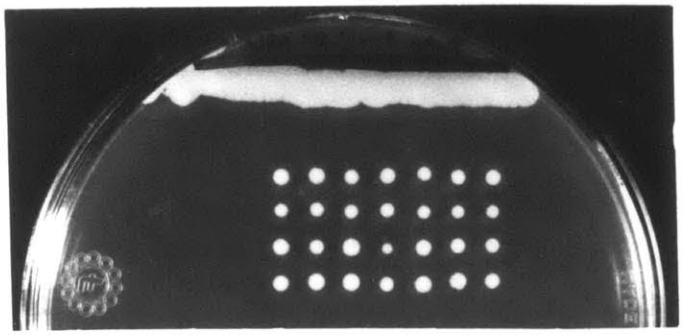
Figure 5-2. 2:2 segregation of lethality in tetrads from +/kem3::HIS3.

(a) Tetrads from a His^+ transformant (b) Tetrads from the parent diploid JM191.

(a)



(b)



sporulated and tetrads were dissected. As shown in Figure 5-2a, every tetrad gave two viable spores and two inviable spores. All viable spores were His^-, suggesting that the spore inviability is a consequence of the KEM3 gene disruption. The original His^- parent strain was compared in Figure 5-2b, which shows that all four spores in each tetrad are viable. These results indicate that the KEM3 is essential.

Plasmid constructions. The plasmids pJI1 and pJI2 were isolated from a yeast genomic library constructed in YCp50. The plasmid pJI14 was constructed by inserting a 2.0 Kb ClaI-PvuII fragment of pJI2 between the ClaI site and the PvuII site of pJI13 (pJI13 was derived from YCp50, which has a PvuII linker at the SalI site). The plasmid pJI4 was constructed by insertion of a 1.7 Kb EcoRI fragment from pJI1 at the EcoRI site of YCp50.

The kem3::HIS3 insertion was constructed by inserting a 1.8 Kb BamHI fragment containing the yeast HIS3 gene at the BamHI site of pJI14.

Linker insertion mutagenesis. Linker insertion into the KEM3 gene was peformed by linker tailing method (Lathe et al., 1984). The plasmid pJI14 was digested partially with TaqI or HinFI and the 5′ overhangs were filled with Klenow enzyme. Linear plasmids with a single cut were isolated from an agarose gel and ligated with the non-phosphorylated HindIII linkers (from New England Biolabs). This ligation links one strand of a single unphosphorylated duplex to a normal 5′- phosphorylated terminus of a target plasmid, resulting in DNA termini carrying covalently linked single-stranded tails. Plasmid DNAs were separated from the excess linkers by agarose gel electrophoresis followed by electro-elution. The self complementary tails

were annealed by heating at 65°C in a hybridization buffer (100mM NaCl, 10mM Tris, PH 7.5, and 5mM Na_2EDTA) and cooling slowly to 4°C prior to transformation. The residual nicks are repaired *in vivo*. A total of 124 transformants were analyzed after rapid plasmid preparation. Of 84 linker inserted plasmids, 26 contained a linker insertion in the yeast DNA. Fine mapping of these linker insertions was carried out and shown in Figure 5-1.

LITERATURE CITED

Adams, A. E. M. and J. R. Pringle, 1984 Relationships of actin and tubulin distribution to bud growth in wild-type and morphogenetic-mutant Saccharomyces cerevisiae. J. Cell. Biol. 98:934-945.

Baum, P., L. Goetsch, and B. Byers, 1986a Genetics of spindle pole body regulation. pp. 155-158. In: Yeast Cell Biology, Edited by J. Hicks. Alan R. Liss, Inc., New York.

Baum, P., F. Clement, and B. Byers, 1986b Yeast gene required for spindle pole body duplication: homology of its product with Ca^{2+}-binding proteins. Proc. Natl. Acad. Sci. 83:5512-5516.

Betz, R., V. L. Mackay, and W. Duntze, 1977 α-factor from Saccharomyces cerevisiae: partial characterization of a mating hormone produced by cells of mating type **a**. J. Bacteriol. 132:462-472.

Betz, R. W., Duntze, and T. R. Manney, 1978 Mating-factor-mediated sexual agglutination in Saccharomyces cerevisiae. FEMS. Microbiol. Lett. 4:107-110.

Boeke, J. D., D. J. Garfinkel, C. A. Styles, and G. R. Fink, 1985 Ty elements transpose through an RNA intermediate. Cell 40:491-500.

Boeke, J. D., J. Trueheart, G. Natsoulis, and G. R. Fink, 1987 5-fluoroorotic acid as a selective agent in yeast molecular genetics. Methods Enzymol. 154: 164-175.

Botstein, D., S. C. Falco, S. Stewart, M. Brenner, S. Scherer, D. Stinchcomb, K. Struhl, and R. Davis, 1979 Sterile host yeasts (SHY): a eukaryotic system of biological containment for recombinant DNA experiments. Gene 8:17-24.

Boyer, H. and D. Roulland-Dussoix, 1969 A complementation analysis of the restriction and modification of DNA in E. coli. J. Mol. Biol. 41:469-472.

Broek, D., N. Samiy, O. Fasano, A. Fujiyama, F. Tamanoi, P. J. Northu, and M. Wigler, 1985 Differential activation of yeast adenylate cyclase by wild-type and mutant RAS proteins. Cell 41:763-769.

Broek, D., T. Toda, T. Michaeli, L. Levin, C. Birchmeier, M. Zoller, S. Power, M. Wigler, 1987 The S. cerevisiae CDC25 gene product regulates the RAS/adenylate cyclase pathway. Cell 48:789-799.

Bryan, J. and L. Wilson, 1971 Are cytoplasmic microtubules heterodimers? Proc. Natl. Acad. Sci. U.S.A. 68:1762-1766.

Bucking-Throm, E., W. Duntze, H. Hartwell, and T. Manney, 1973 Reversible arrest of haploid yeast cells at the initiation of DNA synthesis by a diffusible sex factor. Exp. Cell Res. 76:99-110.

Burke, D., L. Mendonca-Previato, and C. E. Ballou, 1980 Cell cell recognition in yeast: purification of Hansenula wingei 21-cell sexual agglutination factor and comparison of the factors from three genera. Proc. Acad. Natl. Sci. U.S.A. 77:318-322.

Buckholder, A. C. and L. Hartwell, 1985 The yeast α-factor receptor: structural properties deduced from the sequence of the STE2 gene. Nuc. Acids Res. 13:8463-8475.

Byers, B., 1981a Cytology of the yeast life cycle. pp. 59-96. In: The Molecular Biology of the Yeast Saccharomyces. vol. 1, Edited by Strathern,J. N., E. W. Jones, and J. R. Broach, Cold Spring Harbor, New York.

Byers, b., 1981b Multiple roles of the spindle pole bodies in the life cycle of Saccharomyces cerevisiae. pp. 119-131. In: Molecular Genetics in Yeast, vol. 17, Edited by Wettstein, D. V., J. Friis, M. Kielland-Brandt, and A. Stenderup, Copenhagen, Munksgaard.

Byers, B. and L. Goetsch, 1974 Duplication of spindle plaques and integration of the yeast cell cycle. Cold Spring Harbor Symp. Quant. Biol. 38:123-131

Byers, B. and L. Goetsch, 1975 Behavior of spindles and spindle plaques in the cell cycle and conjugation of Saccharomyces cerevisiae. J. Bacteriol. 124: 511-523.

Byers, B., K. Shriver, and L. Goetsch, 1978 The role of spindle pole bodies and modified microtubule and in the initiation of microtubule assembly in Saccharomyces cerevisiae. J. Cell Sci. 30:331-352.

Carle, G. F. and M. V. Olson, 1985 An electrophoretic karyotype for yeast. Proc. Natl. Acad. Sci. U.S.A. 82:3756-3760.

Chan, R. K., L. M. Melnick, L. M., L. C., and J. Thorner, 1983 Extracellular suppression allows mating by pheromone-deficient sterile mutants of Saccharomyces cerevisiae. J. Bacteriol. 155:903-906.

Conde, J. and G. R. Fink, 1976 A mutant of Saccharomyces cerevisiae defective for nuclear fusion. Proc. Natl. Acad. Sci. U.S.A. 73:3651-3655.

Curran, B. P. G. and B. L. A. Canter, 1986 α-factor enhancement of hybrid formation by protoplast fusion in Saccharomyces cerevisiae. Curr. Genetics 10:943-945.

Davis, R., D. Botstein, and J. Roth. 1980 Advanced Bacterial Genetics. Cold Spring Harbor Lab. Cold Spring Harbor, New York.

DeFeo-Jones, D., K. Tatchell, L. Robinson, I. Sigal, W. Vass, D. Lowy, and E. Scolnick, 1985 Mammalian and yeast ras gene products: biological function in their heterologous system. Science 228:179-184.

Delgano, M. A. and J. Conde, 1984 Benomyl prevents nuclear fusion in Saccharomyces cerevisiae. Mol. Gen. Genet. 193:188-189.

Dietzel, C. and J. Kurjan, 1987 The yeast SCG1 gene: a G_{α}-like protein implicated in the a- and α-factor response pathway. Cell 50:1001-1010.

Dutcher, S., 1982 The genetic control of karyogamy in the yeast Saccharomyces cerevisiae. Ph.D. thesis, University of Washington, Seattle.

Dutcher, S. K. and L. H. Hartwell, 1982 The role of cell division cycle genes in nuclear fusion in Saccharomyces cerevisiae. Genetics 100:175-184.

Dutcher, S. K. and L. Hartwell, 1983 Genes that act before conjugation to prepare the Saccharomyces cerevisiae nucleus for caryogamy. Cell 33:203-210.

Fehrenbacher, G., K. Perry, and J. Thorner, 1978 Cell-cell recognition in Saccharomyces cerevisiae: regulation of mating-specific adhesion. J. Bacteriol. 134:893-901.

Fink, G. R., 1970 The biochemical genetics of yeast. Methods Enzymol. 17A:59-78.

Fink, G. R. and J. Conde, 1976 Studies on KAR1, a gene required for nuclear fusion in yeast. pp. 414-419. In: International Cell Biology 1976-1977, Edited by Brinkley, B. R. and K. R. Porter, Rockfeller University Press, New York.

Haarer, B. K. and J. R. Pringle, 1987 Immunofluorescence localization of the Saccharomyces cerevisiae CDC12 gene product to the vicinity of the 10-nm filaments in the mother-bud neck. Mol. Cell Biol. 7:3678-3687.

Hagen, D. C., G. McCaffrey, and G. F. Sprague, 1986 Evidence the yeast STE3 gene encodes a receptor for the peptide pheromone a factor: gene sequence and implications for the structure of the presumed receptor. Proc. Natl. Acad. Sci. U.S.A. 83:1418-1422.

Hagiya, M., K. Yoshida, and N. Yanagishima, 1977 The release of sex-specific substances responsible for sexual agglutination from haploid cells of Saccharomyces cerevisiae. Exp. Cell Res. 104:263-272.

Hartwell, L. H., 1973 Synchronization of haploid yeast cell cycles, a prelude to conjugation. Exp. Cell Res. 76:111-117.

Hartwell, L. and D. Smith, 1985 Altered fidelity of mitotic chromosome transmission in cell cycle mutants of S. cerevisiae. Genetics 110:381-395.

Herskowitz, I. and Oshima, 1981 Control of cell type in Saccharomyces cerevisiae: mating type and mating-type interconversion. In: The Molecular Biology of the Yeast Saccharomyces. vol. 1, Edited by Strathern,J. N., E. W. Jones, and J. R. Broach, Cold Spring Harbor, New York.

Herskowitz, I. and L. Marsh, 1987 Conservation of a receptor/signal transduction system. Cell 50:995-996.

Holmes, D. S. and M. Quigley, 1981 A rapid boiling method for the preparation of bacterial plasmids. Anal. Biochem. 114:193-197.

Huffaker, T. C., M. A. Hoyt, and D. Botstein, 1987 Genetic analysis of the yeast cytoskeleton. Ann. Rev. Genet. 21:258-284.

Huffaker, T. C., J. H. Thomas, and D. Botstein, 1988 Diverse effects of β-tubulin mutations on microtubule formation and function. in press.

Huisman, O., W. Raymond, K. Froehlich, P. Errada, N. Klekner, D. Botstein, and M. A. Hoyt, 1987 A Tn10-lacZ-kanR-URA3 gene fusion transposon for insertion mutagenesis and fusion analysis and bacterial genes. Genetics 116:191-197.

Ito, H., Y. Fukada, K. Murata, and A. Kimura, 1983 Transformation of intact yeast cells with alkai cation. J. Bacteriol. 153:163-168.

Kaiser, C. A., 1987 Analysis of a protein export sequence in yeast. Ph,D. thesis, Massachusetts Institute Technology, Cambridge.

Kataoka, T., S. Powers, C. McGill, O. Fasano, J. Strathern, J. Broach, and M. Wigler, 1984 Genetic analysis of yeast RAS1 and RAS2 genes. Cell 37:437-445.

Kataoka, T., D. Broek, and M. Wigler, 1985a DNA sequence and characterization of the S. cerevisiae gene encoding adenylate cyclase. Cell 43:493-505.

Kataoka, T., S. Powers, S. Cameron, O. Fasano, M. Goldfarb, J. Broach, and M. Wigler, 1985b Functional homology of mammalian and yeast RAS genes. Cell 40:19-26.

Kawanabe, Y., K. Yoshida, and N. Yanagishima, 1979 Sexual cell agglutination in relation to the formation of zygotes in Saccharomyces cerevisiae. Pland and Cell Physiol. 20:423-433.

Kilmartin, J. and A. Adams, 1984 Structural rearrangements of tubulin and actin during the cell cycle of the yeast Saccharomyces. J. Cell Biol. 98:922-933.

Lathe, R., S. Skory, and M. Kieny, 1984 Insertion new restriction sites by linker tailing. Focus 6:1-7.

Levi, J. D., 1956 Mating reaction in yeast. Nature 177:753-754.

Lipke, P., A. Taylor, and C. Ballou, 1976 Morphogenic effects of α-factor on Saccharomyces cerevisiae a cells. J. Bacteriol. 127:610-618.

Lipke, P. and C. Ballou, 1980 Altered immunochemical reactivity of Saccharomyces cerevisiae a cells after α-factor-induced morphogenesis. J. Bacteriol. 141:1170-1177.

Ma, H., S. Kunes, P. J. Schatz, and D. Botstein, 1987 Construction of plasmids by recombination in yeast. Gene 58:201-216.

Mackay, V. and T. Manney, 1974a Mutations affecting sexual conjugation and related processing in Saccharomyces cerevisiae. I. Isolation and phenotypic characterization of nonmating mutants. Genetics 76:255-271. Yeast Cell Biology, Edited by J. Hicks. Alan R. Liss, Inc., New York.

Mackay, V. and T. Manney, 1974b Mutations affecting sexual conjugation and related processing in Saccharomyces cerevisiae. II. Genetic analysis of nonmating mutants. Genetics 76:273-288.

Mandel, M. and A. Higa, 1970 Calcium dependent bacteriophage DNA infection. J. Mol. Biol. 53:159-162.

Manney, T. and S. V. Woods, 1976 Mutants of Saccharomyces cerevisiae resistant to the α mating-type factor. Genetics 82:639-644.

Miyajima, I., M. Nakafuku, N. Nakayama, C. Brenner, A. Miyajima, K. Kaibuchi, K. Arai, Y. Kaziro, and K. Matsumoto, 1987 GPA1, a haploid-specific essential gene, encodes a yeast homology of mammalian G protein which may be involved in mating factor signal transduction. Cell 50:1011-1019.

Mortimer, R. K. and D. Schild, 1981 Genetic mapping in Saccharomyces cerevisiae. pp. 11-26. In: The Molecular Biology of the Yeast Saccharomyces. vol. 1, Edited by Strathern,J. N., E. W. Jones, and J. R. Broach, Cold Spring Harbor, New York.

Nakayama, N., A. Miyajima, and K. Arai, 1985 Nucleotide sequences of STE2 and STE3, cell type-specific sterile genes from Saccharomyces cerevisiae. EMBO J. 4:2643-2648.

Nasmyth, K., 1982 Molecular genetics of yeast mating type. Ann. Rev. Genet. 16:439-500.

Natsoulis, G., F. Hilger, and G. R. Fink, 1986 The HTS1 gene encodes both the cytoplasmic and mitochondrial histidine tRNA synthetases of S. cerevisiae. Cell 46:235-243.

Neff, N. F., J. H. Thomas, P. Grisafi, and D. Botstein, 1983 Isolation of the β-tubulin gene from yeast and demonstration of its essential function in vivo. Cell 33:211-219.

Oakley, B. and N. R. Morris, 1980 Nuclear movement is β-tubulin dependent in Asperigillus nidulans. Cell 19:255-262.

Ohsumi, Y. and Y. Anraku, 1985 Specific induction of Ca^{2+} transport activity in MATa cells of Saccharomyces cerevisiae by a mating pheromone, α-factor. J. Biol. Chem. 260:10482-10486.

Osumi, M., C. Shimoda, and N. Yanagishima, 1974 Mating reaction in S. cerevisiae: V. Changes in the fine structure during the mating reaction. Arch. Microbiol. 97:27-38.

Pickett-Heaps, J. D., 1969 The evolution of the mitotic apparatus: an attempt at comparative ultrastructural cytology in dividing plant cells. Cytobios 1:257-280.

Pickett-Heaps, J. D., 1971 The anatomy of the centriole: fact or fallacy? Cytobios 3:205-214.

Polaina, J. and J. Conde, 1982 Genes involved in the control of Nuclear fusion during the sexual cycle of Saccharomyces cerevisiae. Mol. Gen. Genet. 186:253-258.

Powers, S., T. Kataoka, O. Fasano, M. Goldfarb, J. Strathern, J. Broach, M. Wigler, 1984 Genes in S. cerevisiae encoding proteins with domains homologous to the mammalian ras proteins. Cell 36:607-612.

Pringle,J. R., S. H. Lillie, A. E. M. Adams, C. W. Jacobs, B. K. Haarer, K. G. Coleman, J. S. Robinson, L. Bloom, and R. A. Preston, 1986 Cellular morphogenesis in the yeast cell cycle. pp. 47-80. In: Yeast Cell Biology, Edited by J. Hicks. Alan R. Liss, Inc., New York.

Robinow, C. F. and J. Mark, 1966 A fiber apparatus in the nucleus of the yeast cell. J. Cell Biol. 29:129-151.

Rose, M. D. B. Price, and G. R. Fink, 1986 Saccharomyces cerevisiae nuclear fusion requires prior activation by alpha factor. Mol. Cell. Biol. 6:3490-3497.

Rose, M. D. and G. R. Fink, 1987 KAR1, a gene required for function of both intranuclear and extranuclear microtubules in yeast. Cell 48:1047-1060.

Rothstein, R. J., 1983 One-step gene disruption in yeast. Methods Enzymol. 101:202-211.

Salminen, A. and P. Novick, 1987 A ras-like protein is required for a post-golgi event in yeast secretion. Cell 49:527-538.

Schatz, P. J., L. Pillus, P. Grisafi, F. Solomon, and D. Botstein., 1986a Two functional α-tubulin genes of the yeast Saccharomyces cerevisiae encode divergent proteins. Mol. Cell Biol. 6:3711-3721.

Schatz, P. J., F. Solomon, and D. Botstein., 1986b Genetically essential and nonessential α-tubulin genes specify functionally interchangeable proteins. Mol. Cell Biol. 6:3722-3733.

Schatz, P. J., 1987 Analysis of α-tubulin in yeast. Ph.D. thesis, Massachusetts Institute Technology, Cambridge.

Schekman, R. and V. L. Brawley, 1979 Localized deposition of chitin on the yeast cell surface in response to mating pheromone. Proc. Natl. Acad. Sci. U.S.A. 76:645-649.

Scherman, F., G. R. Fink, and C. W. Lawrence, 1979 Methods in Yeast Genetics, Cold Spring Harbor Lab. Cold Spring Harbor, New York.

Schmitt, H. D., P. Wagner, E. Pfaff, and D. Gallwitz, 1986 The ras-lelated YPT1 gene product in yeast: a GTP-binding protein that might be involved in microtubule organization. Cell 47:401-412.

Segev, N. and D. Botstein, 1987 The ras- like yeast YPT1 gene is itself essential for growth, sporulation and starvation response. Mol. Cell Biol. 7:2367-2377.

Sheirr-Neiss, G., M. Lai, and N. Morris, 1978 Identification of a gene for β-tubulin in Aspergillus nidulans. Cell 15:639-647.

Shimoda, C. and N. Yanagishima, 1972 Mating reaction in Saccharomyces cerevisiae: III. Changes in autolytic activities. Arch. Microbiol. 85:310-318.

Shimoda, C. and N. Yanagishima, 1975 Mating reaction in Saccharomyces cerevisiae: VIII. Mating-type-specific substances responsible for sexual cell agglutination. Antonie van Leeuwenhoek 41:521-532.

Shimoda, C. and N. Yanagishima, A. Sakurai, and S. Tamura, 1978 Induction of sexual agglutination of a mating-type cells as the primary action of the peptityl sex factor from α mating-type cells in Saccharomyces cerevisiae. Plant and Cell Physiol. 19:513-517.

Snyder,M. and R. W. Davis, 1986 Molecular analysis of chromosome segregation in yeast. Yeast 2:S363.

Southern, E. M., 1975 Detection of specific sequences among DNA fragments separated by gel electrophoresis. J. Mol. Biol. 98:503-517.

Stryer, L. and H. R. Bourne, 1986 G-proteins: a family of siganl transducers. Ann. Rev. Cell Biol. 2:391-419.

Sumurada, R. and T. G. Cooper, 1978 Control of vacuole permeability and protein degradation by the cell cycle arrest signal in Saccharomyces cerevisiae. J. Bacteriol. 136:234-246.

Tamanoi, F., M. Walsh, T. Kataoke, and M. Wigler, 1984 A product of yeast RAS2 gene is a guanine nucleotide binding protein. Proc. Natl. Acad. Sci. U.S.A. 81:6924-6928.

Terrance, K. and P. Lipke, 1981 Sexual agglutination in Saccharomyces cerevisiae. J. Bacteriol. 148:889-896.

Terrance, K., P. Heller, Y. Wu, and P. Lipke, 1987 Identification of glycoprotein components of α-agglutinin, a cell adhesion from Saccharomyces cerevisiae. J. Bacteriol. 169:475-482.

Thomas, J. H., 1984 Genes controlling the mitotic spindle and chromosome segregation in yeast. Ph,D. thesis, Massachusetts Institute Technology, Cambridge.

Thomas, J. H., N. F. Neff, and D. Botstein, 1985 Isolation and characterization of mutations in the β-tubulin gene of Saccharomyces cerevisiae. Genetics 112:715-734.

Thomas, J. H., P. Novick, and D. Botstein, 1986 Geneticts of the yeast cytoskeleton. pp. 13-34. In: Yeast Cell Biology, Edited by J. Hicks. Alan R. Liss, Inc., New York.

Thomas, J. H. and D. Botstein, 1986 A gene required for the separation of chromosomes on the spindle apparatus in yeast. Cell 44:65-76.

Thorner, J., 1981 Pheromonal regulation of development in Saccharomyces cerevisiae. pp. 143-180. In: The Molecular Biology of the Yeast Saccharomyces. vol. 1, Edited by Strathern,J. N., E. W. Jones, and J. R. Broach, Cold Spring Harbor, New York.

Throm, E. and W. Duntze, 1970 Mating type-dependent inhibition of deoxyribonucleic acid synthesis in S. cerevisiae. J. Bacteriol. 104:1388-

Toda, T., I. Uno, T. Ishikawa, S. Powers, T. Kataoka, D. Broek, S. Cameron, J. Broach, K. Matsumoto, and M. Wigler, 1985 In yeast, RAS proteins are controlling elements of adenylate cyclase. Cell 40:27-36.

Toda, T., S. Cameron, P. Sass, M. Zoller, and M. Wigler, 1987a Three different genes in S. cerevisiae encode the catalytic subunits of the cAMP-dependent protein kinase. Cell 50:277-287.

Toda, T., S. Cameron, P. Sass, M. Zoller, J. D. Scott, B. McMullen, M. Hurwitz, E. G. Krebs, and M. Wigler, 1987b Cloning and characterization of BCY1, a locus encoding a regulatory subunit of the cyclic AMP-dependent protein kinase in Saccharomyces cerevisiae. Mol. Cell Biolol. 7:1371-1377.

Trueheart, J., J. Boeke, and G. R. Fink, 1987 Two genes required for cell fusion during conjugation: evidence for a pheromone-induced surface protein. Mol. Cell Biol. 7:2316-2328.

Uno, I., K. Matsumoto, and T. Ishikawa, 1982 Characterization of cyclic AMP-requiring yeast mutants altered in the regulatory subunit of protein kinase. J. Biol. Chem. 257:14110-14115.

Wilkinson, L. E. and J. R. Pringle, 1974 Transient G1 arrest of S. cerevisiae cells of mating type α by a factor produced by cells of mating type a. Exp. Cell Res. 89:175-187.

Wright, R. E. and J. Lederberg, 1957 Extranuclear inheritance in yeast heterokaryons. Proc. Natl. Acad. Sci. U.S.A. 43:919-923.